ERCC1-XPF NUCLEASE: ROLES IN THE REPAIR OF DNA INTERSTRAND CROSSLINKS AND CHEMOTHERAPY RESISTANCE

by

Nikhil R. Bhagwat

M.B., B.S., University of Mumbai, India, 2003

Submitted to the Graduate Faculty of

Department of Human Genetics

Graduate School of Public Health in partial fulfillment

of the requirements for the degree of

Doctor of Philosophy

University of Pittsburgh

2009

UNIVERSITY OF PITTSBURGH

Graduate School of Public Health

This dissertation was presented

by

Nikhil R. Bhagwat

It was defended on

November 18, 2009

and approved by

Dissertation Advisor:
Laura J. Niedernhofer, MD, PhD
Associate Professor
Department of Microbiology and Molecular Genetics
School of Medicine
University of Pittsburgh

Committee Member:
Robert E. Ferrell, PhD
Professor
Department of Human Genetics
Graduate School of Public Health
University of Pittsburgh

Committee Member:
Susanne M. Gollin, PhD
Professor
Department of Human Genetics
Graduate School of Public Health
University of Pittsburgh

Committee Member:
Patricia L. Opresko, PhD
Assistant Professor
Department of Environmental and Occupational Health
Graduate School of Public Health
University of Pittsburgh

Copyright © by Nikhil R. Bhagwat
2009

Laura J. Niedernhofer, MD, PhD

ERCC1-XPF NUCLEASE: ROLES IN THE REPAIR OF DNA INTERSTRAND CROSSLINKS AND CHEMOTHERAPY RESISTANCE

Nikhil R. Bhagwat, PhD

University of Pittsburgh, 2009

ERCC1-XPF is a mammalian structure-specific endonuclease that incises at the junction of double and 3'-single-stranded DNA. ERCC1-XPF and its homologs are implicated in multiple DNA repair pathways including, nucleotide excision repair, interstrand crosslink repair, double strand break repair, repair of AP sites, and telomere maintenance, making it essential for viability. The pleiotropic phenotypes of ERCC1-XPF deficiency in humans, range from the cancer-predisposition syndrome xeroderma pigmentosum to the XPF-ERCC1 progeroid syndrome, a disease of accelerated aging.

This document concentrates on dissecting the role of ERCC1-XPF in crosslink repair, elucidating the mechanisms underlying the dramatic phenotypic differences in patients with inherited *XPF* mutations, and exploring the utility of ERCC1 and XPF as biomarkers of tumor prognosis.

Ercc1 and *Xpf* knockout mice are phenocopies, illustrating that the two proteins function exclusively as a heterodimer. These models present a progeroid phenotype, reflected in some patients with *XPF* or *ERCC1* mutations. We hypothesize that this accelerated aging is consequent on a failure to repair crosslinks, which are highly cytotoxic DNA lesions. The crosslink repair mechanism in animals remains poorly elucidated and the exact relationship of ERCC1-XPF to other players in this pathway, largely unexplored. Herein we show that ERCC1-XPF functions in the same pathway of crosslink repair as the Fanconi anemia proteins and that

crosslink unhooking by ERCC1-XPF is required for the efficient binding of FANCD2 to the chromatin.

The pleiotropy of phenotypes associated with human ERCC1-XPF deficiency is puzzling. Often, the severity of phenotype does not correlate with the DNA incising ability of the mutant proteins. We show here that the phenotypic heterogeneity is at least partially explained by the mislocalization of mutant proteins to the cytoplasm.

The public health importance of this work comes from the increasing interest in the regulation of ERCC1-XPF expression and activity, due to its involvement in DNA repair pathways implicated in the resistance of tumors to platinum-based chemotherapy. A panel of antibodies was tested extensively and optimized for use in clinical measurement of ERCC1-XPF. This will facilitate improved measurement of DNA repair proteins in clinical specimens and greater understanding of the mechanisms of tumor resistance to genotoxic therapy.

TABLE OF CONTENTS

LIST OF TABLES

LIST OF FIGURES

PREFACE

The work compiled herein would not have been possible without the help and support of some wonderful people, to whom I'll forever owe a debt of gratitude. I would not be here without the enduring support and sacrifice of my family. I am in debt to my parents for always trusting me and backing me up all the way. Ruta, my wife, always stood by me and kept me going through the thick and the thin; a task I know to be a very difficult one. I cannot thank her enough for that. I thank my best friend Vishal, for helping me become more persistent in my efforts, less temperamental and many other things than one can shake a stick at; and Rahul without whose advice I would not have ended up in Laura's lab.

Laura is an incredibly good mentor. She is always fair and encouraging, while maintaining a stringent standard for the quality of science, and that means a lot when you are a student trying to navigate a bewildering and brutal world of science. But she is also a great role model and that helps a lot too. So for all the science and life lessons that I received, I am eternally thankful to her.

In last five years, I have gone from not knowing which end of the pipette to hold (a side-effect of my medical training) to being totally independent in the lab, and even teaching others a few tricks. Anwaar and Andria bore the brunt of my ignorance and taught me the ropes. They are both, my friends and my mentors. I thank everyone in the lab not just for the interesting scientific

discussions and advice but also for making these five years such an enjoyable time, by incessantly quoting Monty Python, appreciating bad science-nerd jokes and maintaining a continuous supply of baked goodies.

I would like to thank my thesis committee, Dr. Susanne Gollin, Dr. Patricia Opresko and Dr. Robert Ferrell, for their support and guidance, and for taking the time out of their very busy schedules.

Through these years there have been a number of productive collaborations. Dr. Rick Wood led us to the antibody project and collaborated for two manuscripts. I thank him and Vera Roginskaya for a wonderful collaboration. The work related to Fanconi anemia was done in collabortion with Dr. Peter McHugh, his student Anna Olsen and Post-doc Anderson Wang. I thank them for an efficiently run transatlantic collaboration. Last but not least, I am grateful to Dr. Julie DeLoia and Dr. Tom Krivak for the ongoing collaboration to measure the ERCC1-XPF expression in ovarian tumors.

1.0 INTRODUCTION

ERCC1-XPF is a structure-specific endonuclease initially discovered for its role in nucleotide excision repair (NER), a DNA repair pathway that removes helix distorting lesions from the nuclear genome (Sijbers *et al.*, 1996a). ERCC1-XPF and its homologs in yeast, *Drosophila* and plants have been found to function in a plethora of DNA damage repair and tolerance mechanisms. Humans and mice deficient in ERCC1-XPF show symptoms of accelerated aging and predisposition to cancer (Niedernhofer *et al.*, 2006). This makes ERCC1-XPF deficient cells and organisms attractive models for the study of mechanisms and treatment of age-related degenerative disorders and cancer.

1.1 PUBLIC HEALTH RELEVANCE

As the average life expectancy increases, cancers and other age-related disorders escalate in prevalence. This can create a significant burden on health care and the economy. Although the treatment of early stage cancers and their outcome has improved over the past decades, for many types of cancers, especially for cancers at later stages, the survival rates have not improved over the last decade (Jemal *et al.*, 2009). Chemotherapy and radiotherapy are used in surgically non-resectable cases as the treatment of choice. Resistance to chemotherapy is common, especially for platinum-based chemotherapy, which is the workhorse of chemotherapies (Modesitt and

Jazaeri, 2007). In many cases, this method of treatment does not improve overall patient survival (Armstrong, 2002; Jemal *et al.*, 2008; McGuire *et al.*, 2002). It is therefore of great importance to identify the mechanisms behind chemotherapy resistance and to find a way to either circumvent these or to tailor the chemotherapy for the best outcome in each individual case. Many of the chemotherapeutic drugs including platinum derivatives (Eastman, 1987) and radiotherapy (Ward, 1988) act through their ability to damage genomic DNA. It therefore follows that the efficiency of DNA damage repair mechanisms could act as a predictor of sensitivity to these therapies. As far as the chemotherapy with crosslinking agents such as platinum derivatives, nitrogen mustards and mitomycin C (MMC) is concerned, ERCC1-XPF is extremely important for both pathways – nucleotide excision repair (NER) and interstrand crosslink (ICL) repair – required for tolerance to these drugs (De Silva *et al.*, 2000; Sijbers *et al.*, 1996a). Therefore, it is important to study the mechanism of action of ERCC1-XPF in these pathways.

Age-associated diseases, such as cardiovascular disease, Alzheimer's disease, diabetes, osteoporosis, hearing and visual impairment, arthritis and cancers, accompany aging. For many of these diseases, age is the single most important risk factor. People over the age of 65 years have a 10-fold higher risk of cancers compared to their younger counterparts (Finkel, 2005). Many of these diseases show a similar trend with advancing age (Kirkwood, 2005) and seem to increase exponentially with a linear increase in age (Finkel, 2005). By 2030 the number of people above 65 in the US will nearly double and their proportion in the population will go up from about 12% to greater than 19% (Greenberg, 2008). Thus, over the next decades, treatment of age-associated diseases can make a significant impact on the health care system and the national economy. Therefore, it is important to understand the mechanisms regulating and

causing the process of aging. The foremost theory is the stochastic theory of aging, which states that the organism ages as a result of an accumulation of cellular damage due to genomic mutations, mitochondrial dysfunction, damage to proteins and DNA due to endogenous and exogenous genotoxic agents, telomere shortening and accumulation of waste products (Kirkwood, 2005). Thus, DNA repair plays an important role in the process of aging, highlighting the importance of deciphering DNA repair mechanisms. *Ercc*$^{-/-}$ mice have a progeroid phenotype (Niedernhofer *et al.*, 2006), while a milder depletion of ERCC1-XPF leads to cancer (Sijbers *et al.*, 1996a). Studying ERCC1-XPF therefore allows us to study both aging and cancer, two processes that are responsible for considerable morbidity and mortality in the general population.

1.2 XPF FAMILY MEMBERS

ERCC1-XPF is a member of the XPF family of endonucleases. The XPF family has no known homologs in bacteria (Aravind *et al.*, 1999). It likely arose in archaea, in which there is just one family member, Hef (Figure 1-1) (Komori *et al.*, 2002). The N-terminal region of the XPF-family shows similarities to the archaeal superfamily 2 (SF2) RNA helicases, and the C-terminal region has a conserved (V/I)ERKX$_3$D nuclease motif similar to SF2-helicases (Sgouros *et al.*, 1999). Euryarchaeal Hef orthologs retain the DExH helicase motif (Komori *et al.*, 2002), though crenarchaea, e.g., *Aeropyrum pernix* and *Sulfolobus solfataricus*, do not (Figure 1-1) (Nishino *et al.*, 2003). Eukaryotic XPF homologs show conservation of the N-terminal half without conservation of the DExH motif itself and are therefore, helicase inactive (Sgouros *et al.*, 1999).

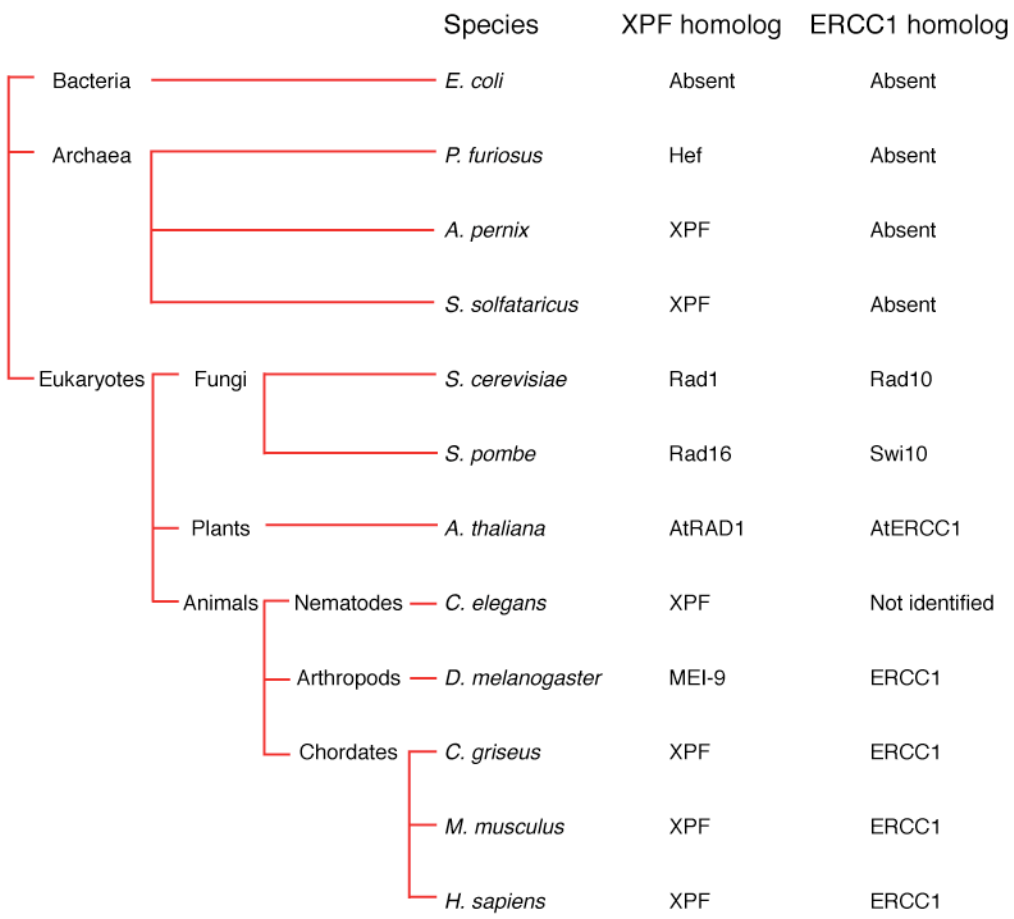

Figure 1-1: Homologs of ERCC1-XPF

Homologs of XPF and ERCC1 in various model organisms ranging from bacteria to vertebrates

In eukaryotes, the functional homolog is the ERCC1-XPF heterodimer, with XPF retaining the nuclease motif, whereas in archaea, Hef homodimerizes. ERCC1-XPF is highly conserved throughout evolution and all eukaryotes studied so far have homologs of ERCC1-XPF (Figure 1-1). The eukaryotic XPF has three major domains: a DExH helicase-like domain, an ERKX3D nuclease domain and a helix-hairpin-helix like domain (Figure 1-2) (Aravind *et al.*, 1999; Sgouros *et al.*, 1999). ERCC1, the smaller of the two partners, does not have the helicase-like domain and has lost its nuclease motif through gene divergence (Gaillard and Wood, 2001).

It only has two domains: the central domain, which is nuclease-dead and the C-terminal HhH2 domain (Figure 1-2), which interacts with the corresponding domain of XPF (de Laat *et al.*, 1998b). The heterodimeric interaction of ERCC1 and XPF stabilizes these proteins *in vivo* (Niedernhofer *et al.*, 2006). Consequently, XP-F cells have a reduced expression of ERCC1 (Biggerstaff *et al.*, 1993; Yagi *et al.*, 1997), which is restored by the expression of exogenous wild-type XPF (Yagi *et al.*, 1998), and *Ercc1* mutant cells have a reduced level of XPF, which is restored by exogenous expression of ERCC1 (Houtsmuller *et al.*, 1999). ERCC1-XPF is a versatile endonuclease that plays a role in many genome maintenance pathways (Figure 1-3) described in detail later.

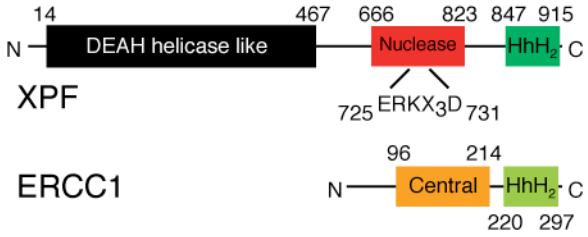

Figure 1-2: Major domains in XPF and ERCC1

Schematic representation of XPF and ERCC1 showing the extents in amino acid numbers of the helicase-like (*black box*), the nuclease (*red box*) and the HhH_2-like (*dark green box*) domains of XPF and the central (*orange box*) and HhH2 (*light green box*) domains of ERCC1.

All XPF family members in eukaryotes function as heterodimers (Bailly *et al.*, 1992; Bardwell *et al.*, 1992; Boddy *et al.*, 2001; Ciccia *et al.*, 2007; Sijbers *et al.*, 1996a). In vertebrates there are three types of proteins in the XPF family: those that have nuclease activity (XPF and MUS81), one with translocase activity (FANCM), and those that do not have either of these

activities, but are binding partners of proteins with these activities (ERCC1, EME1 and 2, and FAAP24). Together, they form three endonucleases and one translocase (Figure 1-3).

The EME1-MUS81 and EME2-MUS81 endonucleases show specificity for flap structures and replication forks (Bastin-Shanower *et al.*, 2003; Ciccia *et al.*, 2003; Ciccia *et al.*, 2007). Their yeast counterparts can also process recombination intermediates, such as D-loops and nicked Holliday junctions (Gaillard *et al.*, 2003; Osman *et al.*, 2003). Physiologically, the yeast homologs of EME1-MUS81 play a role in meiotic recombination in generating crossover products. This role is more pronounced in *S. pombe* (Osman *et al.*, 2003; Smith *et al.*, 2003) than in *S. cerevisiae* (de los Santos et al., 2003; de los Santos et al., 2001), indicating the presence of other redundant pathways. MUS81 deficiency in humans leads to decreased mitotic recombination (Blais *et al.*, 2004). The major role of EME1-MUS81 is the resolution of stalled replication forks. It is required for formation of a double strand-break (DSB) when a replication fork is stalled by an ICL (Hanada *et al.*, 2006). Similarly, yeast homologs are required for repair of stalled forks produced by various DNA damaging agents such as camptothecin, methylmethanesulfonate, UV irradiation and Hydroxyurea (Bastin-Shanower *et al.*, 2003; Boddy *et al.*, 2000; Doe *et al.*, 2002).

The most recently discovered members of the XPF family are FANCM and FAAP24 (Ciccia *et al.*, 2007; Meetei *et al.*, 2005). These proteins heterodimerize to form a translocase that has an affinity for splayed arm substrates (Ciccia *et al.*, 2007). It lacks helicase or nuclease activity and may be involved in loading of the FA core complex on to the chromatin during ICL repair (Kim *et al.*, 2008a).

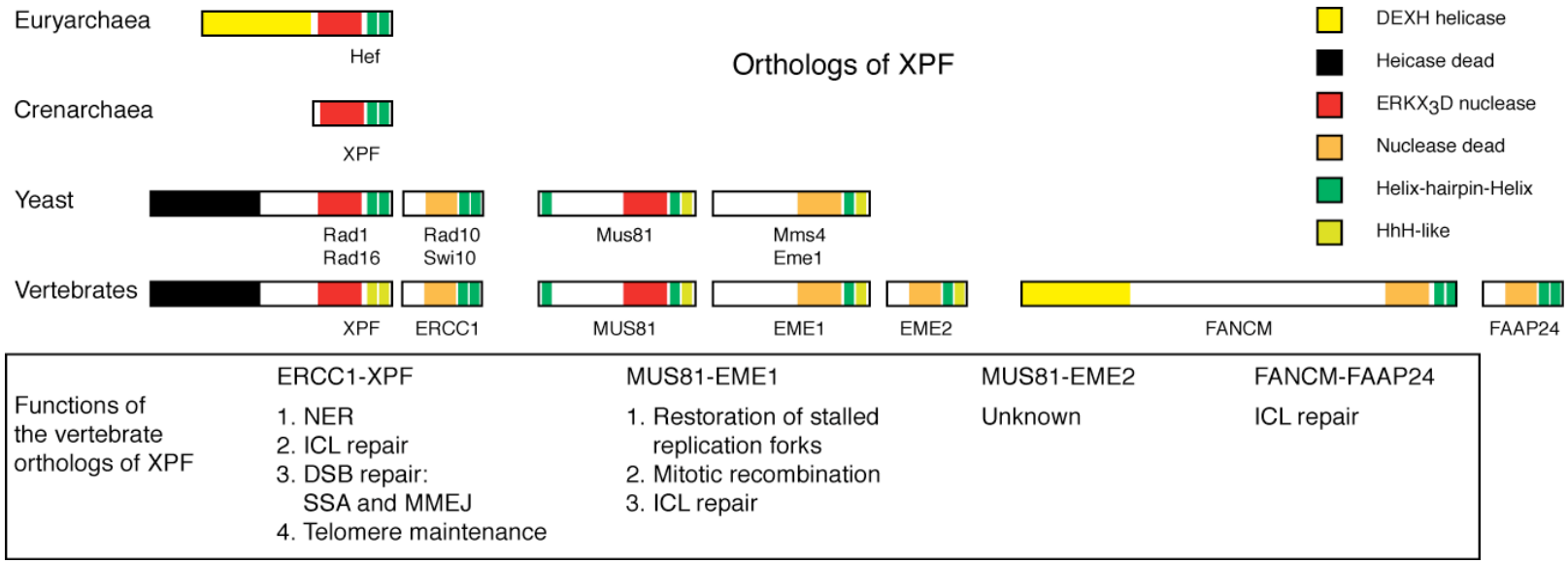

Figure 1-3: Orthologs of XPF

Orthologs of XPF: members of the XPF family in archaea, yeast and vertebrates. Archaea have only one member of the family (Hef/XPF). Yeasts *S. cerevisiae* and *S. pombe* have 4 members, the homologs of ERCC1 (Rad10/Swi10) and XPF (Rad1/Rad16) and homologs of MUS81 (Mus81) and EME1 (Mms4/Eme1). Vertebrates possess three additional members, EME2, which dimerizes with MUS81 to form the EME2-MUS81 endonuclease, and FANCM and FAAP24, which participate in the Fanconi anemia pathway. Heterodimers formed by these proteins and their functions in vertebrates are listed in the box.

1.3 BIOLOGICAL FUNCTIONS OF ERCC1-XPF AND ITS HOMOLOGS

1.3.1 Nucleotide excision repair

NER is a DNA repair pathway that repairs a wide variety of helix-distorting lesions affecting one strand of DNA. It is a complex pathway involving as many as 30 proteins that perform a highly coordinated excision of the damage as a single-stranded oligonucleotide leading to the formation of a gap, which is subsequently filled in by replicative polymerases (de Laat *et al.*, 1999; Gillet and Scharer, 2006).

The role of ERCC1-XPF homologs in NER was first identified in *S. cerevisiae*. *RAD1* and *RAD10* mutants were found to be hypersensitive to UV irradiation and defective in the incision step of NER (Reynolds *et al.*, 1981; Wilcox and Prakash, 1981). Studies of the *S. cerevisiae* Rad10-Rad1 showed that it was only functional as an endonuclease when it was a heterodimer (Davies *et al.*, 1995). It showed specificity for substrates with junctions of ssDNA (ssDNA) and double-stranded DNA (dsDNA) with 3' single-stranded overhangs; releasing the 3' overhangs (Bardwell *et al.*, 1994; Davies *et al.*, 1995). Similarly, ERCC1 and XPF were discovered from their roles in NER and the ability of these proteins to restore UV resistance to NER-deficient CHO cell lines (Brookman *et al.*, 1996; van Duin *et al.*, 1986). Subsequently, ERCC1-XPF was shown to possess structural specificity similar to Rad10-Rad1 in incising junctions of single- and double-stranded DNA (de Laat *et al.*, 1998a; Sijbers *et al.*, 1996a).

NER consists of two pathways, global genome NER (GG-NER) and transcription-coupled NER (TC-NER) that feed into a common nucleotide excision repair pathway (Hanawalt,

2002). As the name suggests, GG-NER deals with DNA damage throughout the genome, whereas TC-NER allows the cell to preferentially repair the transcribed strand of genes (Bohr *et al.*, 1985; Mellon and Hanawalt, 1989; Mellon *et al.*, 1987). GG-NER is initiated by the XPC/hHR23B, which detects helix distortion (Araki *et al.*, 2001; Sugasawa *et al.*, 1998; Volker *et al.*, 2001), while TC-NER is initiated when transcription by RNA polII is blocked a DNA lesion (Leadon and Lawrence, 1991; Venema *et al.*, 1992). Recognition of damage by either initiates a sequential recruitment and assembly of the downstream proteins (Houtsmuller *et al.*, 1999; Volker *et al.*, 2001). TFIIH, a basal transcription factor is recruited to the site of damage. XPG, a structure specific endonuclease, is present in stable association with TFIIH and is required for its role in NER as well as transcription (Ito *et al.*, 2007). DNA strands are separated into a bubble intermediate by the helicase activity of the TFIIH-component helicases, XPB (Schaeffer *et al.*, 1993) and XPD (Schaeffer *et al.*, 1994). This is followed by the recruitment of XPA and RPA (Tapias *et al.*, 2004; Wakasugi and Sancar, 1998). In TC-NER, CSA (Henning *et al.*, 1995), CSB (Troelstra *et al.*, 1992) and XAB2 (Nakatsu *et al.*, 2000) are also required in addition to TFIIH. XPA then recruits ERCC1-XPF through its interaction with ERCC1 (Li *et al.*, 1994; Li *et al.*, 1995; Park and Sancar, 1994; Saijo *et al.*, 1996). Recruitment of ERCC1-XPF allows the release of TFIIH from the bubble (Riedl *et al.*, 2003). The 5'-end of the repair bubble produced by the NER machinery is an ideal substrate for incision by ERCC1-XPF (Bardwell *et al.*, 1994; de Laat *et al.*, 1998a; Sijbers *et al.*, 1996a). The physical presence of XPG, although not its nuclease activity, is required for the 5' incision by ERCC1-XPF (Mu *et al.*, 1997; Wakasugi *et al.*, 1997). On the other hand, the nuclease activity of ERCC1-XPF is required for efficient strand cleavage by XPG and the 5' incision by ERCC1-XPF precedes the 3' incision by XPG (Staresincic *et al.*, 2009). Following the incision, recruitment of RF-C releases ERCC1-

XPF from the DNA (Mocquet *et al.*, 2008). PCNA, RPA, RF-C and pol δ/ε (Shivji *et al.*, 1995) assemble to release XPG (Mocquet *et al.*, 2008) and fill in the gap, and ligase I (Shivji *et al.*, 1995) or ligase III/XRCC1 seal the nick (Moser *et al.*, 2007).

1.3.2 Interstrand crosslink repair

ICLs are formed when a bifunctional alkylating agent covalently binds a base on each strand of duplex DNA, thereby preventing strand separation necessary for replication or transcription (McHugh *et al.*, 2001). In S-phase cells ICLs are converted into DSBs. This makes crosslinks extremely cytotoxic. The ICL repair mechanism in mammals remains poorly defined. Proteins from multiple DNA damage repair and tolerance pathways appear to be involved in ICL repair. Data from genetic analysis and crosslink hypersensitivity of mutant cells and organisms shows the involvement of ERCC1-XPF (Collins, 1993), HR proteins such as XRCC2 and XRCC3 (De Silva *et al.*, 2000; Liu *et al.*, 1998), MutS β (Zhang *et al.*, 2002), RPA, PCNA (Li *et al.*, 2000; Zhang *et al.*, 2003), PSO4 complex (PSO4/PRP19, CDC5L, PLRG1, SPF27) (Zhang *et al.*, 2005), WRN (Zhang *et al.*, 2005), BRCA2 (Yu *et al.*, 2000), EME1-MUS81 (Abraham *et al.*, 2003; McPherson *et al.*, 2004), SNM1a and SNM1b (Bae *et al.*, 2008; Dronkert *et al.*, 2000; Hazrati *et al.*, 2008; Ishiai *et al.*, 2004) and the Fanconi anemia (FA) proteins (Auerbach and Wolman, 1976; Fujiwara and Tatsumi, 1977; Sasaki and Tonomura, 1973; Thompson and Hinz, 2009).

When the replication machinery encounters a crosslink, because the two strands of DNA cannot be separated, it cannot move past the damage, and the replication fork is therefore blocked. This activates ATR (Stiff *et al.*, 2006), which along with its downstream target CHK1 phosphorylates multiple proteins, which include the FA proteins FANCA, FANCG, FANCE,

FANCD2, FANCI and FANCM (Andreassen *et al.*, 2004; Collins *et al.*, 2009; Matsuoka *et al.*, 2007; Meetei *et al.*, 2005; Pichierri and Rosselli, 2004; Qiao *et al.*, 2004; Smogorzewska *et al.*, 2007; Wang *et al.*, 2007; Yamashita *et al.*, 1998), and H2AX (Ward and Chen, 2001) and NBS1 (Pichierri and Rosselli, 2004). These phosphorylations activate the FA pathway leading to monoubiquitination of FANCD2 and FANCI – the ID complex – that act as a signal for cell cycle checkpoints and DNA repair (Meetei *et al.*, 2003; Smogorzewska *et al.*, 2007). This step is not dependent on ERCC1-XPF, and FANCD2 monoubiquitination appears to be normal although persistent in ERCC1-XPF deficient cells (Bhagwat *et al.*, 2009a). To repair a crosslink it must be removed from both strands of DNA, one at a time, and therefore poses a considerable challenge to cells. Initial incision is probably made by the ERCC1-XPF ortholog EME1-MUS81, producing a DSB (Hanada *et al.*, 2007; Hanada *et al.*, 2006). ICL-induced DSBs can occur even in the absence of ERCC1-XPF (Niedernhofer *et al.*, 2004). However, ERCC1-XPF is required for the resolution of these breaks. It makes the incision on the other side of the crosslink, thereby releasing it from one strand, a process known as "unhooking" (De Silva *et al.*, 2000; Kuraoka *et al.*, 2000; Niedernhofer *et al.*, 2004). This function of ERCC1-XPF is necessary for the efficient binding of FANCD2 to the chromatin (Bhagwat *et al.*, 2009a; McCabe *et al.*, 2008). Once the ICL is unhooked, a translesion polymerase, such as polζ could fill the gap in an error prone fashion (Raschle *et al.*, 2008). The FA proteins then coordinate the repair of the replication fork through recruitment of the homologous recombination repair (HRR) (Thompson and Hinz, 2009).

The ICL repair mechanism in *S. cerevisiae* is well studied and appears to be different from its mammalian counterpart. In this case, unlike ERCC1-XPF in mammals, Rad10-Rad1 seems to be involved in ICL repair as a part of the NER machinery. In yeast, ICL repair is

performed by a combination of NER, HRR (Jachymczyk *et al.*, 1981), PSO2/SNM1 (Henriques and Moustacchi, 1980; Henriques *et al.*, 1989; Ruhland *et al.*, 1981), base excision repair (McHugh *et al.*, 1999), mismatch repair (Durant *et al.*, 1999) and translesion synthesis (Sarkar *et al.*, 2006).

1.3.3 Double strand break repair

HRR is a mechanism for repair of DSBs utilizing a homologous DNA sequence. The role of ERCC1-XPF in DSB repair was first described in the yeast homolog, Rad10-Rad1. Rad10-Rad1 was initially described to function in a subtype of HRR, independent of Rad52 (Schiestl and Prakash, 1988, 1990) and involves the formation of intrachromosomal heteroduplex intermediates between regions containing repeat sequences (Klein, 1988). During the process of HRR, the template strand and the invading strand must be completely homologous for the stability of the intermediate and for the repair to proceed. Rad10-Rad1 in complex with Msh2 and Msh3 is required to process 3' ends that have more than 30 overhanging nucleotides (Paques and Haber, 1997). This mechanism of recombination is responsible for gene conversion.

Similarly, Rad10-Rad1 functions in the error prone DSB repair subtypes: single strand annealing (SSA) and microhomology mediated end joining (MMEJ), which can repair DSBs in regions of DNA containing sequence repeats. After exonuclease-processing of ends, 3' overhangs are formed on both sides, which may contain non-homologous sequences. Rad10-Rad1 can prune the ends to remove nonhomologous sequences and allow repair to occur (Fishman-Lobell and Haber, 1992; Ivanov and Haber, 1995). SSA is independent of Msh2 and Msh3 for regions of homology >1kb (Sugawara *et al.*, 1997), but is dependent on Rad52 (Mortensen *et al.*, 1996).

ERCC1-XPF was found to interact with RAD52 and enhance the ability of the nuclease in incising 3' flaps (Motycka *et al.*, 2004). It was later discovered that ERCC1-XPF has a role in SSA and in gene conversions similar to yeast (Al-Minawi *et al.*, 2008). Also, *Ercc1* mutant CHO cells are deficient in processing heteroduplex intermediates of the recombination between repeat sequences (Sargent *et al.*, 2000; Sargent *et al.*, 1997). ERCC1-XPF is required to remove 3' tails that are formed in these intermediates and failure to remove these, leads to deletions at the sites of recombination. Irrespective of the sequence homology status, ERCC1-XPF is required for integration of exogenous DNA into the genome, for example, the targeted gene replacement in mouse ES cells (Niedernhofer *et al.*, 2001).

MMEJ is independent of Rad52 and Ku86, but requires Mre11-Rad50-Xrs2 (the MRX complex) (Haber, 2006), Msh2, Pms1 (Decottignies, 2007), Nej1, multiple DNA polymerases including Pol4, Rad30, Rev3, and Pol32, the flap endonuclease Sae2, and Tel1 (Lee and Lee, 2007). In mammals, the existence of the MMEJ pathway is evident from persistent end joining repair in non-homologous end joining (NHEJ) deficient cells (Kabotyanski *et al.*, 1998). *Ercc1*$^{-/-}$ *Ku86*$^{-/-}$ mice are not viable and the double knockout MEFs are more sensitive to radiation than the single mutants. However, *Ercc1-/-* mouse ES cells are not hypersensitive to radiation, suggesting that this is not a defect of HRR. Linearized plasmid DNA with microhomologies on both ends, which are substrates for MMEJ, shows large deletions after repair in *Ercc1* mutant CHO cells. Overall, these data suggest that ERCC1-XPF functions in a Ku-independent error prone pathway of end joining (Ahmad *et al.*, 2008).

In *S. pombe*, individual cells undergo spontaneous mating-type switch during growth. This involves formation of a DSB at a switching signal locus followed by recombination-mediated repair. Strains *rad16 (swi9)* and *swi10* have a defect in the mating-type switching

recombination mechanism (Carr *et al.*, 1994; Schmidt *et al.*, 1989). Additionally, they are also sensitive to ionizing radiation (Schmidt *et al.*, 1989). In *A. thaliana*, deficiency of AtERCC1 led to radiation sensitivity, indicating a role in DSB repair (Hefner *et al.*, 2003). In Drosophila, mutation of *mei-9* also leads to radiation sensitivity (Baker *et al.*, 1978). Thus, ERCC1-XPF and its homologs function in multiple subtypes of DSB repair.

1.3.4 Meiotic recombination

Meiosis is accompanied by crossover events between homologous chromosomes, allowing for segregation of polymorphisms. This crossover is brought about by meiotic recombination, a mechanism akin to the HRR mechanism, but between homologous chromosomes with divergent sequences, instead of sister chromatids that are identical at the sequence level. *Drosophila mei-9* mutants are defective in meiotic crossover. They display a marked decrease in crossovers and an increase in chromosome non-disjunctions (Carpenter and Baker, 1982; Yildiz *et al.*, 2004). There is also an increase in postmeiotic segregation, indicating a failure to repair heteroduplex DNA formed during noncrossover recombination events (Yildiz *et al.*, 2004). These findings suggest that MEI-9 is required for the resolution of Holliday junctions (HJ) formed during meiosis. MEI-9 interacts with MUS312, and disruption of MUS312-MEI-9 interaction produces a phenotype similar to the loss of either MUS312 or MEI-9 (Yildiz *et al.*, 2002). Recent evidence suggests that HDM, a single-stranded-DNA binding protein forms a complex with MUS312, MEI-9 and ERCC1 that resolves the HJs (Joyce *et al.*, 2009). Interestingly, the human ortholog of MUS312, BTBD12 (SLX4) binds multiple different endonucleases including ERCC1-XPF (Fekairi *et al.*, 2009; Svendsen *et al.*, 2009).

Mice have elevated *Xpf* and *Ercc1* mRNA levels in the meiotic and early postmeiotic cells involved in spermatogenesis (Shannon *et al.*, 1999). Both male and female *Ercc1*-mutant mice are infertile. ERCC1-XPF is important at all stages of development and maturation of both male and female gametes, but there is no evidence that it is required for meiotic crossovers (Hsia *et al.*, 2003).

1.3.5 Telomere maintenance

Telomeres have 3' overhangs with G-rich repeat sequences. This is an ideal substrate for cleavage by ERCC1-XPF. ERCC1-XPF was found to be associated with the telomeric TRF2 complex, and prevents recombination of telomeric DNA with interstitial telomere-like repeats. The absence of ERCC1-XPF produces telomeric DNA-containing double minute (TDM) chromosomes. On the other hand, in the absence of TRF2, ERCC1-XPF cleaves the 3' overhangs allowing telomeres to be subjected to NHEJ. This leads to telomere fusions and dicentric chromosomes (Zhu *et al.*, 2003). In essence, ERCC1-XPF and TRF2 seem to be acting antagonistically, preventing each other from damaging the telomere. Strangely, TRF2-dependent loss of telomeres, caused by TRF2 overexpression is dependent on ERCC1-XPF (Munoz *et al.*, 2005). What is even more perplexing is that this action requires the physical presence of ERCC1-XPF, but not its nuclease activity (Wu *et al.*, 2007). Also, overexpression of wild-type but not nuclease-dead XPF reduces the telomere binding of TRF2. Apparently, ERCC1-XPF acts on the telomere through two distinct mechanisms, a nuclease-dependent mechanism that affects TRF2 binding, and a nuclease-independent mechanism that limits telomere length (Wu *et al.*, 2008). ERCC1-XPF interacts with TRF1 in a very similar way and contributes to telomere shortening and end-fusions in the absence of TRF1 (Munoz *et al.*, 2009). A similar mechanism exists in *A.*

thaliana, where ERCC1-XPF prevents recombination of telomeres with interstitial telomeric repeats (Vannier *et al.*, 2009).

1.3.6 Repair of TopI lesions

Progression of replication forks along DNA creates superhelical strain on the unreplicated duplex. Topoisomerase I releases this supercoiling by transiently cutting one strand of the duplex and forming a protein-DNA complex with that strand, allowing it to unwind in an ATP dependent mechanism (Champoux, 2001). When a replication fork collides with a Top1-DNA intermediate, it is blocked, leading to a DSB (Hsiang *et al.*, 1989). Top1 poisons such as camptothecin cause the Top1 protein to remain attached to the 3' end of the unreplicated DNA rendering it inaccessible to repair. Tdp1 removes the Top1 molecule and creates a 3' phosphate (Pouliot *et al.*, 1999). In *S. cerevisiae* this substrate is further processed by the activities of Tpp1, Apn1 and Apn2 to convert it from a repair-blocking lesion to a 3' hydroxyl group amenable to repair (Vance and Wilson, 2001). Although the yeast *RAD1* and *RAD10* mutants are not sensitive to Top1 poisons such as camptothecin, Rad10-Rad1 was found to function in a backup pathway for repair of Top1 lesions (Liu *et al.*, 2002; Vance and Wilson, 2002). In the absence of Tdp1, Rad10-Rad1 likely incises a 3' single stranded flap, removing an oligonucleotide containing the Top1-DNA intermediate and allowing for a Rad52-dependent homologous recombination to repair the fork (Vance and Wilson, 2002).

1.3.7 Repair of abasic sites

Apurinic/apyrimidinic (AP) sites are produced as a result of depurination or depyrimidination of DNA due to spontaneous hydrolysis of the bond between the base and the DNA backbone. In a mammalian cell, over a span of 24 hours approximately 10,000 purines (Lindahl, 1979) and about 500 pyrimidines (Lindahl and Karlstrom, 1973) are lost by this process. AP sites are also produced by DNA glycosylases as intermediates of base excision repair (BER) (Duncan *et al.*, 1976; Lindahl, 1976). In *S. cerevisiae* removal of misincorporated uracil by uracil DNA glycosylase appears to be the major endogenous contributor towards AP sites (Guillet and Boiteux, 2003). *S. cerevisiae* mutants defective in both yeast AP endonucleases are viable, but triple mutants *apn1 apn2 rad1* and *apn1 apn2 rad10* are not viable, suggesting that Rad10-Rad1 functions in a backup pathway of AP site repair (Guillet and Boiteux, 2002). Although NER plays a role in removal of AP sites (Swanson *et al.*, 1999; Torres-Ramos *et al.*, 2000) this mechanism seems to be independent of NER, as evident from the viability of *apn1 apn2 rad14* strains (Guillet and Boiteux, 2002). In this case, the genetic evidence suggests that similar to the Top1 lesion repair, Rad10-Rad1 works by removing the 3' flap resulting from the spontaneous hydrolysis of the abasic site (Boiteux and Guillet, 2004).

1.4 PHYSIOLOGICAL FUNCTIONS OF ERCC1-XPF

1.4.1 Human diseases associated with defects in ERCC1-XPF

The severity and manifestation of ERCC1-XPF deficiency in humans varies significantly. Interpretation of the phenotype is complicated by the involvement of ERCC1-XPF in multiple genome maintenance mechanisms.

1.4.1.1 Xeroderma pigmentosum

Xeroderma pigmentosum (XP) was the first hereditary condition to be associated with defect in a DNA repair pathway. It is an autosomal recessive syndrome characterized by sun sensitivity with a 2000-fold increase in skin cancers over sun-exposed areas, which include basal cell carcinoma, squamous cell carcinoma, malignant melanoma, keratoacanthoma, fibrosarcoma, and angioma (Kraemer *et al.*, 1987). There is also evidence for increased incidence of sarcomas. Patients with mutations affecting both global and transcription-coupled NER present with progressive neurodegeneration, probably due to accumulation of damage in transcribed genes (Brooks, 2008). The severity and age of presentation varies widely amongst patients, depending on the mutation and the protein affected. XP has eight complementation groups from XP-A through G and the variant form, XP-V. XP-F was first reported in Japan and usually presents with a mild phenotype with late onset of disease (Matsumura *et al.*, 1998), although in some cases a late onset neurodegenerative phenotype is seen. Mutant XPF protein may fail to localize to the nucleus, leading to mislocalization of both ERCC1 and XPF to the cytoplasm. This produces a phenotype disproportionate to the ability of these mutants to reconstitute NER *in vitro* (Ahmad *et al*, submitted manuscript). There is no known *ERCC1* mutation that presents as XP.

1.4.1.2 XFE progeroid syndrome

Most patients with *XPF* mutations have a mild XP phenotype. However, a patient with XPF R153P mutation presented with a progeroid phenotype in addition to sun sensitivity (Niedernhofer *et al.*, 2006). Arginine-153 lies in the helicase-like domain of XPF and is highly conserved. To date this remains the only published case of the XFE (XPF-ERCC1) progeroid syndrome. Remarkably, despite photosensitivity and abnormal skin pigmentation, there was no evidence of skin cancer. There was evidence of growth retardation, including short stature, microcephaly and developmental delay. Further investigations showed an array of aging-related degenerative changes. Although the patient had a normal birth-weight, he was cachexic at presentation. His skin was dry and atrophic, and lacked subcutaneous fat. He had bird-like facies with prominent bones and an aged appearance. Neurodegeneration was evident from cerebral atrophy, tremors and ataxia with loss of coordination, impaired hearing and vision loss with optic atrophy. Scoliosis, muscle wasting and hypotonia suggested musculoskeletal degeneration. In addition, there was hypertension, renal and hepatic insufficiency, and anemia, which distinguished this case from the DeSanctis-Cacchione and Cockayne syndromes. The patient died at the age of 16 years from multi-organ failure following pneumonia. These symptoms are remarkably similar to the presentation of the *Ercc1*$^{-/-}$ (Niedernhofer *et al.*, 2006) and the *Xpf*$^{m/m}$ (Tian *et al.*, 2004) mouse models which also show an accelerated aging phenotype.

Fibroblasts obtained from skin biopsy of the patient showed markedly decreased UV induced unscheduled DNA synthesis (UV-UDS) (~5% of wild-type). They were more sensitive to UV than XP-F patient fibroblasts, though less so than XP-A fibroblasts. They were exquisitely hypersensitive to the crosslinking agent MMC, indicating that a deficiency in ICL repair may have a significant contribution to this phenotype.

1.4.1.3 Cranio-occulo-facio-skeletal syndrome (COFS)

The only known patient of *ERCC1* mutation was born with low birth-weight, microcephaly with premature closure of the fontanels, bilateral microphthalmia, blepharophimosis, high nasal bridge, short filtrum, micrognathia, low-set and posterior-rotated ears, arthrogryposis with rocker-bottom feet, flexion contractures of the hands, and bilateral congenital hip dislocation. MRI showed a simplified gyral pattern and cerebellar hypoplasia. This was diagnosed as COFS. The classic COFS is defined by microcephaly, hypotonia, microphthalmia, cataracts, blepharophimosis, large ear pinnae, prominent root of the nose, micrognathia, wide set nipples, camptodactyly, flexure contractures at the elbows and knees, generalized osteoporosis, dysplastic acetabula, coxa valga, rocker-bottom feet and failure to thrive (Pena and Shokeir, 1974). Previously, COFS has been diagnosed in patients with mutations of either *CSB* (Meira *et al.*, 2000) or *XPD* (Graham *et al.*, 2001).

The cerebellar hypoplasia seen in this patient was also seen in *Ercc1*$^{-/-}$ mice at the age of 1 day. This was alleviated almost completely by the age of 4 days, suggesting that this was in fact a defect in neuronal migration. This is analogous to the *Xpa* and *Csb* double knockout mouse model, which shows a reduced cerebellar foliation and stunted Purkinje cell dendrites (Murai *et al.*, 2001). The child failed to thrive and did not pas any developmental milestones, dying at the age of 14 months (Jaspers *et al.*, 2007). The phenotype of growth retardation, neurological deficit and shortened lifespan matches with the phenotype of *Ercc1*$^{-/-}$ mice. Together, these observations show that ERCC1 is essential for human development and viability.

1.4.2 Mouse models of ERCC1-XPF deficiency

1.4.2.1 *Ercc1*$^{-/-}$ mouse

Two groups independently made *Ercc1*$^{-/-}$ mice (McWhir *et al.*, 1993; Weeda *et al.*, 1997). In the first case, *Ercc1* was targeted with a *neo* insert between exons 4 and 6 using an HPRT minigene based system (Selfridge *et al.*, 1992). In the second case, two mouse models were made, one with a *neo* insert in exon 7 (*Ercc1*-knockout mouse) and the other with a stop codon at position 292 of ERCC1, producing a truncated version of the transcript (*Ercc1*^{*292} or *Ercc1*$^{7\Delta}$ allele, discussed further under *Ercc1* hypomorphs). The *Ercc1*-knockout mice are born at sub-Mendelian ratios due to an early embryonic lethality. All mutant mice are runted at birth and display shortened lifespan of about 3 - 4 weeks. The mutant mice show abnormalities of liver, with large polyploid nuclei. Mice die of hepatic failure and show increased p53 in liver, kidneys and brain (McWhir *et al.*, 1993). The primary MEFs isolated from these mice grow slower than their wild-type counterparts (Niedernhofer *et al.*, 2006; Weeda *et al.*, 1997). These MEFs and mouse livers have elevated p21 levels, suggesting that they are undergoing senescent changes (Nunez *et al.*, 2000; Weeda *et al.*, 1997). Also, as noted before, the *Ercc1*$^{-/-}$ mice have delayed cerebellar development (Jaspers *et al.*, 2007). This phenotype is dramatically different from that of *Xpa*$^{-/-}$ mice, which are phenotypically nearly indistinguishable from the wild-type littermates (de Vries *et al.*, 1995). *Ercc1*$^{-/-}$ mice have reduced hematopoietic reserve and demonstrate a multilineage cytopenia with reduction in stress induced erythropoiesis and fatty replacement of the bone marrow (Prasher *et al.*, 2005). This resembles Fanconi anemia, a disease characterized by hypersensitivity to ICL repair (Parmar *et al.*, 2009). This suggests that at least a part of the phenotype of *Ercc1*$^{-/-}$ mice is due to a deficiency in ICL repair. Additionally, these mice show neurodegenerative changes including dystonia and ataxia, musculoskeletal degeneration evident

from sarcopenia and kyphosis and renal failure. Combined with the cellular senescence these findings suggest accelerated aging and led to the identification of anew humn progeria cased by the reduced expression of ERCC1-XPF (Niedernhofer *et al.*, 2006).

1.4.2.2 *Xpf*$^{m/m}$ mouse

Mouse *Xpf* was mutated with a *neo* insert between exons 7 and 8 and a stop codon at position 445 (Tian *et al.*, 2004). In keeping with the obligate heterodimeric nature of ERCC1 and XPF, the mouse is a phenocopy of the *Ercc1*$^{-/-}$ mouse. The mice are runted, with enlarged and polyploid hepatocytes and die within 3 weeks of birth. Further analysis was not done.

1.4.2.3 *Ercc1* hypomorphs

The *Ercc1*$^{\Delta/\Delta}$ mice were generated by inserting a stop codon at position 292 of *Ercc1* (Weeda *et al.*, 1997). This resulted in a truncated transcript and presumably a protein that is seven amino acids short at the C-terminus. The C-terminus of ERCC1 is indispensible for its function (Sijbers *et al.*, 1996b) and so the truncation should significantly affect the function of ERCC1-XPF. In fact, the transcript from the Δ allele is reduced to about 15% of the wild-type allele (Weeda *et al.*, 1997). The *Ercc1*$^{\Delta/\Delta}$ mice live for about 6 months from birth, a lifespan intermediate between the *Ercc1*$^{-/-}$ and wild-type mice. Aside from liver changes reminiscent of the knockout mice, they also display ferritin deposition in the spleens, thin skin lacking subcutaneous fat and renal tubular dilatation with abnormal nuclei and proteinuria indicative of renal insufficiency. Unlike the *Ercc1*$^{-/-}$ mice, TUNEL assay shows no evidence of increased apoptosis in tissues. The mice are infertile, but histologically both ovaries and testes appear normal. *Ercc1*$^{-/\Delta}$ mice with LacZ transgene were analyzed by recovery of LacZ containing plasmid and isolating clones lacking LacZ expression. LacZ mutants were further analyzed to determine the type of mutations leading

to inactivation of the gene. This LacZ mutation analysis shows a rapid accumulation of mutations in the livers of these animals. Mutations included point mutations similar to the NER deficient *Xpa*$^{-/-}$ mice and deletions and translocations, probably stemming from the loss of ICL repair and DSB repair related functions of ERCC1-XPF (Dolle *et al.*, 2006).

1.4.2.4 *Ercc1* conditional mutants

In order to correct the hepatic failure of *Ercc1*$^{-/-}$ mice, transgenic *Ercc1* was expressed with a liver specific transthyretin promoter (Selfridge *et al.*, 2001). This prevented the polyploidy of hepatocytes and liver failure, and increased lifespan up to 61 – 88 days, but the mice died of renal failure with a similar polyploid phenotype in the proximal tubule cells. These mice also had elevated plasma lactate levels, pointing towards possible mitochondrial consequences of ERCC1 deficiency. Neurodegeneration was evident from lack of coordination, ataxia and loss of visual acuity, but no histological changes in the brain were detected (Lawrence *et al.*, 2008).

Ercc1$^{-/-}$ mice have an extremely short lifespan, making it difficult to study the UV sensitivity of their skin. To overcome this problem, mice were made with a floxed *Ercc1* allele under bovine *K5* promoter. These mice showed 20-fold increase in sensitivity to the short-term erythematous changes in epidermis with UV-B irradiation. They also displayed a rapid onset of tumors, mainly squamous cell carcinomas, which grew faster than those in wild-type animals (Doig *et al.*, 2006).

1.4.3 Altered expression of ERCC1-XPF in cancers

ERCC1-XPF functions in major genome maintenance pathways including NER (Sijbers *et al.*, 1996a), ICL repair (De Silva *et al.*, 2000), DSB repair (Murray *et al.*, 1996; Murray and

Rosenberg, 1996) and telomere maintenance (Wu *et al.*, 2008; Zhu *et al.*, 2003). Various chemotherapeutic agents and radiotherapy kill cancer cells by damaging their DNA. If ERCC1-XPF expression is variable in cancers, it may have a bearing on the growth characteristics of tumors, their response to various therapies and patient survival. This promise has led to extensive attempts at devising strategies to evaluate the effect of both ERCC1 and XPF, but mainly ERCC1, on tumor biology. These include studies of short nucleotide polymorphisms (SNP), mRNA levels, and Immunohistochemistry for protein levels.

1.4.3.1 SNPs

SNPs may affect protein expression or function based on their nature and location. A non-conservative base substitution may change amino acid sequence, thereby directly affecting protein function. A conservative substitution may alter rate of mRNA translation by altering the choice of tRNA or effect on protein folding due to slow translation. Polymorphisms near promoters or introns can affect protein expression through transcription. There is however no direct evidence that polymorphisms of *ERCC1* or *XPF* can affect protein levels. A survey of polymorphisms in NER genes found that *ERCC1* contains at least seven SNPs that do not alter amino acid sequence; *XPF* has six. *ERCC1* contains no SNPs with amino acid substitutions, while *XPF* has one that leads to P379S substitution (Shen *et al.*, 1998). A commonly studied silent polymorphism of ERCC1, codon 118(C/T) changes a commonly used codon AAC to AAT, one that is used infrequently. This can potentially reduce the translation of the mRNA leading to reduced protein levels (Yu *et al.*, 1997). Once again, there is no evidence of a difference in protein or mRNA levels caused by this SNP. Despite this, *ERCC1* SNPs have shown correlation with outcomes of many different types of tumors. Of these, non-small cell lung carcinoma (NSCLC) has been the most extensively studied. Numerous studies have found

correlation between risk, survival and treatment response in NSCLC with either or both of codon 118 and C8092A polymorphisms of *ERCC1* (Isla *et al.*, 2004; Kalikaki *et al.*, 2009; Park *et al.*, 2006; Su *et al.*, 2007; Takenaka *et al.*, 2009; Zienolddiny *et al.*, 2006). On the other hand, a large meta-analysis of multiple studies failed to find any correlation (Kiyohara and Yoshimasu, 2007). Several other cancers, including esophageal cancer (Doecke *et al.*, 2008; Pan *et al.*, 2009), ovarian cancer (Steffensen *et al.*, 2008), squamous cell carcinoma of head and neck (Quintela-Fandino *et al.*, 2006), basal cell carcinoma (Yin *et al.*, 2003) and bladder cancer (Garcia-Closas *et al.*, 2006) have shown correlation of outcome or chemotherapy resistance to *ERCC1* genotypes. However, studies involving pancreatic adenocarcinoma (McWilliams *et al.*, 2008), carcinoma of prostate (Hooker *et al.*, 2008), colorectal carcinoma (Hansen *et al.*, 2008; Monzo *et al.*, 2007), glioma (Chen *et al.*, 2007), renal cell carcinoma (Hirata *et al.*, 2006) and cervical carcinoma (Chung *et al.*, 2006) did not find any link to *ERCC1* SNPs.

1.4.3.2 mRNA

Interest in *ERCC1* mRNA levels stemmed from the thought that these may be representative of the functional ERCC1 in cells. There is no evidence to suggest that ERCC1 is regulated at the level of transcription. In fact, mRNA levels of *ERCC1* and *XPF* have absolutely no correlation to their respective protein levels (Niedernhofer *et al.*, unpublished data). All the same, multiple studies have suggested a correlation between the level of *ERCC1* mRNA in tumors or tumor cell lines from gastric, ovarian, colorectal, esophageal and non-small cell lung cancer and resistance to cisplatin (Altaha *et al.*, 2004; Dabholkar *et al.*, 1992; Dabholkar *et al.*, 1994; Joshi *et al.*, 2005; Langer *et al.*, 2005; Lord *et al.*, 2002; Metzger *et al.*, 1998; Reed *et al.*, 2000; Rosell *et al.*, 2002; Shirota *et al.*, 2001; Warnecke-Eberz *et al.*, 2004). Similar to SNPs, mRNA levels of *ERCC1* are the most extensively studied in NSCLC. Based on findings that patients with low

ERCC1 expression in tumors respond better to cisplatin-based therapy (Lord *et al.*, 2002), a clinical trial was carried out. Patients who received tailored chemotherapy based on the *ERCC1* expression performed better than those who received a standard control therapy with docetaxel and cisplatin (Cobo *et al.*, 2007). Patients with low *ERCC1* levels performed somewhat better than those with high *ERCC1* levels.

1.4.3.3 Protein levels in tumors

Measurement of ERCC1 levels by IHC of paraffin-embedded tumor samples is an attractive biomarker to study the effect of ERCC1 levels on tumor response to various chemotherapeutic agents and patient survival. This is due to the relative ease of availability of samples, relative stability of proteins over RNA and advantage of processing large sets of samples economically over a short period of time. NSCLC remains the most studied tumor type (Hwang *et al.*, 2008; Lee *et al.*, 2008; Olaussen *et al.*, 2006; Zheng *et al.*, 2007). However, there are mixed results as to whether ERCC1 levels are predictive of resistance depending on the type of therapy administered. High ERCC1 expression correlated with poor response to cisplatin chemotherapy and poor survival outcome (Olaussen *et al.*, 2006). On the other hand high ERCC1 was associated with better survival following surgery (Lee *et al.*, 2008; Zheng *et al.*, 2007). Unfortunately, the antibody (8F1) used in almost all studies is not specific for ERCC1 (Niedernhofer *et al.*, 2007). It recognizes human ERCC1, but also a second unknown nuclear antigen, and is unable to discriminate between cells expressing ERCC1-XPF and cells that do not (Niedernhofer *et al.*, 2007). We rigorously tested antibodies against ERCC1 and XPF and found ones that are best suited for clinical measurement of ERCC1-XPF (Bhagwat *et al.*, 2009b). Our results show that ERCC1 and XPF levels in lung tumors vary considerably between tumors, but are closely correlated to each other and either of these proteins can be used as a surrogate

biomarker. More study however, remains to be performed to fully evaluate the utility of ERCC1 and XPF as cancer biomarkers.

2.0 XPF-ERCC1 PARTICIPATES IN THE FANCONI ANEMIA PATHWAY OF CROSSLINK REPAIR

This chapter was accepted for publication as a research article in Molecular and Cellular Biology:

Bhagwat, N., Olsen, A.L., Wang, A.T., Hanada, K., Stuckert, P., Kanaar, R., D'Andrea, A., Niedernhofer, L.J., and McHugh, P.J. (2009a). XPF-ERCC1 participates in the Fanconi anemia pathway of crosslink repair. Mol Cell Biol, MCB.00086-00009

Copyright © American Society for Microbiology, Molecular and Cellular Biology, doi: 10.1128/MCB.00086-09

2.1 INTRODUCTION

The XPF-ERCC1 heterodimer is a structure-specific endonuclease that incises double-strand DNA immediately adjacent to a 3'-single-stranded region, removing 3'-overhangs or opening bubbles (de Laat *et al.*, 1998a; Sijbers *et al.*, 1996a). ERCC1 is required for DNA binding (Tsodikov *et al.*, 2005) and XPF harbors the catalytic domain (Enzlin and Scharer, 2002). XPF-ERCC1 makes the incision 5' to the lesion during nucleotide excision repair (NER), the pathway responsible for removing helix-distorting DNA lesions (Sijbers *et al.*, 1996a). Defects in NER cause xeroderma pigmentosum (XP), a syndrome characterised by photosensitivity and

dramatically increased risk of skin cancers, due to failure to repair UV-photolesions. Cells from all XP complementation groups (XP-A to -G) and the recently reported ERCC1-deficient patient (Jaspers *et al.*, 2007) are hypersensitive to UV irradiation. However, cells deficient in XPF-ERCC1 differ from other XP cells in that they are also exquisitely sensitive to chemicals that induce DNA interstrand crosslinks (ICLs) (De Silva *et al.*, 2000; Hoy *et al.*, 1985; Niedernhofer *et al.*, 2006) ICLs are extremely cytotoxic lesions formed when bifunctional agents covalently link both strands of DNA, preventing strand separation, which is necessary for replication or transcription (McHugh *et al.*, 2001). Crosslinking agents such as nitrogen mustards (HN2) (Kohn *et al.*, 1966) and mitomycin C (MMC) (Iyer and Szybalski, 1963) produce a mixture of monoadducts and ICLs. However, cytotoxicity correlates with the number of ICLs formed, rather than monoadducts (O'Connor and Kohn, 1990; Palom *et al.*, 2002).

ICLs present a unique challenge to cells in that they affect both strands of DNA and therefore cannot be repaired by a simple excision and re-synthesis mechanism. The mechanism of ICL repair in *E. coli* is well characterized. It involves the NER complex UvrABC, the recombination repair machinery or DNA polymerase II-dependent translesion synthesis (Berardini *et al.*, 1999; Cheng *et al.*, 1991; Cole, 1973; Van Houten *et al.*, 1986). In *S. cerevisiae,* ICL repair requires both the NER and the homologous recombination (HR) machinery (Jachymczyk *et al.*, 1981). There is also evidence for the involvement of PSO2/SNM1 (Henriques and Moustacchi, 1980; Henriques *et al.*, 1989; Ruhland *et al.*, 1981), as well as base excision repair (McHugh *et al.*, 1999), mismatch repair (Durant *et al.*, 1999) and translesion polymerases (Sarkar *et al.*, 2006). ICL repair in mammalian cells, however, remains poorly understood. Genetic evidence implicates XPF-ERCC1 (Collins, 1993), HR proteins such as XRCC2 and XRCC3 (De Silva *et al.*, 2000; Liu *et al.*, 1998), MutS β (Zhang *et al.*, 2002), RPA,

PCNA (Li *et al.*, 2000; Zhang *et al.*, 2003), PSO4 complex (PSO4/PRP19, CDC5L, PLRG1, SPF27) (Zhang *et al.*, 2005), WRN (Zhang *et al.*, 2005) , BRCA2 (Yu *et al.*, 2000), MUS81-EME1 (Abraham *et al.*, 2003; McPherson *et al.*, 2004), SNM1a and SNM1b (Bae *et al.*, 2008; Dronkert *et al.*, 2000; Hazrati *et al.*, 2008; Ishiai *et al.*, 2004) and the Fanconi anemia proteins (Auerbach and Wolman, 1976; Fujiwara and Tatsumi, 1977; Sasaki and Tonomura, 1973; Thompson and Hinz, 2009). Of these, the Fanconi anemia family of proteins are unique in that they appear to be conserved only in higher eukaryotes (D'Andrea and Grompe, 2003; Joenje and Patel, 2001).

Fanconi anemia (FA) is a rare and clinically heterogeneous disease characterised by congenital skeletal abnormalities, growth retardation, bone marrow failure, aplastic anemia, genomic instability and susceptibility to cancer (D'Andrea and Grompe, 2003; Joenje and Patel, 2001). The patients have been grouped into 13 distinct complementation groups (FANC-A, -B, -C, -D1, -D2, -E, -F, -G, -I, -J, -L, -M, and -N) each representing deficiency of one protein in the Fanconi anaemia pathway. Of these, FANCA, B, C, E, F, G, L, M, and FAAP100 and FAAP24 - newly discovered components without complementation groups - form the FA core complex (Ciccia *et al.*, 2007; Garcia-Higuera *et al.*, 1999; Ling *et al.*, 2007; Medhurst *et al.*, 2001; Meetei *et al.*, 2003; Meetei *et al.*, 2004; Meetei *et al.*, 2005). FANCL is an E3 ubiquitin ligase that monoubiquitinates FANCD2 in response to genotoxic stress (Meetei *et al.*, 2003) during S phase of the cell cycle (Taniguchi *et al.*, 2002). FANCI – a newly discovered paralog of FANCD2, which is also monoubiquitinated – forms a chromatin bound complex with FANCD2. Monoubiquitination of both proteins is required for complex stability and ICL repair (Smogorzewska *et al.*, 2007). FANCD2 monoubiquitination is commonly used as a read-out to define which FA proteins act ‘upstream’ and therefore participate in damage signalling or

'downstream' and therefore are more likely to directly contribute to ICL repair. Monoubiquitinated FANCD2 co-localizes with proteins involved in HR including RAD51 and BRCA1 (Digweed *et al.*, 2002; Garcia-Higuera *et al.*, 2001; Taniguchi *et al.*, 2002). FANCD1 is identical to BRCA2 (Howlett *et al.*, 2002) and interacts with XRCC3 along with FANCG (Hussain *et al.*, 2006), as well as RAD51 (Marmorstein *et al.*, 1998). These data indicate a direct physical interaction between the FA proteins and the HR machinery (Wilson *et al.*, 2008).

The emerging model for the mechanism of ICL repair in mammals suggests that the FA pathway is activated in response to ICL damage in an ATR-dependent manner (Andreassen *et al.*, 2004; Pichierri and Rosselli, 2004). ATR is activated by blocked replication forks (Stiff *et al.*, 2006) and also phosphorylates numerous downstream effectors including FA proteins (Andreassen *et al.*, 2004; Meetei *et al.*, 2005; Pichierri and Rosselli, 2004) and H2AX (Ward and Chen, 2001). Before a replication fork that is blocked by an ICL can be restarted, the ICL must be completely unhooked from one strand of DNA, requiring two incisions 5' and 3' of the lesion and potentially producing a DSB at the fork. MUS81-EME1 is thought to be responsible for the first incision, creating a DSB (Hanada *et al.*, 2007; Hanada *et al.*, 2006). The second incision, or unhooking of the crosslink, has been proposed to be a key function of XPF-ERCC1 in ICL repair (Niedernhofer *et al.*, 2004). Once the ICL is completely unhooked from one strand, translesion synthesis can fill the gap, albeit in an error-prone fashion. The repaired strand can now act as a template for re-establishing the replication fork via HR (Niedernhofer *et al.*, 2005).

To further elucidate the mechanism of ICL repair in mammals, it is necessary to define the relationship between the nucleolytic cleavage of crosslinked DNA and the FA pathway. Herein we provide evidence that XPF-ERCC1 nuclease participates in the same ICL repair mechanism as the FA proteins and that nucleolytic processing of damaged DNA is not required

for FA pathway activation, but is required for stable localization of monoubiquitinated FANCD2 on chromatin.

2.2 MATERIAL AND METHODS

2.2.1 Cell culture and drug treatment

Human fibroblast lines immortalized by stable expression of human telomerase, C5RO (normal), XP51RO (XFE), XP42RO (XP-F), and XP25RO (XP-A) (Niedernhofer *et al.*, 2006) were cultured in Ham's F-10 with 10% fetal bovine serum, antibiotics and non-essential amino acids. Cells were treated for 12 hrs with 0.3 μM MMC or for 1 hr with 3 μM MMC diluted in media. At the end of the treatment, cells were washed twice with PBS, the media was replaced and the cells incubated at 5% CO_2 at 37°C under humidity. Time points were calculated with this as 0 hr. Wild-type and *Ercc1*$^{-/-}$ mouse embryonic fibroblasts (MEFs), transformed with SV40 large-T antigen, were cultured in 1:1 mixture of Ham's F-10 and DMEM with 10% fetal bovine serum, antibiotics and non-essential amino acids. Wild type, *Ercc1*$^{-/-}$ (Niedernhofer *et al.*, 2001) and *Mus81*$^{-/-}$ (Hanada *et al.*, 2006) mouse embryonic stem (ES) cells were cultured on gelatin-coated plates in a 1:1 mixture of DMEM and Buffalo Rat Liver (BRL) cell conditioned media with 10% FBS, antibiotics, non-essential amino acids, 0.1 mM 2-mercaptoethanol and leukemic inhibitory factor (1000 U/ml, Gibco). Wild-type (AA8), UV47 (*Xpf* mutant), UV96 (*Ercc1* mutant) and UV135 (*Xpg* mutant) CHO cells were grown as a monolayer in F12-Ham Hepes medium (Sigma) supplemented with 5 mM glutamine and 10% fetal calf serum. Cells were grown at 37°C in a 5% CO_2 humidified incubator. Cells were treated with 1 μM mitomycin C for 12 hrs, or for 1 hr with the stated doses of nitrogen mustard (mechlorethamine hydrochloride, Aldrich) dissolved in culture medium (without FCS) immediately prior to use. Following nitrogen

mustard or mitomycin C treatment, media were removed, cells washed twice with PBS and returned to the incubator in drug-free complete media for the stated times.

2.2.2 Immunoblotting

Cells were trypsinized, washed with PBS and lysed with 1 ml NETT buffer (100 mM NaCl, 50 mM Tris base pH 7.5, 5 mM EDTA pH 8.0, 0.5% Triton X-100) containing Complete™ mini protease inhibitor cocktail and phosphatase inhibitor cocktail (Roche Molecular Biochemicals). From each sample, 50 μg protein was resolved on 6% SDS-PAGE gels. FANCD2 was detected with rabbit anti-FANCD2 (for human cells, 1:10000, Novus Biologicals), rabbit anti-murine FANCD2 (for mouse cells, 1:1000) or rabbit anti-FANCD2 (for CHO cells, 1:1000, Abcam). The loading control used for whole cell extracts (WCEs) was tubulin (rabbit anti-tubulin, 1:1000 or 1:15,000, Abcam and Sigma, respectively). The loading control for cytoplasmic protein from HeLa cells was GRB2 (anti-GRB2, 1:5000, BD Biosciences). The loading control for chromatin and nuclear fractions of ES cells was TATA binding protein (mouse anti-TBP, 1:500, Abcam) and for hamster cells was ORC2 (mouse anti-ORC2 BD-Pharmingen, 1:800). The loading controls for human fibroblasts and MEFs were: nucleophosmin (mouse anti-nucleophosmin, 1:5000, Millipore) for the soluble nuclear fraction, and Histone H3 (rabbit anti-H3, 1:20,000, Abcam) for the chromatin fraction. Secondary antibodies used were: mouse AP (1:7500, Promega), rabbit AP (1:1000, Promega), rat HRP (1:5000, Abcam), Rabbit HRP (1:1200, Dako) and mouse HRP (1:1500 or 1:2500, Promega).

2.2.3 Depletion of ERCC1 by siRNA

HeLa cells were obtained from Cancer Research UK Clare Hall Cell Services and maintained in RPMI supplemented with 10% fetal calf serum and glutamine without antibiotics. Cells were transfected with siRNA duplexes using Hiperfect transfection reagent (Qiagen). Cells were seeded at 50% confluency immediately before the transfection complex containing 5 nM siRNA oligonucleotides was added. This transfection step was repeated 24 hours later. siRNA transfected cells were harvested for subsequent drug treatment 72 hours after the first transfection. The siRNA duplexes were purchased from Qiagen and the sequence used to deplete Ercc1 was: 5'-GCCCUUAUUCCGAUCUACATT-3', which has been previously characterized in detail (Lan *et al.*, 2004). For negative controls, HeLa cells were transfected with Hiperfect with Qiagen AllStars RNAi negative control duplex.

2.2.4 Cell cycle analysis

Cells were plated at 50% confluence, then 16 hrs later exposed to 0.3 μM MMC for 12 hrs or left untreated. At 12, 24, 48 and 72 hrs after exposure, the cells were fixed with ice cold 70% ethanol and stored at 4°C overnight. CHO cells were treated with 5 μM HN2, as described above, and samples removed at the stated times for fixing. The fixed cells were washed with PBS, treated with RNase A (Roche) at a final concentration of 100 U/ml for 30 min at room temperature and then stained with 1 μg/ml propidium iodide in PBS. Cell cycle analysis was performed on Dako MoFlo flow cytometer or a Becton Dickinson FACS caliber.

2.2.5 Modified Comet assay

The modified version of the Comet assay for the detection of ICLs was performed exactly as previously described (De Silva *et al.*, 2000).

2.2.6 Cell fractionation

Cells were fractionated into cytosolic, nuclear and chromatin fractions with a modification of a published protocol (Kapetanaki *et al.*, 2006). In brief, cells were trypsinized, pelleted and washed twice with PBS. The pellet was vortexed at full speed for 15 sec with 200 µl of CERI reagent from the Pierce NE-PER fractionation kit (Pierce Biotech) with Complete™ mini protease inhibitor cocktail, then incubated on ice for 10 min. This was followed by addition of 11 µl of CERII, vortexing for 5 sec and incubation on ice for 1 min. The mixture was spun down at 13,000 rpm for 5 min and the supernatant was collected as the cytosolic fraction. The nuclei were suspended in extraction buffer (15 mM Tris-HCl pH 7.3, 1 mM EDTA, 0.4 M NaCl, 1 mM $MgCl_2$, 10% glycerol, 10 mM β -mercaptoethanol and Complete™ mini protease inhibitor cocktail), mixed for 1 hr at 4°C and spun down at 13,000 rpm for 10 min. The supernatant was collected as the soluble nuclear fraction and the pellet was suspended in micrococcal nuclease buffer (20 mM Tris·HCl pH 7.5, 100 mM KCl, 2 mM $MgCl_2$, 1 mM $CaCl_2$, 0.3 M sucrose, 0.1% Triton X-100 and Complete™ mini protease inhibitor cocktail) and digested with 400 U/ml S7 micrococcal nuclease (Roche) at 37°C for 30 min. The reaction was spun down at 13,000 rpm for 10 min and supernatant was collected as the chromatin fraction. For CHO and HeLa cells, fractionation was performed exactly as described (Qiao *et al.*, 2001).

2.2.7 Immunodetection of FANCD2 foci

C5RO and XP51RO human fibroblasts (Niedernhofer *et al.*, 2006) were plated on glass coverslips at 50% confluence, then 16 hrs later exposed to 3 μM MMC for 1 hr or left untreated. At 6, 12, 24 and 48 hrs following exposure, cells were fixed as described (Wang *et al.*, 2004) with some modifications. Briefly, cells were washed with PBS, permeabilized with ice-cold 0.5% Triton X-100 in PBS, then fixed with 2% paraformaldehyde and blocked with 5% bovine serum albumin at room temperature. FANCD2 was detected by incubation with rabbit polyclonal anti-FANCD2 antibody (1:1000, Novus Biologicals) for 90 min at RT and goat anti-rabbit Alexa-488 (1:1000, Invitrogen). Images were taken of 20 fields of cells for each genotype. The total number of nuclei and the number of nuclei with foci were counted in each field. The sum from all fields was used to calculate the percent of nuclei with foci. The experiment was done in triplicate. Student's t-test was used to probe significant differences between cell lines.

2.3 RESULTS

2.3.1 FANCD2 is monoubiquitinated in XPF-ERCC1 and MUS81-EME1 deficient cells

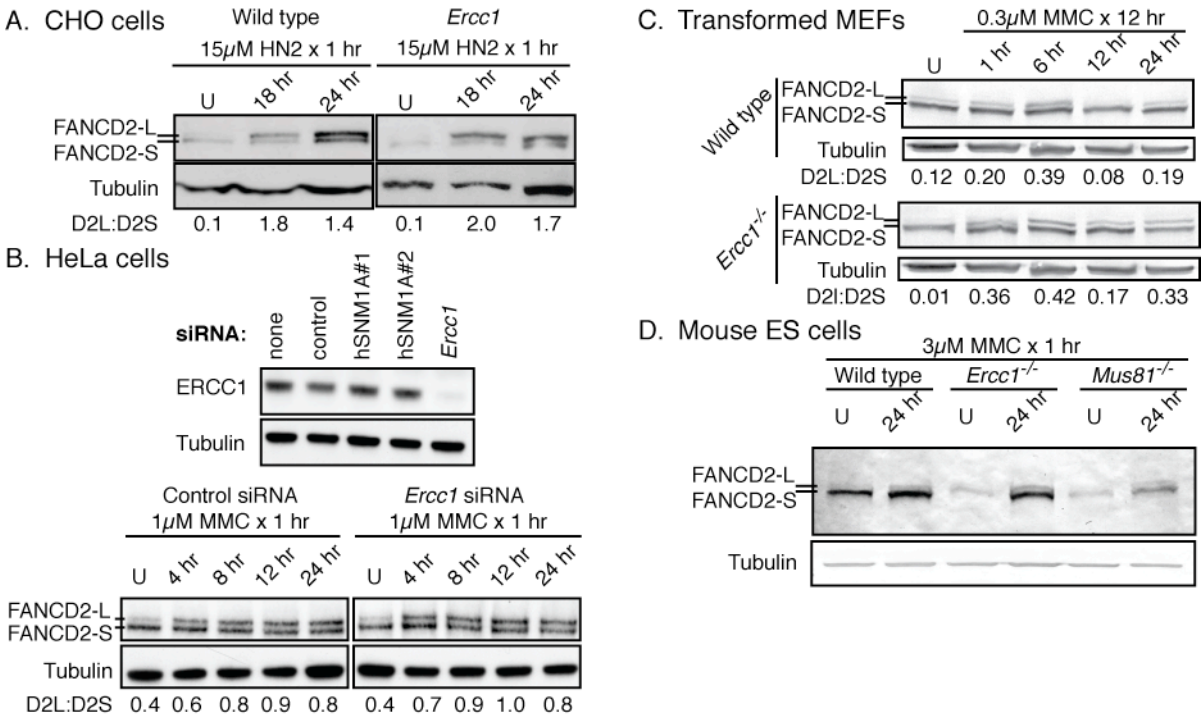

Figure 2-1: FANCD2 monoubiquitination in ERCC1-XPF deficient cells

FANCD2 is monoubiquitinated in XPF-ERCC1 and MUS81-EME1 deficient cells after crosslink damage. *A*, wild type and *Ercc1* mutant CHO cells were exposed to 15 μM nitrogen mustard (HN2) for 1 hr, then whole cell extracts (WCEs) were collected 18 or 24 hrs later for immunodetection of FANCD2. FANCD2-L is the monoubiquitinated protein and FANCD2-S is the non-ubiquitinated form. U indicates cells that were untreated. *B*, wild type HeLa cells were transfected with either control siRNA, or one of two siRNAs against hSNM1A as further controls for specificity, or with siRNA against *Ercc1*. After confirming specific knockdown of ERCC1 by immunoblotting, cells were treated with 1 μM MMC for 1 hr and WCEs were collected at multiple time points after exposure for immunodetection of FANCD2. *C*, wild type and

***Ercc1*$^{-/-}$ mouse embryonic fibroblasts (MEFs) were exposed to 0.3 µM mitomycin C (MMC) for 12 hrs then WCEs were collected at multiple time points after exposure for immunodetection of FANCD2. *D*, wild type, *Mus81*$^{-/-}$ and *Ercc1*$^{-/-}$ mouse embryonic stem (ES) cells were exposed to 3 µM MMC for 1 hr then WCEs were collected 24 hrs later for immunodetection of FANCD2.**

To determine if XPF-ERCC1 deficiency affects activation of the FA pathway, FANCD2-L (monoubiquitinated form) and –S (non-ubiquitinated form) were measured in mutant cells exposed to crosslinking agents. Wild-type and *Ercc1* mutant Chinese hamster ovary (CHO) cells were exposed to the crosslinking agent nitrogen mustard (HN2) for 1 hr, then WCEs collected 18 or 24 hrs later. The levels of FANCD2-L were similarly increased in both cell types after exposure to HN2 relative to untreated samples (Figure 2-1A and Figure 2-5A). This was confirmed in an isogenic pair of human cell lines by knocking down ERCC1 expression in HeLa cells using siRNA and exposing them to a different crosslinking agent, MMC (Figure 2-1B and Fi. 2-5B). Comparable results were obtained with *Ercc1*$^{-/-}$ mouse embryonic fibroblasts (MEFs) exposed to MMC (Figure 2-1C and Figure 2-5C). Since XPF-ERCC1 nuclease appeared not to be required for FA pathway activation, we also screened cells deficient in MUS81, a second nuclease required for ICL repair (Hanada *et al.*, 2006). Mouse embryonic stem cells (ES) genetically deleted for either *Ercc1* or *Mus81* were exposed to MMC for 1 hr then WCEs collected 24 hrs later. Immunodetection of FANCD2 revealed increased levels of FANCD2-L in all cells exposed to the crosslinking agents relative to the untreated cells (Figure 2-1D). These data demonstrate that FANCD2 is monoubiquitinated in response to crosslink damage in the absence of XPF-ERCC1 or MUS81-EME1. This indicates that nucleolytic processing of crosslinks by MUS81-EME1 or XPF-ERCC1 is not necessary for FA pathway activation, as defined by FANCD2 monoubiquitination.

2.3.2 FA pathway activation persists in XPF-ERCC1 deficient cells

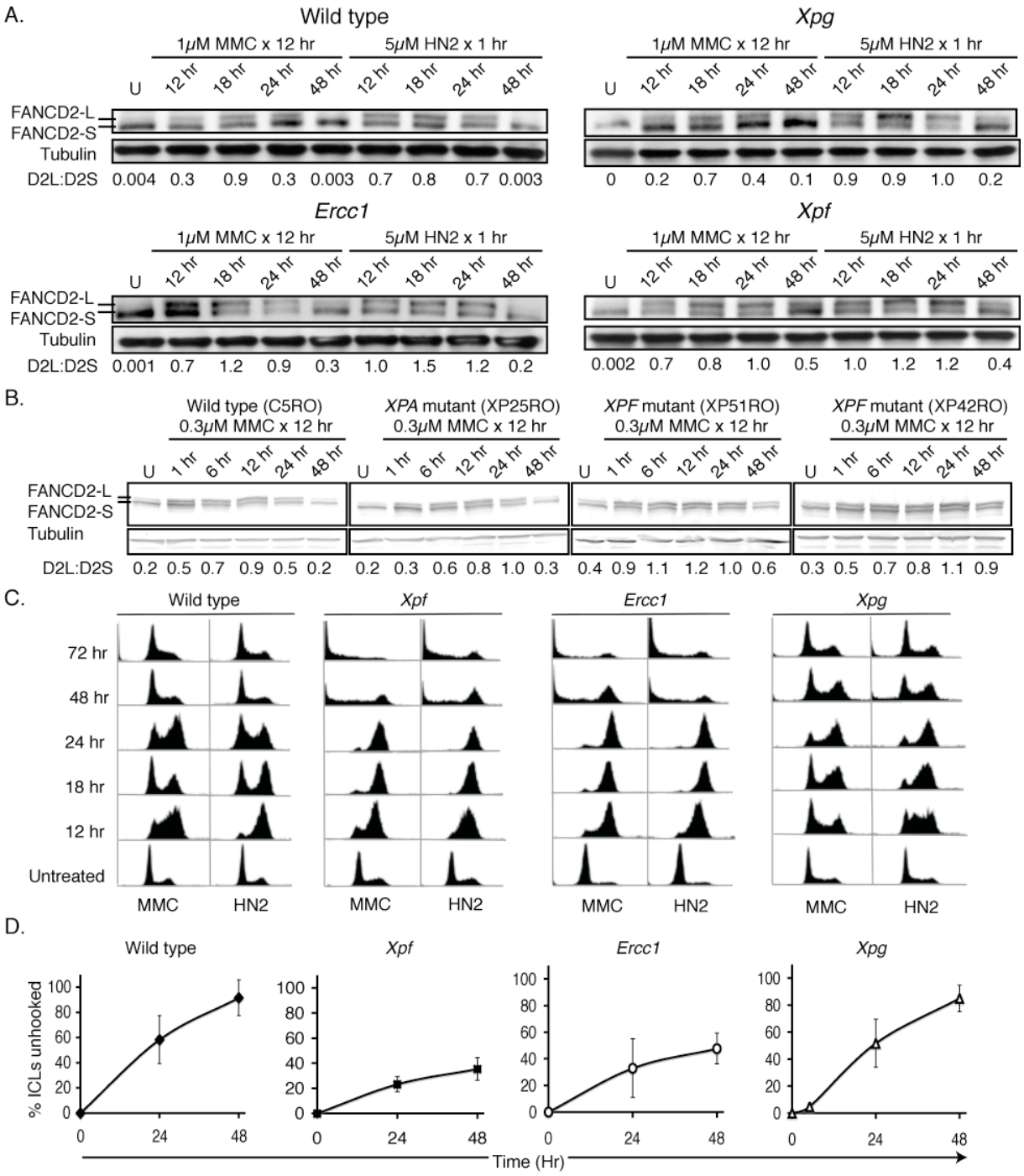

Figure 2-2: Persistence of FANCD2 monoubiquitination in ERCC1-XPF deficient cells

Monoubiquitination of FANCD2 persists in XPF-ERCC1 deficient cells. *A*, AA8 (wild type), UV135 (*Xpg* mutant), UV96 (*Ercc1* mutant) and UV47 (*Xpf* mutant) CHO cells were exposed to 1 μM MMC for 12 hr

or 5 μM nitrogen mustard (HN2) for 1 hr then WCEs were collected at multiple time points following exposure for immunodetection of FANCD2. U indicates cells that were untreated. *B*, wild type, XP-A (XP25RO) and XP-F (XP51RO and XP42RO) immortalized human fibroblasts were exposed to 0.3 μM MMC for 12 hrs then WCEs were collected at multiple time points after exposure for immunodetection of FANCD2. *C*, CHO cells were treated as described in *A* then fixed at the same time points, and stained with propidium iodide for cell cycle analysis by flow cytometry. *D*, The efficiency of unhooking of interstrand crosslinks determined by modified Comet assay, following 1 hr treatment with 5 μM HN2 in *Xpg*, *Xpf* and *Ercc1* mutant and wild type parent cell lines.

Although FANCD2 is monoubiquitinated in XPF-ERCC1 deficient cells, initial data from the MEFs suggested that FANCD2-L levels remained elevated longer in *Ercc1*$^{-/-}$ cells exposed to MMC compared to wild-type cells (Figure 2-1C and Figure 2-5C). To investigate this further, wild-type and mutant CHO cells and human fibroblasts were exposed to MMC or HN2, and FANCD2 was visualized by immunoblot at multiple time points following DNA damage. Both MMC and HN2 induced an increase in the ratio of FANCD2-L to FANCD2-S in wild-type and NER deficient *Xpg* mutant CHO cells (Figure 2-2A). By 48 hrs after HN2 or MMC exposure, FANCD2-L levels returned to near-normal in these cell lines. In contrast, the ratio of FANCD2-L to FANCD2-S was still elevated in both *Xpf* and *Ercc1* mutant CHO cells at 48 hrs after exposure to HN2 or MMC (Figure 2-2A and Figure 2-5D). The results were recapitulated in cells derived from human XP patients (Figure 2-2B). In wild-type and NER deficient XP-A human fibroblasts, MMC induced a rapid increase in the ratio of FANCD2-L to FANCD2-S that persisted for 24 hrs. The levels of monoubiquitinated FANCD2 returned to those of untreated cells by 48 hrs. In two different XP-F cell lines, the ratio of FANCD-L to –S was increased by MMC, like wild-type cells. However, in the XPF-ERCC1 deficient cells, the ratio of FANCD2-L to -S remained elevated at 48 hrs after exposure to MMC (Figure 2-2B and Figure 2-5E). This

suggests that in the absence of XPF-ERCC1 the FA pathway remains activated in response to crosslink damage.

Because FANCD2 monoubiquitination is cell cycle-dependent (Kim *et al.*, 2008a), the cell cycle profile of the CHO cell lines was measured at multiple time points after exposure to crosslinking agents (Figure 2-2C). HN2 and MMC caused an accumulation of cells in S and G2/M phases at 12 and 18 hrs in all cells. By 48 hrs following MMC treatment, some wild-type and *Xpg* mutant cells had escaped G2/M arrest, but XPF-ERCC1 defective cells remained arrested in late S and G2/M. Therefore, persistent FANCD2-L correlates with G2/M accumulation. The *Xpg* mutant cells were somewhat slower to escape the G2/M arrest compared to wild-type cells, and this might be attributable to the role of NER in repairing the monoadducts produced by crosslinking agents. The persistence of FANCD2-L also correlates with impaired unhooking of crosslink damage (Figure 2-2D). The modified comet assay (De Silva *et al.*, 2000) was used to measure nucleolytic processing of crosslink damage in CHO cells following HN2 exposure. In wild-type and *Xpg* mutant cells crosslink unhooking was greater than 85% at 48 hrs. In contrast, in *Ercc1* and *Xpf* mutant cells in which FANCD2 monoubiquitination persisted, crosslink unhooking was only approximately 40% at 48 hrs. These data indicate that nucleolytic processing of ICLs coincides with the deactivation of FA pathway, marked by a decrease in the FANCD2-L to FANCD2-S ratio, and is associated with escape from G2/M.

2.3.3 FANCD2 foci are reduced in XPF-ERCC1 deficient human fibroblasts

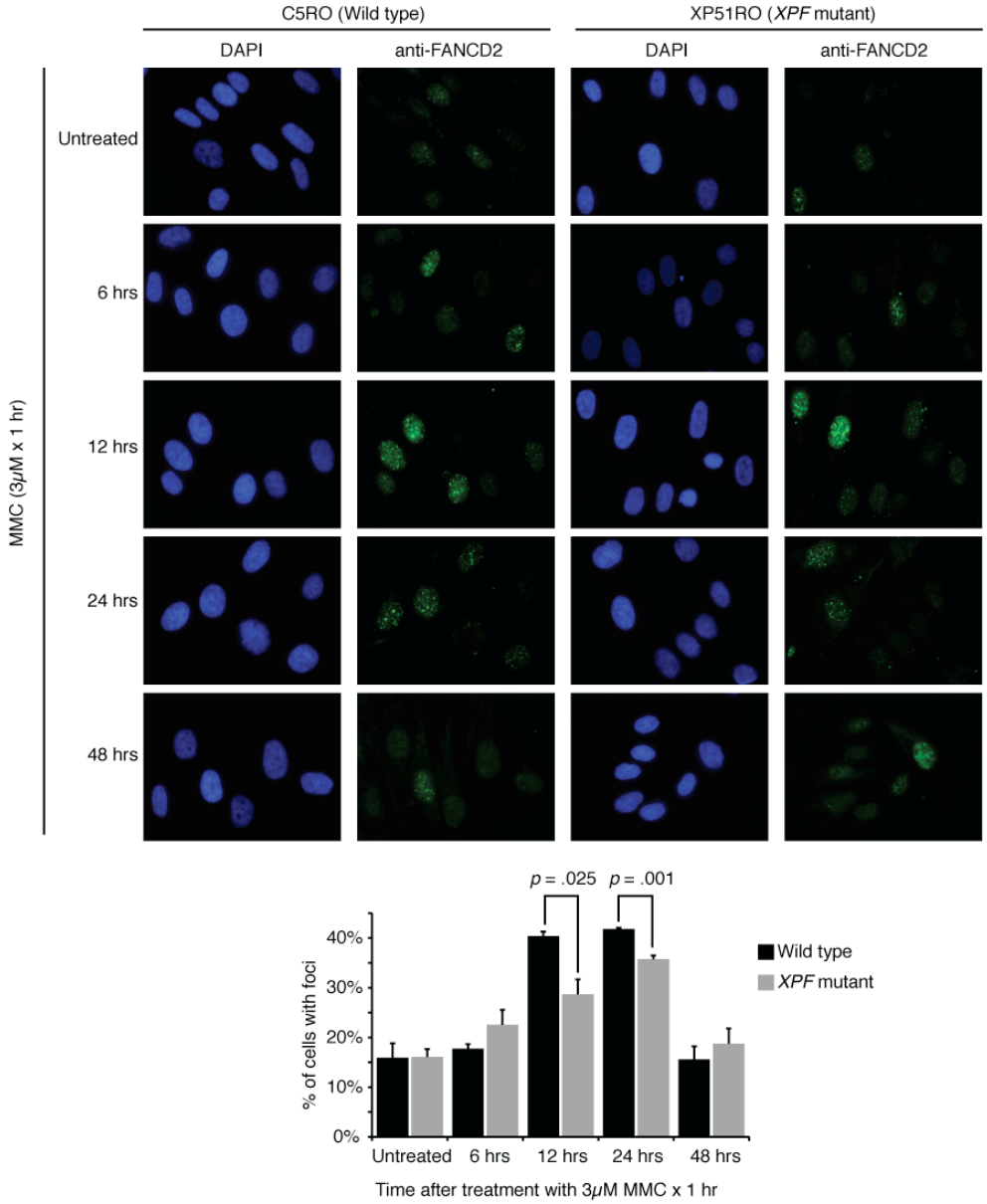

Figure 2-3: FANCD2 focus formation in ERCC1-XPF deficient cells in response to ICL damage

FANCD2 focus formation is impaired in XPF-ERCC1 deficient cells. Wild type (C5RO) and XP-F (XP51RO) human fibroblasts were seeded on glass coverslips. Sixteen hours later the cells were exposed to 3 μM MMC for 1 hr, then fixed at multiple time points. FANCD2 was detected by immunofluorescence. Cells with FANCD2 foci were counted. Representative images are shown and the average of three experiments plotted. A paired Student's t-test was used to calculate significance.

Another way to quantify FA pathway activation is to measure chromatin bound FANCD2 (Oestergaard *et al.*, 2007). Surprisingly, in human fibroblasts the number of cells with FANCD2 foci was significantly reduced in the XPF-ERCC1 deficient cell line (Figure 2-3). We measured FANCD2 foci in human fibroblasts exposed to MMC, after detergent extraction of soluble proteins. FANCD2 foci were detected in approximately 15% of untreated wild-type and *XPF* mutant cells. Twelve hours after exposure to MMC, 40% of wild-type cells had FANCD2 foci whereas 29% of *XPF* mutant cells had foci (p=0.025) and 24 hrs after the exposure, 42% of wild-type cells and 36% of *XPF* mutant cells had FANCD2 foci (p=0.001). By 48 hrs after crosslink damage the fraction of cells with FANCD2 foci had returned to normal in both cell types. These data suggest that although FANCD2 is efficiently ubiquitinated in XPF-ERCC1 deficient cells in response to crosslink damage, the localization of FANCD2 to the chromatin is impaired, a critical step for subsequent HR-mediated repair of replication induced DSBs.

2.3.4 Chromatin bound FANCD2 is reduced in XPF-ERCC1 deficient cells

FANCD2 levels were normal in XPF-ERCC1 deficient cells exposed to crosslinking agents, yet chromatin-bound FANCD2 focus formation was diminished, suggesting aberrant subcellular localization of FANCD2 in the absence of this nuclease. To further explore this, ERCC1 was depleted in HeLa cells by siRNA; the cells were then exposed to HN2 and fractionated. Immunodetection of FANCD2 in WCEs revealed that, as previously observed (Figure 2-1B), FANCD2 was efficiently monoubiquitinated in both control and ERCC1-depleted cells (Figure 2-4A and Figure 2-5F). In control cells, the level of FANCD2-L in the chromatin fraction increased dramatically following exposure of the cells to HN2 (Figure 2-4A). In contrast, in

ERCC1-depleted cells, the amount of FANCD2-L in the chromatin fraction did not increase following exposure of cells to HN2, but instead was elevated in the soluble nuclear fraction (Figure 2-4A).

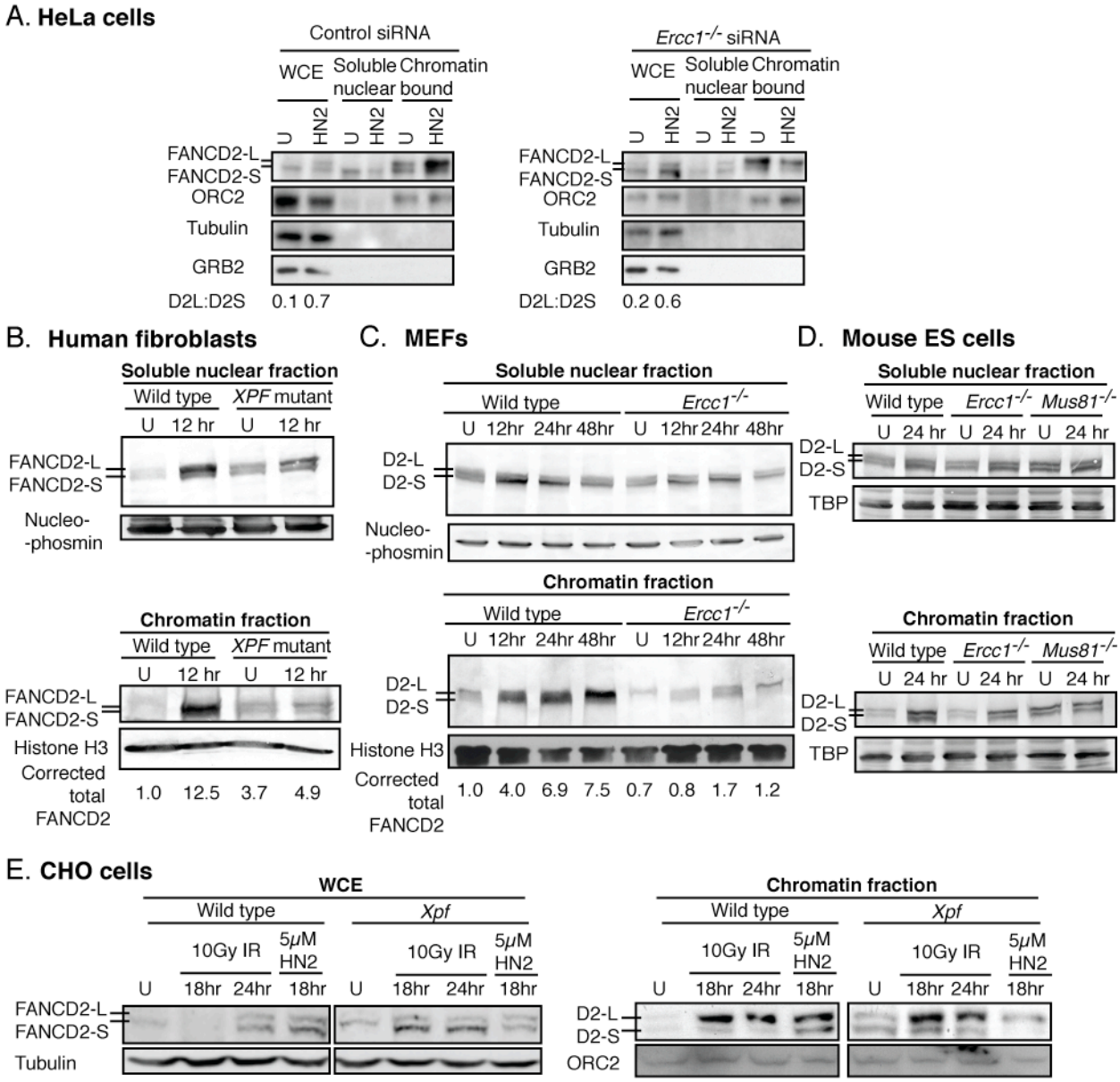

Figure 2-4: Chromatin binding of FANCD2 in ERCC1-XPF deficient cells

Chromatin localization of FANCD2 is impaired in XPF-ERCC1 deficient cells exposed to crosslinking agents, but not ionizing radiation. *A*, HeLa cells depleted for ERCC1, or mock depleted with a control siRNA duplex were treated with 1 μM HN2 for 1 hr. At 18 hrs after exposure WCEs were prepared

or cells were fractionated to isolate the soluble nuclear and chromatin bound protein fractions. Samples were immunoblotted for FANCD2. Immunodetection of ORC2 (origin recognition complex 2) was used as a loading control for chromatin-bound protein and GRB2 for cytoplasmic protein. *B*, wild type (C5RO) and XP-F (XP51RO) human fibroblasts were exposed to 3 μM MMC for 1 hr then fractionated 12 hrs later. The fractions were immunoblotted for FANCD2. Nucleophosmin and histone H3 were used as loading controls for the soluble nuclear and chromatin fractions, respectively. *C*, wild type and *Ercc1*$^{-/-}$ mouse embryonic fibroblasts (MEFs) were exposed to 3 μM MMC for 1 hr and fractionated at multiple time points after exposure. Fractions were immunoblotted for FANCD2 and the loading controls. *D*, Wild type (IB10) and *Ercc1*$^{-/-}$ (Clone 49) mouse embryonic stem (ES) cells were exposed to 3 μM MMC for 1 hr and fractionated at 24 hrs after exposure. Fractions were immunoblotted for FANCD2 with TATA binding protein (TBP) as the loading control. *E,* wild type and *Xpf* mutant CHO cells were exposed to 5 μM HN2 for 1 hr or 10 Gy of ionizing radiation. Cells were processed as described in *A* at 18 and 24 hrs after radiation and samples were immunoblotted for FANCD2. Tubulin was used as loading control for WCE and ORC2 was used as loading control for the chromatin fraction.

In human fibroblasts, the level of FANCD2-L was comparable for XP-F and wild-type cells before and after exposure to MMC (Figure 2-4B). However, the amount of FANCD2 detected in the chromatin fraction of XP-F fibroblasts treated with MMC was substantially lower than that detected in normal human fibroblasts (Figure 2-4B and Figure 2-5G). This is consistent with the observation that XP-F cells had significantly fewer FANCD2 foci than wild-type cells after MMC treatment (Figure 2-3). Similar results were obtained using congenic *Ercc1*$^{-/-}$ MEFs exposed to MMC (Figure 2-4C and Figure 2-5H), where again there was less chromatin-bound FANCD2 in the knock-out cells compared to wild-type in response to crosslink damage. The subcellular localization of FANCD2 was less dramatically affected in ES cells (*Ercc1*$^{-/-}$ and *Mus81*$^{-/-}$) than fibroblasts (Figure 2-4D). One possible explanation is that ES cells differ dramatically from fibroblasts in their cell cycle profile and checkpoint responses to crosslink

damage (Supplemental Figure 2-2A-C). Finally, an equivalent level of FANCD2-L was detected in wild-type and *Xpf* mutant CHO cells exposed to HN2 (Figure 2-4E). However, substantially less FANCD2-L was detected in the chromatin fraction of the mutant cells. In contrast, chromatin localization of FANCD2-L was not impaired in *Xpf* mutant cells exposed to ionizing radiation (Figure 2-4E). This indicates that the aberrant subcellular localization of FANCD2-L seen in XPF-ERCC1 deficient cells was specific for ICLs and not other forms of DNA damage, such as direct DSBs, where XPF-ERCC1 is not required prior to HR-mediated repair (Ahmad *et al.*, 2008).

Taken together these data, obtained in three mammalian cell systems exposed to two different crosslinking agents, support the conclusion that FANCD2 is not stably localized to the chromatin in the absence of XPF-ERCC1. This suggests that nucleolytic processing of crosslink damage is required for the stable accumulation of FANCD2 at or near the sites of damage. The data also imply that FANCD2 monoubiquitination does not always correlate with chromatin localization and should be considered as distinct steps in the response to crosslink damage.

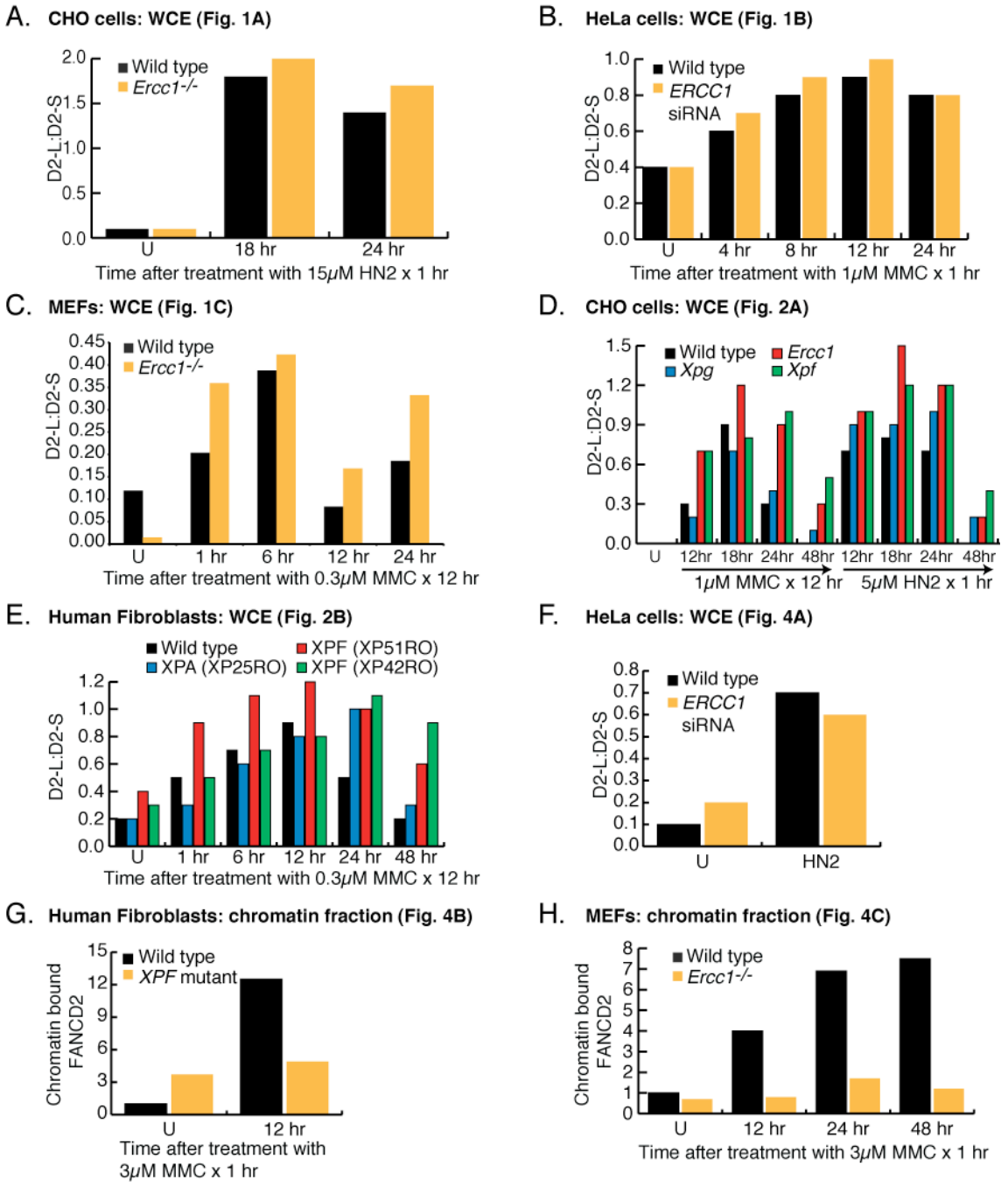

Figure 2-5: Immunoblot band intensities

Graphical representation of FANCD2 band intensities in immunoblots, measured by densitometry: *A-F*, ratio of FANCD2-L and FANCD2-S band intensities. *G* and *H*, total chromatin bound FANCD2 (FANCD2-L + FANCD2-S) corrected by the loading control.

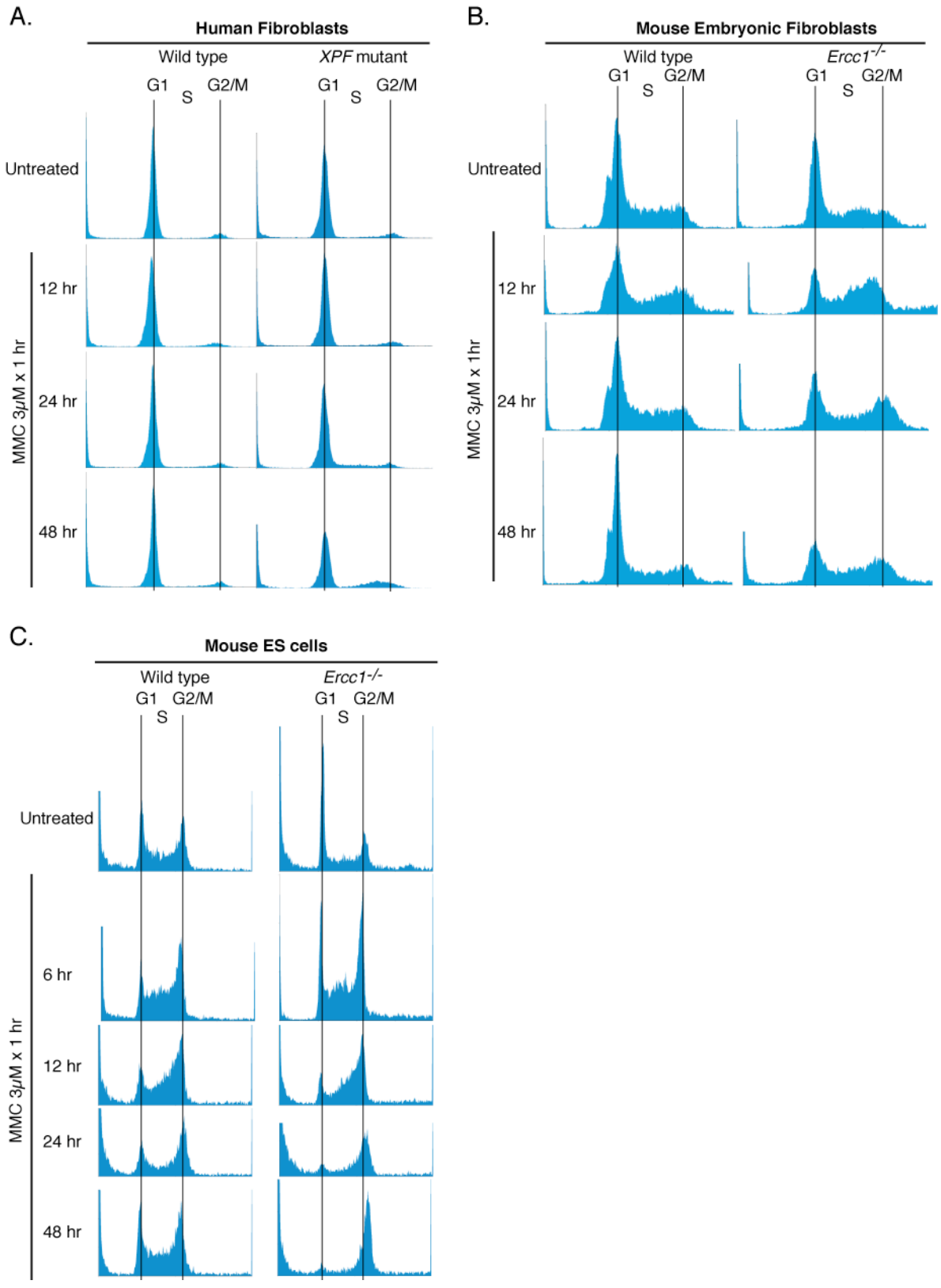

Figure 2-6: Cell cycle profile of ERCC1-XPF cells after ICL damage

Crosslink damage induces an S/G2 arrest that persists in ERCC1-XPF deficient cells. *A*, wild type (C5RO) and XPF mutant (XP51RO) immortalized human fibroblasts were exposed to 3 μM MMC for 1 hr and harvested at multiple time points after exposure. Cells were then fixed and stained with propidium iodide, and subjected to flow cytometry for cell cycle analysis. *B*, wild type and *Ercc1*$^{-/-}$ mouse embryonic fibroblasts were processed as above. *C*, wild type (IB10) and *Ercc1*$^{-/-}$ (Clone 49) mouse ES cells were processed as above.

2.4 DISCUSSION

Two sets of proteins that are critical for the response to and repair of ICLs are the FA family of proteins and the XPF-ERCC1 complex (McHugh *et al.*, 2001; Niedernhofer *et al.*, 2005). Whether or not these proteins function in the same DNA damage detection and repair mechanism is not established. A significant body of biochemical and cellular data indicates an essential role for XPF-ERCC1 endonuclease in the unhooking of ICLs (De Silva *et al.*, 2000; Kuraoka *et al.*, 2000). However, it is not known if unhooking of ICLs must occur prior to activation of the FA pathway. Our studies revealed that XPF-ERCC1 nuclease is not required for activation of the FA pathway, as defined by the monoubiquitination of FANCD2. In the same experiments, we confirmed that both XPF and ERCC1 are required for efficient ICL unhooking using the modified comet assay. Thus nucleolytic processing of ICLs by XPF-ERCC1 is not a pre-requisite for FA pathway activation. This is consistent with the results of numerous other laboratories, indicating that replisome stalling at DNA lesions and secondary structures, as occurs with ICLs, is sufficient to generate the signal which ultimately leads to FANCD2 ubiquitination (D'Andrea and Grompe, 2003; Gregory *et al.*, 2003; Montes de Oca *et al.*, 2005). Given that ATR activation is also required for the timely ubiquitination of FANCD2 in response to ICLs (Andreassen *et al.*, 2004), it is tempting to speculate that tracts of single-stranded DNA (ssDNA) that occur at stalled replisomes are what trigger ATR-dependent FANCD2 monoubiquitination. In the case of ICLs, ssDNA likely results from nucleolytic processing of stalled forks rather than uncoupling of leading and lagging strand synthesis (Paulsen and Cimprich, 2007), which is what activates ATR when replication is blocked by lesions that affect only one strand of DNA.

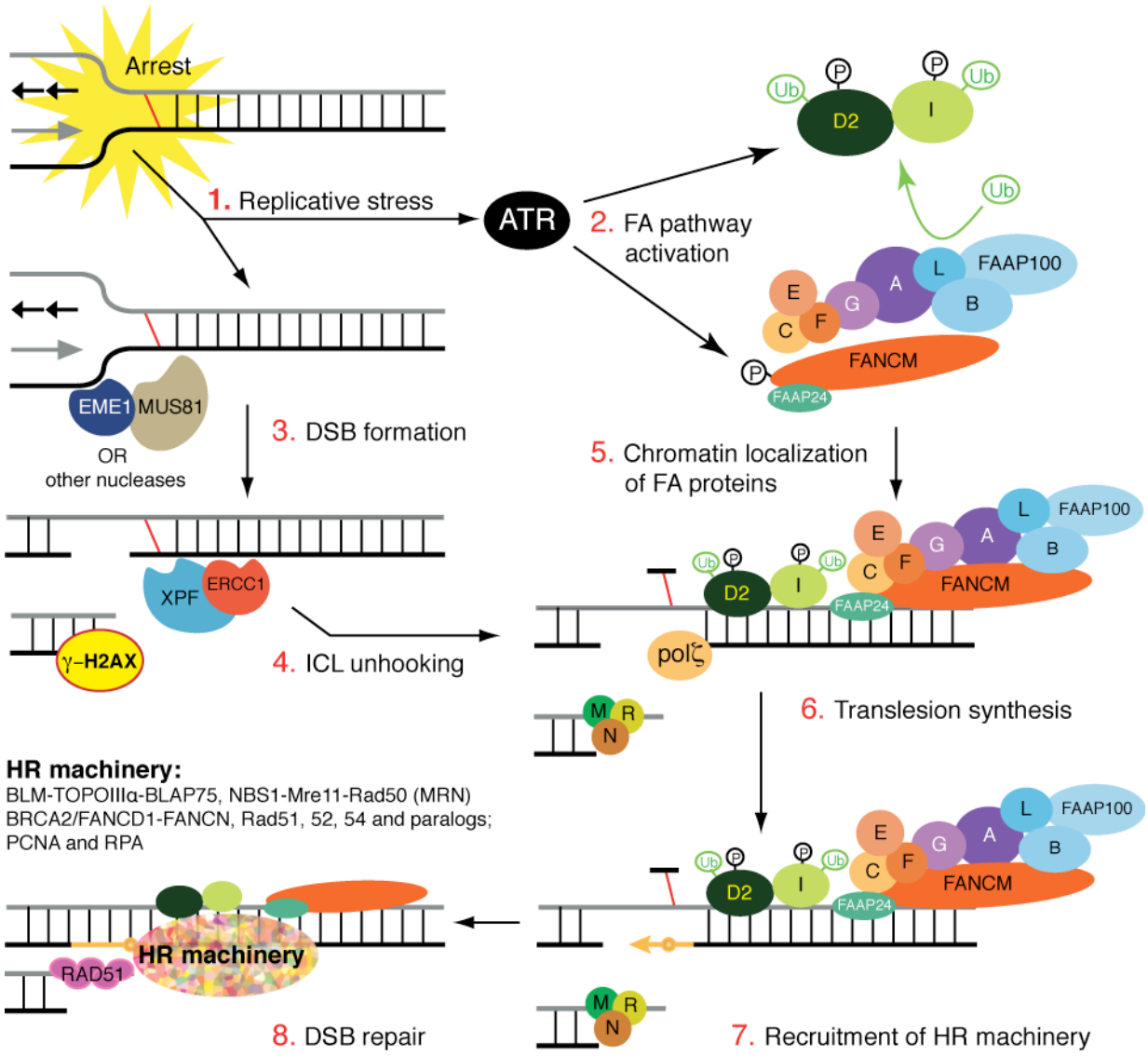

Figure 2-7: A model of crosslink repair

Model of how XPF-ERCC1 and MUS81-EME1 nucleases function in the same S-phase specific DNA interstrand crosslink repair mechanism as the Fanconi anemia proteins. See text for more details.

Although XPF-ERCC1 dependent nucleolytic processing of ICLs is not required for FA pathway activation, our data did reveal a difference in the kinetics of FANCD2 modification in XPF-ERCC1 deficient cells. These nuclease-deficient cells show a persistence of monoubiquitinated FANCD2 in whole cell extracts following ICL induction. In contrast to our

results, McCabe *et al* reported decreased monoubiquitination of FANCD2 in cells depleted of ERCC1 by siRNA (McCabe *et al.*, 2008). However, like us, these authors did observe that MMC causes an induction of FANCD2 monoubiquitination in ERCC1-depleted cells and that the relative increase in the ratio of FANCD2-L to -S was similar in ERCC1-depleted and control cells upon crosslink damage. We observed persistent FANCD2 monoubiquitination in XPF-ERCC1 deficient cells from three species in response to two different crosslinking agents. Prolonged FANCD2 monoubiquitination has not previously been reported in other crosslink sensitive mutants, suggesting that incision of crosslinked DNA by XPF-ERCC1 is essential for the repair of ICLs and termination of the DNA damage response.

In addition, chromatin localization of FANCD2 in response to crosslink damage is impaired in XPF-ERCC1 deficient cells, as demonstrated by cellular fractionation and FANCD2 foci formation. This suggests that stable association of monoubiquitinated FANCD2 with chromatin requires (at a minimum) an unhooked ICL. Indeed, the persistent FANCD2-L observed in *Xpf* and *Ercc1* mutant WCEs might reflect continued attempts to target FANCD2 to sites of damage in chromatin, which are non-productive when crosslinked DNA is not incised.

The XPF-ERCC1-related nuclease, MUS81-EME1 is also implicated in ICL repair by virtue of the hypersensitivity of *Mus81*$^{-/-}$ and *Eme1*$^{-/-}$ mouse cells to crosslinking agents (Hanada *et al.*, 2006). Specifically, MUS81 is required for the cleavage of replication forks stalled by ICLs, producing DSBs with one accessible end (Hanada *et al.*, 2007; Hanada *et al.*, 2006). However, ICL-induced monoubiquitination of FANCD2 is normal in *Mus81*$^{-/-}$ cells (Figure 2-1) and genetic disruption of *FANCB* and *MUS81* does not render cells hypersensitive to crosslinking agents relative to deletion of *FANCB* alone (Nomura *et al.*, 2007). These data support the conclusion that the generation of DSBs at ICLs during S-phase by MUS81-EME1 is

not a pre-requisite for activation of FANCD2. Taken together, these data suggest a model for ICL repair (Figure 2-7; see also a recent review by Thompson and Hinz (Thompson and Hinz, 2009)) in which stalling of a replication fork at an ICL leads to the formation of a DSB created by MUS81-EME1 nuclease. Fork stalling, but not the generation of a DSB, is sufficient for activation of ATR and the monoubiquitination of FANCD2. However, in the absence of unhooking of the ICL by XPF-ERCC1, FANCD2 and, therefore, presumably the HR machinery do not stably associate at the sites of damage. This results in failure to repair ICL-dependent DSBs in XPF-ERCC1 deficient cells (Niedernhofer *et al.*, 2004).

The data presented herein demonstrate that there is not an absolute correlation between the level of monoubiquitinated FANCD2 and its chromatin association. In XPF-ERCC1 deficient cells in which ICL-dependent DSBs are not repaired (Niedernhofer *et al.*, 2004), the levels of monoubiquitinated FANCD2 persist longer than in wild-type cells after crosslink damage, but chromatin localization of FANCD2 is reduced. This suggests that in the absence of ICL repair, damage signalling persists. In accordance, it was recently reported that FANCD2 deubiquitination by USP1 (Nijman *et al.*, 2005), is required for efficient ICL repair (Oestergaard *et al.*, 2007). Thus when chromatin association of FANCD2 is compromised, for instance in the absence of ICL unhooking by XPF-ERCC1, deubiquitination of FANCD2 by USP1 does not occur. This is supported by the observation that FANCD2 deubiquitination is concurrent with release of FANCD2 from chromatin (Oestergaard *et al.*, 2007). The eviction of FANCD2 from chromatin likely coincides with the recruitment of factors that undertake post-unhooking steps of ICL repair, including homologous recombination-mediated DSB repair and translesion synthesis to fill the gap created by ICL unhooking (Niedzwiedz *et al.*, 2004; Wang *et al.*, 2004).

3.0 MISLOCALIZATION OF DNA REPAIR NUCLEASE XPF-ERCC1: THE MOLECULAR BASIS FOR REDUCED DNA REPAIR IN XP-F PATIENTS

This chapter is under review for publication in PLoS Genetics:

Ahmad, A.*, Enzlin, J.H.*, Bhagwat, N.R.*, Wijgers, N., Raams, A., Appledorn, E., Theil, A.F., Hoeijmakers, J.H.J., Vermeulen, W., Jaspers, N.G.J., Scharer, O.D. and L.J. Niedernhofer (2009) Aberrant sub-cellular localization of DNA repair protein XPF: the molecular basis for reduced DNA repair in XP-F patients. (*Contributed equally)

3.1 INTRODUCTION

Xeroderma pigmentosum (XP) is a rare autosomal recessive disease characterized by photosensitivity and greater than a 1000-fold increased risk of skin cancer in sun-exposed areas of the skin (Kraemer *et al.*, 1987). In approximately 20% of patients, there is also progressive neurodegeneration leading to loss of coordination motion, vision and hearing (Nouspikel, 2008; Robbins *et al.*, 1991). XP is caused by mutations in genes that encode proteins required for nucleotide excision repair (NER) of DNA. Eight complementation groups of XP have been identified based on fusion studies with XP patient cells. These complementation groups include XP-A through XP-G and a variant, XP-V. The severity of XP varies tremendously, with

diagnosis occurring anywhere from infancy to adulthood. The severity of the disease is determined largely by which gene is mutated and to what extent the mutation affects NER.

NER removes helix-distorting lesions in DNA, for example cyclobutane pyrimidine dimers (CPDs) and pyrimidine pyrimidone photoproducts (6-4PPs) caused by the ultraviolet (UV) component of sunlight (Gillet and Scharer, 2006). There are two ways by which DNA damage is recognized in NER. Lesions anywhere in the genome can be recognized by the complex XPC-RAD23B (Sugasawa *et al.*, 1998; Volker *et al.*, 2001). For some lesions, this is facilitated by a second complex XPE/DDB2-DDB1 (Sugasawa, 2006). Alternatively, lesions that occur in the coding strand of DNA, within transcribed regions, can trigger NER if they stall progression of RNA polymerase II (Hanawalt and Spivak, 2008; Laine and Egly, 2006). This requires CSA, CSB and XAB2 (Henning *et al.*, 1995; Nakatsu *et al.*, 2000; Troelstra *et al.*, 1992). Once the damage is recognized, the subsequent steps of damage excision are believed to be uniform. The basal transcription factor TFIIH is recruited to the site of helix-distortion to unwind the DNA around the lesion, using two of its ten subunits, XPB and XPD (Evans *et al.*, 1997; Laine and Egly, 2006). RPA and XPA bind the unwound repair intermediate to stabilize it and recruit subsequent factors. The damaged strand of DNA is then incised by two structure-specific endonucleases, the heterodimer of XPF-ERCC1 and XPG, which cut 5' and 3' of the lesion, respectively (Bardwell *et al.*, 1994; O'Donovan *et al.*, 1994; Sijbers *et al.*, 1996a; Staresincic *et al.*, 2009). This leads to removal of the lesion as part of a 24-32 base oligonucleotide. The resultant gap is filled by the replication machinery including RPA, PCNA, RF-C, DNA polymerase δ/ε, and the backbone is sealed by DNA LIGI or LIGIIIα-XRCC3 (Moser *et al.*, 2007; Ogi and Lehmann, 2006; Shivji *et al.*, 1995).

XPF-ERCC1 is a highly conserved endonuclease that nicks double-stranded DNA 5' to a junction with single-stranded DNA (de Laat *et al.*, 1998a). In addition to NER, XPF-ERCC1 is involved in the repair of DNA interstrand crosslinks (ICL) (Niedernhofer *et al.*, 2004) and double-strand break (DSB) repair (Ahmad *et al.*, 2008). XPF and ERCC1 are paralogs thought to have arisen by gene duplication of the conserved nuclease and helix-hairpin helix protein-interaction domains (Gaillard and Wood, 2001). The proteins interact via their C-terminal helix-hairpin-helix domains and this interaction is required to stabilize both proteins in vivo (Biggerstaff *et al.*, 1993; de Laat *et al.*, 1998b). XPF contains the nuclease catalytic domain (Enzlin and Scharer, 2002), whereas ERCC1 mediates the interaction with XPA and recruitment to NER complexes (Li *et al.*, 1994; Tsodikov *et al.*, 2007). Unlike NER-specific proteins XPA and XPC, XPF-ERCC1 appears to be essential for human development or viability since no early nonsense or frameshift mutations in either gene have yet been identified.

XP-A and XP-C are among the most common complementation groups in XP (Zeng *et al.*, 1997). XP-C patients have severe skin abnormalities but generally lack neurological symptoms (Moriwaki and Kraemer, 2001). In contrast, XP-A patients show profound neurodegeneration, in addition to cutaneous features (Kraemer *et al.*, 1987). XP-F patients typically have very mild cutaneous features of XP, including late onset of skin cancer, but often have neurological complications. It was recently discovered that mutations in *XPF* can lead to a second disease, XFE progeroid syndrome (short for XPF-ERCC1), characterized by spontaneous, accelerated aging of multiple organ systems including the nervous system (Niedernhofer *et al.*, 2006). It is highly unlikely that this disease is caused by a defect in NER alone, but instead is caused by additional defects in other XPF-ERCC1 dependent DNA repair mechanisms, such as ICL or DSB repair.

Genetic deletion of *Xpf* or *Ercc1* in the mouse causes accelerated aging and a severely reduced lifespan of 3-4 weeks (Tian *et al.*, 2004; Weeda *et al.*, 1997). However, mice expressing 10% of the normal level of XPF-ERCC1 have a less severe phenotype and live 28 weeks (Weeda *et al.*, 1997). This leads to the hypothesis that the level of the XPF-ERCC1 nuclease available to engage in DNA repair mechanisms in the cell nucleus is the primary determinant in disease severity associated with mutations in *XPF*. Herein, we test this hypothesis using human patient cell lines and make the surprising discovery that in patients with mutations in *XPF*, the XPF-ERCC1 DNA repair complex is frequently mislocalized into the cytoplasmic compartment of cells, where it cannot participate in DNA repair.

3.2 RESULTS

3.2.1 Characterization of $R^{153}P$-XPF-ERCC1 activity in vitro

We first asked if mutations in XPF that cause mild or severe disease differentially affect the biochemical properties of XPF-ERCC1. To test this, we compared the biochemical properties of XPF-ERCC1 from two patients, XP42RO (an XP-F patient homozygous for $R^{799}W$ in *XPF* (Sijbers *et al.*, 1998)) and XP51RO (a patient with XFE progeroid syndrome homozygous for $R^{153}P$ in *XPF* (Niedernhofer *et al.*, 2006)) to that of wild type XPF-ERCC1. Recombinant XPF-ERCC1, XPF ^{R153P}-ERCC1 and XPF ^{R799W}-ERCC1 were purified from baculovirus-infected Sf9 insect cells using a His_6 tag on ERCC1. We previously reported [25] that our purified preparations of XPF^{WT}-ERCC1 elute from a gel-filtration column in three fractions: (1) a minor fraction in the void volume (~45 ml) containing aggregated, inactive protein; (2) active heterodimeric XPF-ERCC1 at ~65 ml, which corresponds to a molecular weight of ~ 200 kD, as expected, and (3) monomeric ERCC1, which peaks at ~78 mL, which corresponds to ~50 kD. Recombinant XPF^{WT}-ERCC1 eluted as expected (Figure 3-1A). In contrast, the majority of the mutant XPF-ERCC1 proteins eluted at ~45 mL in the void volume of the column, indicating that it was aggregated, likely due to protein misfolding. Nonetheless, we were able to purify a small amount of XPF ^{R153P}-ERCC1 and XPF ^{R799W}-ERCC1 from the fractions eluting at 65 ml (Figure 3-1B), indicating that at least some of the mutant protein formed a heterodimer, indicating that it is likely to be properly folded. SDS PAGE analysis of the complexes purified in an additional step over a heparin column, revealed dramatically reduced yields of the complexes of XPF^{R153P}-

ERCC1 and XPF^{R799W}-ERCC1 compared to XPF^{WT}-ERCC1 (Figure 3-1B). Similarly, in vivo, the amount of XPF detectable by immunoblot was substantially reduced in cells harboring the XPF^{R153P} and XPF^{R799W} mutations (XP51RO and XP42RO, respectively) compared to wt cells (C5RO) (Figure 3-1C).

The catalytic activity of the purified heterodimers was investigated by measuring their ability to incise a ^{32}P-end-labeled stem–loop DNA substrate at the single-strand/double-strand DNA junction in the presence of 0.4 mM $MnCl_2$ or 2 mM $MgCl_2$ and a 2-fold molar excess of protein over substrate. We previously observed that mutant XPF-ERCC1 complexes tend to be more active in the presence of Mn^{2+}, since this metal has less stringent requirements for the proper alignment of the active site residues (Enzlin and Scharer, 2002). Consistent with this, reactions in the presence of Mn^{2+} yielded the greatest activity leading to greater than 80% cleavage of the stem-loop substrate by wild type XPF-ERCC1 (Figure 3-1D). Incision was reduced to approximately 50% of the total substrate for XPF ^{R153P}-ERCC1 and XPF ^{R799W}-ERCC1. When Mg^{2+} was used as a cation, incision activity of wild type XPF-ERCC1 was not affected. However, catalytic activity of both mutant protein complexes was dramatically reduced in the presence of Mg^{2+} relative to Mn^{2+}. Notably, there was no dramatic difference in enzymatic activity between XPF^{R153P}-ERCC1 and XPF^{R799W}-ERCC1 on stem-loop DNA substrates, indicating that the biochemical basis for the more severe phenotype associated with the R^{153}P mutation is unlikely to be a simple loss of catalytic activity.

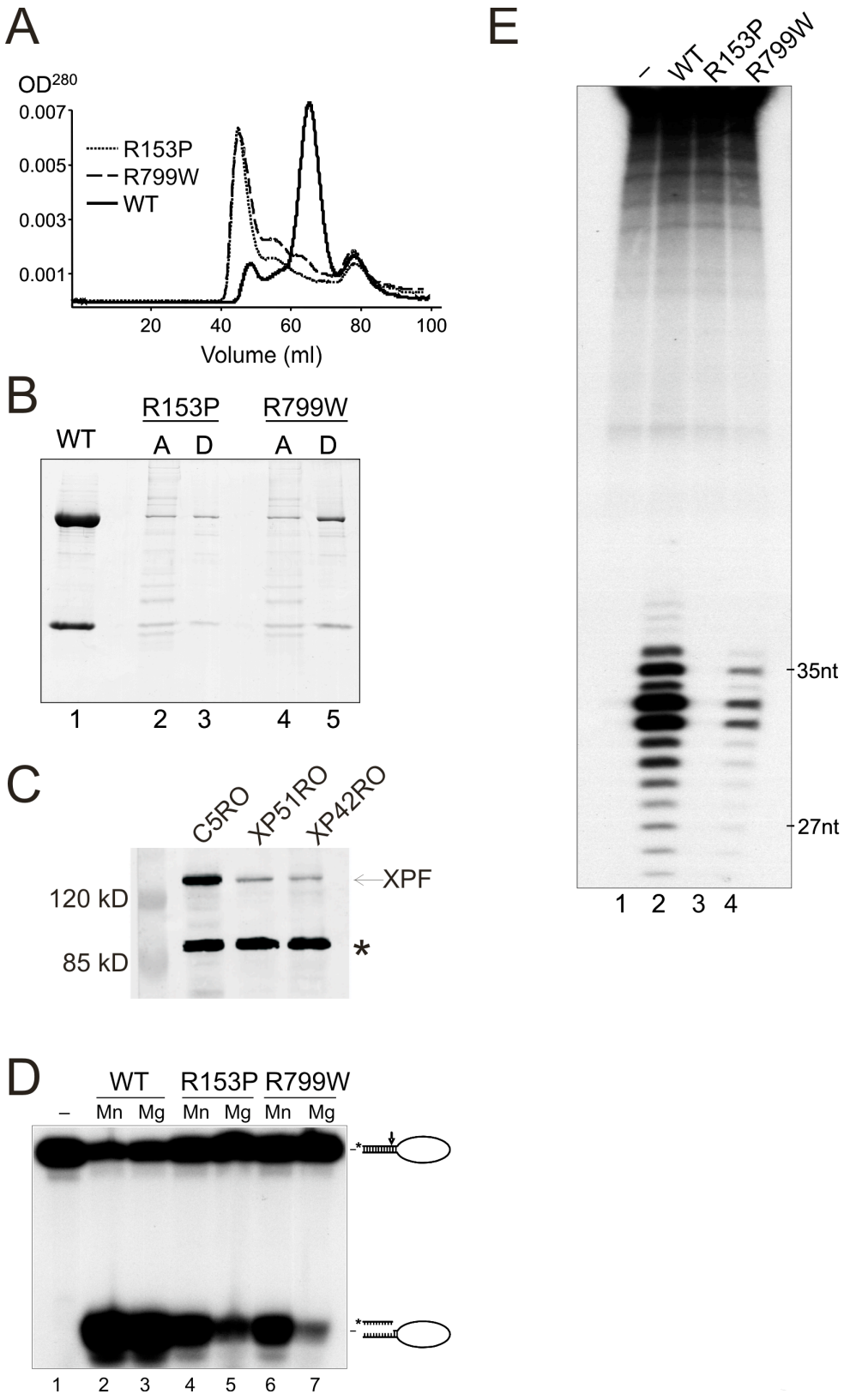

Figure 3-1: Biochemical characterization of XPF^{R153P}-ERCC1 and XPF^{R799W}-ERCC1 mutants

_A,_ Gel filtration profiles from the purification of recombinant XPF-ERCC1, XPF ^{R153P}-ERCC1 and XPF ^{R799W}-ERCC1 from baculovirus-infected Sf9 insect cells using a His_6 tag on ERCC1. Aggregated proteins elute at ~45 ml in the void volume of the column, heterodimeric XPF-ERCC1 elutes at ~65 ml, corresponding to ~ 200 kD, and monomeric ERCC1 elutes at ~78 ml (~50kD). _B,_ SDS PAGE analysis of purified protein complexes. Lane 1, 3 and 5 (labeled D): XPF-ERCC1, XPF ^{R153P}-ERCC1 and XPF ^{R799W}-ERCC1, respectively, after purification over NTA-agarose, gel filtration and heparin columns. Lanes 2 and 4 (labeled A) show the proteins present in the fractions eluting at 45 ml in the gel filtration column step of XPF ^{R153P}-ERCC1 and XPF ^{R799W}-ERCC1, respectively. _C,_ Immunodetection of XPF in normal (C5RO) and _XPF_ mutant cells. The star indicates the migration of a cross-reactive band demonstrating equal loading (Niedernhofer _et al._, 2006). _D_, Incision activities of XPF-ERCC1, XPF ^{R153P}-ERCC1 and XPF ^{R799W}-ERCC1 (200 fmol) on a 5'-^{32}P-labeled stem-loop DNA substrate (100 fmol) in the presence of either 0.4 mM $MnCl_2$ (lanes 2, 4 and 6) or 2 mM $MgCl_2$ (lanes 3, 5 and 7). Reactions were analyzed on a 15% denaturing polyacrylamide gel. The 46-mer substrate and 9-10-mer products are indicated. _E,_ In vitro NER activity of wt XPF-ERCC1, R^{153}P-XPF-ERCC1 and R^{799}W-XPF-ERCC1. A plasmid containing a single 1,3-intrastrand d(GpTpG)-cisplatin adduct was incubated with 500 µg of whole cell extracts expressing XPF-ERCC1, R^{153}P-XPF-ERCC1 and R^{799}-XPF-ERCC1. The excised fragments were detected by radiolabeled probe as described in Materials and Methods. The position of the 35 and 27 nucleotide marker bands from M_spI_ digested pBR322 plasmid are indicated.

To further probe the catalytic activity of these mutant protein complexes, their ability to incise an intrastrand cisplatin adduct was measured. A plasmid containing a single 1,3-intrastrand d(GpTpG)-cisplatin adduct was incubated with 500 µ g of whole cell extracts expressing XPF-ERCC1, XPF^{R153P}-ERCC1 and XPF^{R799W}-ERCC1. Incision yields radiolabeled fragments of 27-35 nucleotides in length, corresponding to the range of excision products in NER (Hohl *et al.*, 2007; Moggs *et al.*, 1996). Incision was observed in WCEs with XPF-ERCC1 and to a lesser extent XPF^{R799W}-ERCC1 (Figure 3-1E, lanes 2 and 4, respectively). No NER incision was observed in extracts from cells complemented with XPF^{R153P}-ERCC1. These

observations raise the possibility that the mutant heterodimers do not properly interact with the NER machinery. The loss of activity may however also be due to the fact that we were only able to obtain the mutant proteins in very low concentrations, which we have found to be problematic in NER assays in WCEs in other cases (JHE and ODS, unpublished observations).

3.2.2 Immunolocalization of XPF protein

$R^{153}P$ is situated in a lysine-rich domain of XPF that might be part of a complex nuclear localization sequence (NLS). Thus we next asked if mutant XPF was mislocalized in cells. Differential immunofluorescence was used to compare the sub-cellular localization of XPF in normal and *XPF* mutant cell lines in a single sample (Vermeulen *et al.*, 2000). Primary fibroblasts derived from an unaffected individual, an XP patient (XP42RO; XPF^{R799W}) and an XFE patient (XP51RO; XPF^{R153P}) were cultured in the presence of different sized beads in order to differentially label them. Subsequently, the labeled cell lines were co-cultured, fixed and immunostained on a single glass coverslip. XPF was detected exclusively in the nucleus of normal fibroblasts (Figure 3-2A, upper panels). In the same sample, XPF was detected in the cytoplasm of XP51RO cells ($R^{153}P$) creating a negative outline of the cell nucleus. In XP42RO cells ($R^{799}W$), the XPF signal was pancellular so that the nucleus and cytoplasm could not be distinguished from one another. To explore this further, we used immunofluorescence to detect XPF in additional XP-F patient cell lines and discovered that in all *XPF* mutant cell lines XPF was frequently detected in the cytoplasm. In fact, in all cases *XPF* mutant cell lines could be discriminated from normal fibroblasts by the staining pattern of the cell population. This was true irrespective of the antibody used [monoclonal 3F2 (Cancer Research UK), monoclonal Ab-1

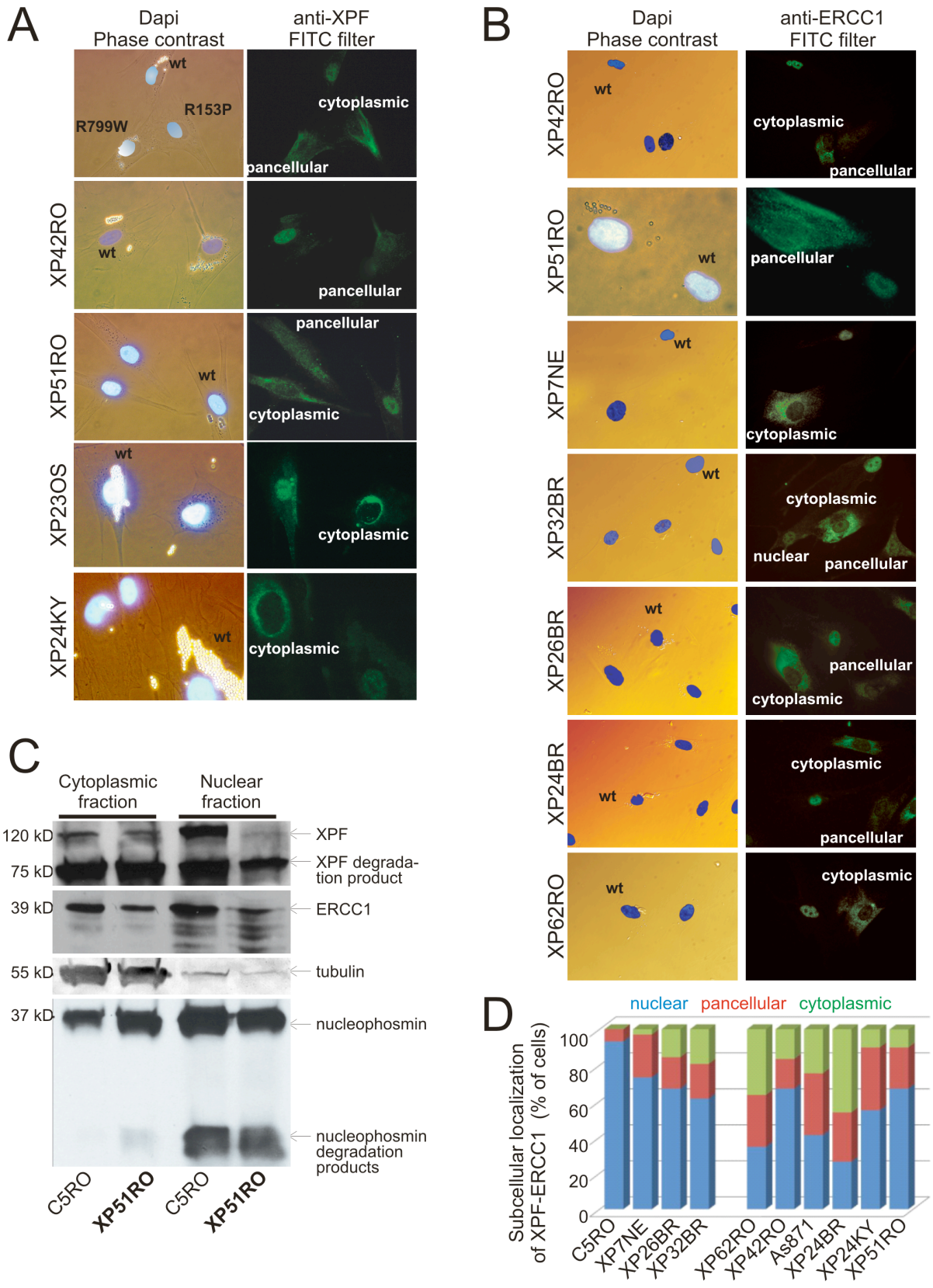

Figure 3-2: Differential immunofluorescence of cells from patients with *XPF* mutations

Fibroblasts from patients with mutations in *XPF* and a normal control were grown in the presence of different size beads. After 24 hr the cultures were washed to remove extracellular beads, mixed and co-plated on glass coverslips. The next day, the cells were fixed and immunostained as indicated. Cells were stained with Dapi to identify nuclei and examined by phase contrast microscopy to identify the cell type by their bead content and by fluorescence microscopy for immunodetection of XPF or ERCC1. *A,* Analysis of XPF protein sub-cellular localization. Cells from an unaffected individual were labeled with 2 μM beads; Xpf mutant cells were labeled with 0.8 μM beads. *B*, Analysis of ERCC1 subcellular localization in patients with mutations in *XPF*. *C*, Immunodetection of XPF and ERCC1 in nuclear and cytoplasmic fractions of normal fibroblasts (C5RO) and Xpf mutant cells (XP51RO). Tubulin is used as a loading control of the cytoplasmic fraction. Nucleophosmin is used as a loading control for the nuclear fraction. *D,* Quantitation of the fraction of cells containing exclusively nuclear XPF-ERCC1, XPF-ERCC1 in the nucleus and cytoplasm (pancellular) or exclusively cytoplasmic complex, as determined from immunofluorescence images (n≥100 cells per cell line).

(Neomarkers), or polyclonal anti-XPF (Erasmus Medical Centre)] (data not shown). This indicates that mislocalization of XPF in the cytoplasm is a common consequence of *XPF* mutation.

This observation raised the possibility that misfolding of mutant XPF caused abnormal subcellular localization of the protein. To address this, we immunostained *XPF* mutant cells for ERCC1, the obligate binding partner of XPF. ERCC1 was detected in the nucleus of normal (wt) fibroblasts. However, like XPF, ERCC1 was frequently detected exclusively in the cytoplasm of *XPF* mutant cells or pancellular (Figure 3-2B). All eight *XPF* mutant cells lines tested were readily distinguished from wt cells by the ERCC1 staining pattern. Furthermore the staining pattern for ERCC1 and XPF correlated for each cell line. This indicates that ERCC1 interacts with the mutant XPF proteins, indicating that mutant XPF is not entirely misfolded or degraded.

Furthermore, these results demonstrate that ERCC1 enters the nucleus as a heterodimer with XPF and that mutant XPF protein fails to target ERCC1 to the nucleus.

To further test this, wt and XPF^{R153P} fibroblasts were fractionated and nuclear and cytoplasmic XPF-ERCC1 was detected by immunoblot (Figure 3-2C). In wt cells, XPF-ERCC1 is predominantly nuclear. XPF-ERCC1 was detected in the cytoplasmic fraction, but to an extent proportional to nuclear contamination, as determined by immunodetection of the nuclear protein nucleophosmin. In the XP51RO cells, substantially more XPF and ERCC1 were detected in the cytoplasm than in the nucleus. Degradation products of both proteins are commonly detected on immunoblot, but were not overrepresented in the mutant cell line. Similar results were obtained for other *XPF* mutant cell lines (XP24BR, XP26BR and XP32BR) and using other antibodies against XPF and ERCC1 (data not shown). These data confirm the immunofluorescence data and support the conclusion that mislocalization of XPF-ERCC1 in the cytoplasm occurs in *XPF* mutant cells.

Remarkably, mislocalization of XPF-ERCC1 does not occur in all *XPF* mutant cells within a population. To quantify the phenomena, the fraction of cells with exclusively nuclear, exclusively cytoplasmic or pancellular XPF-ERCC1 was determined from immunofluorescence images (Figure 3-2D). In wt fibroblasts, 93% of cells have XPF-ERCC1 only in the nucleus and never is the complex seen exclusively in the cytoplasm. In all of the *Xpf* mutant cell lines, XPF-ERCC1 was detected exclusively in the cytoplasm of some cells, ranging from 3-46% of the total population. The fraction of cells with normal, nuclear XPF-ERCC1 ranged from 26-73%. The fact that all known XPF mutations lead to mislocalization of XPF-ERCC1 into the cytoplasm, yet not all cells harboring mutant XPF display cytoplasmic protein suggests that cytoplasmic XPF-ERCC1 may be rapidly degraded. Alternatively, there may be tremendous selection

pressure for cells with nuclear XPF-ERCC1, consistent with the notion that that repair complex is essential for human life. Indeed, serial passaging of XP51RO cells over years led to a striking increase in the fraction of cells with nuclear XPF-ERCC1 and reduced sensitivity to the crosslinking agent mitomycin C (Niedernhofer, unpublished data), likely leading to underrepresentation of the fraction of cells with cytoplasmic XPF-ERCC1 in Figure 3-2D, although these were relatively early passage cells.

3.2.3 Analysis of R153P mutation in *XPF* cDNA

To further rule out the possibility that the cytoplasmic XPF-ERCC1 detected was an artifact generated by non-specific antibodies, XPF^{R153P} and XPF^{WT} were tagged with YFP and expressed in *Xpf* mutant hamster cells (UV41 or UV47) for direct detection. The expression of fusion proteins was confirmed by immunoblot using antibodies against human XPF and GFP (Figure 3-3A). Immunodetection of XPF revealed numerous breakdown products of XPF, likely due to its overexpression, but only a single fusion protein migrating at the expected molecular mass of full length XPF-YFP. To determine if the fusion proteins were functional, transiently transfected cells were tested for their sensitivity to UV to measure NER and mitomycin C (MMC) to measure interstrand crosslink repair (Figure 3-3B). Wild-type XPF-YFP yielded near complete correction of the hypersensitivity of UV41 mutant cells to UV and MMC. By contrast, despite the fact that XPF^{R153P}–YFP was expressed to the same extent as XPF^{WT}-GFP, this protein was unable to correct either DNA repair defect (Figure 3-3B) as expected based on the hypersensitivity of the XP51RO patient cell lines (Niedernhofer *et al.*, 2006). To determine the sub-cellular localization of XPF^{R153P}, cells expressing the YFP-tagged protein was plated on glass coverslips and the protein detected by fluorescence microscopy (Figure 3-3C). XPF^{WT}-YFP

was exclusively in the nucleus. However, XPF^{R153P}–YFP was detected in the cytoplasm of 95% of the transfected cells. These results confirm that mutation of XPF leads to its mislocalization to the cytoplasm of cells.

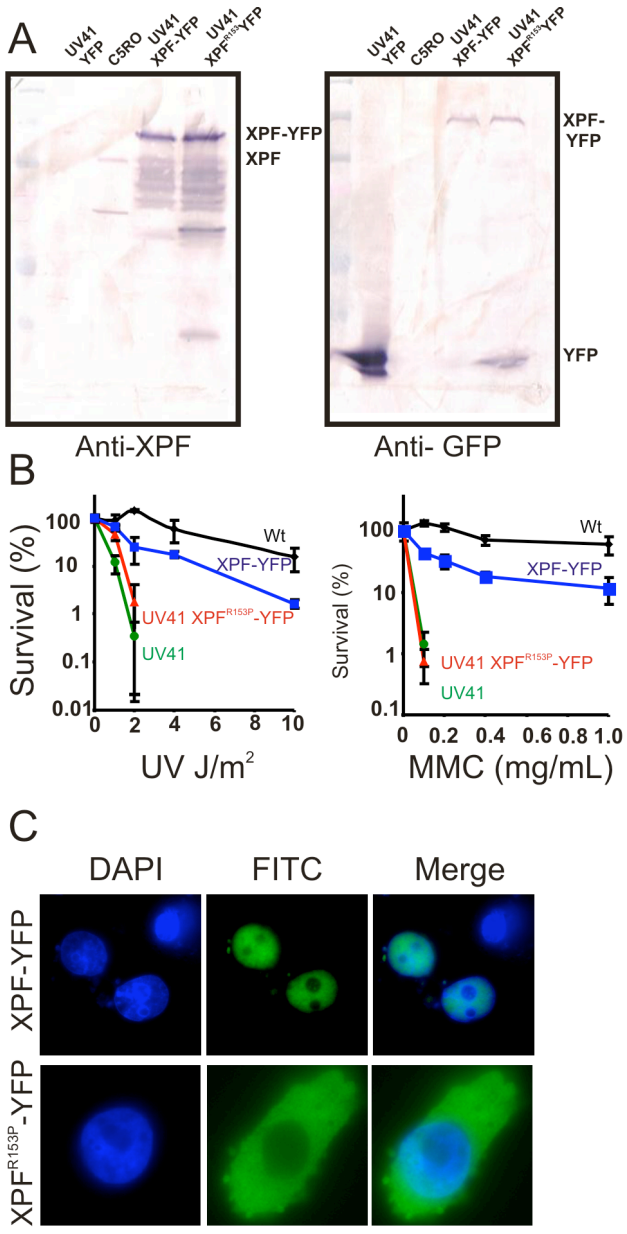

Figure 3-3: Characterization of XPF-YFP and XPF^{153}-YFP in CHO cells

***A,* Western blot analysis of XPF-YFP expressed in *Xpf* mutant cells. XPF-deficient hamster cell line, UV41, was transiently transfected with wild type *XPF-YFP* or *XPF^{153}-YFP* and the fusion proteins were detected using an antibody against XPF or GFP. C5RO was used as positive control for the XPF blot and as a**

negative control for the GFP blot. UV41 cells transfected with YFP alone was used as a negative control for XPF blot and as a positive control for GFP blot. *B,* Clonogenic survival of wild type (wt), XPF-deficient CHO cell line UV41, and UV41 transfected with wild type XPF-YFP and XPF^{153}-YFP after UV and MMC treatment. Colonies were counted 7-10 days after treatment and results are plotted as mean 3 independent experiments. *C,* Subcellular localization of wild type XPF-YFP and XPF^{153}-YFP after transient transfection in XPF-deficient the CHO cell line UV41 detected by fluorescence microscopy.

3.2.4 Characterization of XPF^{R153P}-ERCC1 activity in living cells

Unscheduled DNA synthesis (UDS) measures the incorporation of radiolabeled nucleotides in nuclei of non-S phase cells by autoradiography after exposure of the cells to ultraviolet radiation and is a direct measure of NER (Hoeijmakers *et al.*, 1990). The amount of UDS for patient cells is reported as a percent of UDS relative to that found in cells from an unaffected individual. Previously, UDS in cells from patient XP42RO (XPF^{R799W}) and XP51RO (XPF^{R153P}) was found to be 19% and <5%, respectively (Table 3-1). For all of the patient cell lines with the exception of XP51RO UDS levels are above background. This establishes that the mutant XPF proteins, with the exception of XPF^{R153P}, are catalytically active in vivo.

To test the ability of the mutant XPF-ERCC1 protein complexes to participate in NER in living cells, recombinant, purified XPF^{R153P}-ERCC1 and XPF^{R799W}-ERCC1 (Figure 3-1) were micro-injected into the nuclei of XP51RO primary fibroblasts. XP51RO cells were first fused on slides by treatment with inactivated Sendai virus to produce homopolykaryons (multinucleate cells). Only homopolykaryons were injected with protein, to permit distinction of cells injected. The slides were irradiated with 10 J/m^2 UV-C, cultured in the presence of ^{3}H-thymidine and nuclear grains indicating sites of thymidine incorporation in non-S phase cells measured (Figure 3-4). There was a significant increase in the number of grains detected in homopolykaryons

relative to individual cells in the same culture for all samples. Importantly, a similar level of UDS or NER was detected in homopolykaryons injected with XPF^{R153P}-ERCC1 and XPF^{R799W}-ERCC1 as wild type XPF-ERCC1. These data demonstrate that both mutant XPF complexes are enzymatically active once inside the nucleus and therefore that the severe phenotype seen in XP51RO is likely due to the inability of XPF^{R153P}-ERCC1 to enter the nucleus.

Table 3-1: Characteristics of *XPF* mutant cell lines

Patient	Mutation Allele 1	Mutation Allele 2	Age (yr)	Skin Cancer	Clinical features	UDS	UV sensitivity	% of cells with non-nuclear XPF-ERCC1	Ref
C5RO	none	none		-	normal	100%	1X	7%	(Sijbers *et al.*, 1998)
Father of XP42RO	R799W	none		-	photosensitivity without skin lesions	100%	1X	rare	(Sijbers *et al.*, 1998)
XP23OS	455fs	?*	45	-	mild XP	45%	4X	rare	(Arase *et al.*, 1979)
XP7NE	P379S	silent	28	-	mild XP	30%	2X	27%	(Berneburg *et al.*, 2000)
XP62RO°	R799W	R799W			mild XP with late onset neurodegeneration	20%	not reported	65%	
XP42RO°	R799W	R799W	62	+	mild XP with late onset neurodegeneration	20%	2X	33%	(Sijbers *et al.*, 1998)
XP2YO	T567A♦	657fs	65	+	mild XP	17%	3X	n.d.	(Matsumura *et al.*, 1998)
AS871	R589W	del exon3			severe XP with neurodegeneration	15%	2X	59%	
XP26BR	R799W	R799W			mild XP	15%	not reported	33%	
XP32BR	R589W	P379S	12	-	mild XP	10%	2X	39%	
XP24BR	R799W	R589W	29	-	severe XP with neurodegeneration	5%	3X	74%	(Berneburg *et al.*, 2000)
XP24KY	R799W	537fs + 7bp	50	-	XP with late onset neurodegeneration	7%	3X	45%	(Matsumura *et al.*, 1998)
XP51RO	R153P	R153P	16	-	neurodegeneration severe progeria	<5%	10X	>33%	(Niedernhofer *et al.*, 2006)

UDS unscheduled DNA synthesis
*The patient had normal levels of *XPF* transcript, suggesting one allele encodes a full-length mRNA.
♦Mutation not confirmed on genomic DNA.
°Siblings.

3.2.5 Clinical correlation

To determine if the severity of disease associated with a particular mutation in *XPF* could be predicted by the amount of XPF-ERCC1 detected in cell nuclei, the results in Figure 2D were compared to the clinical information about the patients from which the cells were derived (Table 3-1). In Table I, the cell lines were listed in order of decreasing UDS. Of note, for all patients for which the mutation in *XPF* was confirmed by sequencing genomic DNA, each is harboring one of four recurrent point mutations. The observations that *XPF* mutations are extremely rare, predominantly point mutations and redundant between patients are all consistent with the notion that *XPF* is essential for life.

Patients with mild disease tend to have greater UDS. Patients XP32BR and XP26BR could be exceptions, but they are too young to be certain. In Figure 3-2D, the cell lines are clustered into those from patients in which severe disease/neurodegeneration was documented (right) or not yet observed (left). There is a trend towards those with severe disease to have more non-nuclear XPF-ERCC1, but this trend did not reach significance (p=0.06, unpaired Student's t-test).

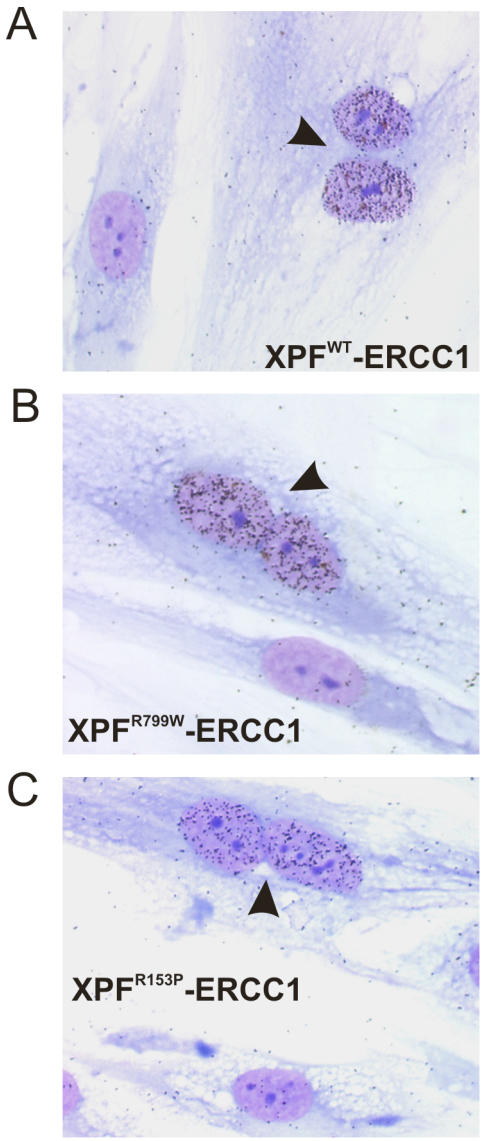

Figure 3-4: Correction of *Xpf* mutant cell NER defect by micro-injection of XPF-ERCC1

Primary fibroblasts from XFE progeroid patient XP51RO were fused to create homokaryons by treatment with inactivated lentivirus then plated on glass coverslips. Homopolykaryons were injected with recombinant XPF-ERCC1 protein complex *A*, wild-type *B*, XPF ^{R799W}-ERCC1 *C*, XPF ^{R153P}-ERCC1. The cultures were irradiated with 10 J/m^2 UV-C and ^{3}H-thymidine was added to the culture. UV-induced unscheduled DNA synthesis was detected by autoradiography. Homopolykaryons are indicated with arrows.

3.3 DISCUSSION

Classically, inherited mutations in a gene are associated with a single disease. However, mutations in several genes involved in the NER pathway can result in more than one disease. The most prominent example is XPD, which if mutated can cause the cancer-prone disease XP but also Cockayne Syndrome (CS), characterized by photosensitivity, growth retardation, developmental abnormalities and profound neurodegeneration, as well as trichothiodystrophy (TTD), which is similar to CS, but also involves the skin and nails (Taylor *et al.*, 1997). Similarly, mutations in XPB can also cause XP, TTD and a combined XP-CS (Vermeulen *et al.*, 1994) and mutations in XPG can lead to XP or XP-CS (Nouspikel *et al.*, 1997). Of all the genes whose products are required for NER, only XPB, XPD and XPG are required for the proper function and stability of the basal transcription factor TFIIH (Ito *et al.*, 2007). Thus the more severe symptoms of CS and TTD are attributed to a combined defect in NER as well as transcription (de Boer *et al.*, 2002; Kraemer *et al.*, 2007; Takayama *et al.*, 1996; Taylor *et al.*, 1997). More recently, mutations in *XPF* were linked to a second disease in addition XP, a disease of systemic accelerated aging termed XFE progeroid syndrome (Niedernhofer *et al.*, 2006). In this study, we investigated the underlying basis of how mutations in *XPF* cause disease.

3.3.1 Mutations in *XPF* do not ablate catalytic activity

Since CS and TTD are attributed to defects in transcription (van Gool *et al.*, 1997; Vermeulen *et al.*, 2000), the prediction is that mutations in XPB, XPD or XPG that cause CS or TTD should affect basal transcription in addition to NER, whereas mutations that affect only NER cause XP. Indeed, mutations in the catalytic domain of *XPG*, for example $A^{792}V$, disrupt the endonuclease activity of the XPG, but not its interaction with TFIIH and therefore causes classical XP (Clarkson, 2003). Similarly, a mutation in the helicase domain of XPD, $D^{234}N$, affects NER, but not basal transcription and therefore leads to XP (Dubaele *et al.*, 2003). By analogy, we examined the enzymatic activity of XPF^{R153P} and XPF^{R799W}, which cause XFE progeroid syndrome and XP respectively, and discovered that neither mutation ablates the catalytic activity of the protein (Figure 3-1). Recombinant proteins harboring either mutation are able to incise a stem-loop substrate in vitro, though less efficiently than the wild type protein. This demonstrates that these mutations in *XPF* do not prevent enzymatic activity of the nuclease.

3.3.2 Stability of XPF^{R799W}-ERCC1 and XPF^{R153P}-ERCC1 is reduced

Mutations in a single gene could potentially lead to distinct clinical outcomes if mutations differentially affect the stability of the gene product. For example, mutations affecting the stability of the TFIIH complex are linked with TTD but not XP (Vermeulen *et al.*, 2000). XPF levels are reduced in cells from patients with accelerated aging, carrying $R^{153}P$ and $R^{799}W$ mutations (Figure 3-1C), and a milder XP patient XP2YO (Niedernhofer *et al.*, 2007), compared to cells from unaffected individuals. Therefore mutant XPF may be rapidly degraded. However, XPF levels are similar all of these *XPF* mutant cells lines despite significantly different levels of

NER (Table 3-1). Therefore, it is unlikely that the severity of the disease caused by mutations in *XPF* is dictated by the level of expression or degradation of the mutant protein.

3.3.3 Mutations in *XPF* affect protein subcellular localization

The novel and unexpected finding is that mutation in *XPF* leads to increased cytoplasmic localization of the XPF-ERCC1 nuclease complex (Figure 3-2 and 3-3) and that this aberrant subcellular localization is what prevents XPF-ERCC1 from participating in DNA repair (Figure 3-4). This was demonstrated by immunofluorescence detection of the complex using multiple antibodies as well as by immunoblot after cellular fractionation (Figure 3-2). The results were confirmed by examining the subcellular localization of fluorescently tagged recombinant XPF (Figure 3-3).

Several human diseases are associated with misrouting or mislocalization of proteins, ranging from metabolic disorders to cancer. Mislocalization of proteins may result from a mutated nuclear localization sequence (NLS) or nuclear export sequence (NES). Remarkably, the majority of the missense mutations in *XPF* is at arginine residues and leads to conversion to a noncharged residues. So these mutations could affect a complex nuclear localization signal (NLS). All of the point mutations (R→P, R→W and P→S) are also predicted to alter protein structure and therefore may affect protein folding and/or protein:protein interactions that are critical for nuclear localization.

Mislocalization of the tumor suppressors p53 (Moll *et al.*, 1992), FOXO (Kau *et al.*, 2004), $p27^{Kip1}$ (Min *et al.*, 2004) and β-catenin (Rosin-Arbesfeld *et al.*, 2003) in the cytoplasm rather than the nucleus, leading to a loss of protein function, are associated with multiple cancers. In contrast, mislocalization of NF-κB (Karin *et al.*, 2002), BRCA1 and BARD1 (Fabbro *et al.*,

2002; Karin *et al.*, 2002) from the cytoplasm into the nucleus is also associated with a variety of tumors. A classic example of a disease caused by protein mislocalization is cystic fibrosis which is caused by retention of the cystic fibrosis transmembrane conductance regulator **(**CFTR) protein in the endoplasmic reticulum, instead of its localizing to the cell surface (Edwards *et al.*, 2000; Welsh and Smith, 1993). In addition, nephrogenic diabetes inspidus, retinitis pigmentosa, emphysema and α1-antitrypsin deficiency liver disease are also caused by mislocalized proteins (Edwards *et al.*, 2000).

Our data add XPF to the list of proteins that when mislocalized cause disease. In the case of XPF, it is the absence of XPF and its binding partner ERCC1 in the nucleus, causing reduced repair of genomic DNA that is disease-causing, rather than toxicity of mislocalized protein. The data also raise the possibility of a novel mechanism by which the DNA repair capacity of a cell is regulated: via proteins required for nuclear localization of XPF-ERCC1. Such proteins would be excellent targets for small molecule inhibitors that would reduce repair and thereby tumor resistance to genotoxic chemotherapeutic agents.

3.4 MATERIALS AND METHODS

3.4.1 Biochemical characterization of XPF^{R153P}-ERCC1 and XPF^{R799W}-ERCC1

Purification of recombinant XPF–ERCC1 was performed essentially as previously reported (Enzlin and Scharer, 2002) from baculovirus-infected Sf9 insect cells using a His_6 tag on ERCC1. In brief, plasmids pFastBac1-*XPF* and pFastBac1-*ERCC1*-His were used to transfect Sf9 insect cells, and to amplify the virus according to the manufacturer's instructions (BAC TO BAC system; Life Technologies). Cell extracts were prepared 65 hr after infection with an MOI of 5 and highly purified protein was obtained using chromatography on Ni−agarose, gel-filtration and heparin columns. Only XPF-ERCC1 eluting as proper heterodimer on the gel filtration column at ~65 ml of eluant was collected. The aggregated protein, eluting in the void volume (~40-50 ml), was not used in experiments.

The endonuclease activity of wild-type and mutant XPF-ERCC1 was performed using a stem−loop substrate also as previously described (Enzlin and Scharer, 2002). A stem12−loop22 oligonucleotide (GCCAGCGCTCGGT_{22}CCGAGCGCTGGC) was 5'-^{32}P end-labeled. Nuclease reactions were performed on 100 fmol of DNA substrate and 20-200 fmol of XPF-ERCC1 protein in a total volume of 15 µl in optimized nuclease buffer (25 mM HEPES pH 8.0, 40 mM NaCl, 10% glycerol, 0.5 mM β-mercaptoethanol, 0.1 mg/ml bovine serum albumin and 0.4 mM $MnCl_2$ or 2 mM $MgCl_2$). The reactions were incubated at 30°C for 2 h and stopped by adding 15 µl of 90% formamide/10 mM EDTA and heating at 95°C for 5 min. Samples were loaded onto

15% denaturing polyacrylamide gels and reaction products were visualized by autoradiography and quantified on a PhosphorImager (STORM860; Molecular Dynamics).

In vitro NER reactions were performed as described previously (Shivji *et al.*, 1999; Tsodikov *et al.*, 2005). In brief, a plasmid containing a single 1,3-intrastrand d(GpTpG)-cisplatin adduct was incubated with 500 µg of whole cell extracts prepared from XPF-deficient XP2YO cells complemented with recombinant XPF-ERCC1, XPF^{R153P}-ERCC1 or XPF^{R799W}-ERCC1. The fragments excised during NER were labeled by annealing them to a complementary oligonucleotide with a four guanosine 5' overhang and filling in the overhang with Sequenase and [α-^{32}P]-dCTP. Products were resolved on a 14% sequencing gel and detected by autoradiography.

3.4.2 Cell lines and culturing

Human fibroblasts immortalized with hTert were cultured in Ham's F10 with 10% fetal calf serum and antibiotics and incubated at 3% oxygen as described previously (Niedernhofer *et al.*, 2006). Cell lines included those derived from a normal individual (C5RO) (Poot *et al.*, 1987), the parent of a patient, heterozygous for a mutation in *XPF* (Sijbers *et al.*, 1998), XP-F patients (XP42RO) (Sijbers *et al.*, 1998), XP23OS (Arase *et al.*, 1979), XP24KY (Matsumura *et al.*, 1998), XP7NE (Berneburg *et al.*, 2000), XP32BR, XP26BR, XP24BR (Berneburg *et al.*, 2000), and XP62RO, and a patient with XFE progeroid syndrome caused by a mutation in *XPF* (XP51RO) (Niedernhofer *et al.*, 2006)

3.4.3 Immunodetection of XPF in patient cells

Cells were trypsinized, washed twice with PBS and lysed with 1 ml NETT buffer (100 mM NaCl, 50 mM Tris base pH 7.5, 5 mM EDTA pH 8.0, 0.5% Triton X-100) containing Complete™ mini protease inhibitor cocktail and phosphatase inhibitor cocktail (Roche Molecular Biochemicals). Then the lysates were freeze-thawed twice in liquid nitrogen to disrupt nuclear membranes. From each sample, 50 μg of protein was resolved on 10% SDS-PAGE gels after boiling for 10 min in the presence of loading buffer. XPF was detected using a human XPF monoclonal antibody (clone 219; Neomarker, Fremont, CA) at a dilution of 1:1000.

3.4.4 Differential immunofluorescence of fibroblasts isolated from patients with mutations in *XPF*

Cultures of primary human fibroblasts from patients with mutations in *XPF* or a normal individual were grown in the presence of different size beads (2 μm or 0.8 μm; Sigma). After 24 hr the cultures were trypsinized and washed extensively with phosphate-buffered saline to remove any extracellular beads. The cells were then mixed in various combinations and co-plated on glass coverslips to provide internal controls of normal XPF-ERCC1 protein levels (Vermeulen *et al.*, 2000). After 16 hr, the cells were fixed with 2% paraformaldehyde in sodium phosphate buffer, pH 7.4, for 15 min then permeabilized with 0.1% Triton X-100 in PBS. The samples were immunostained with polyclonal anti-ERCC1 (1:2000; (van Vuuren *et al.*, 1995)) or polyclonal anti-XPF (1:1000; (Sijbers *et al.*, 1996a)) followed by goat anti-rabbit ALEXA 488 (1:500; Molecular Probes). Samples were stained with Dapi to identify nuclei and examined by

phase contrast microscopy to identify the genotype of the cells according to their bead content and by fluorescence microscopy for immunodetection of repair proteins.

3.4.5 Cell fractionation

Cells were fractionated into nuclear and cytosolic fractions as described (Kapetanaki *et al.*, 2006), with minor modification. In brief, cells were trypsinized, pelleted and washed twice with PBS. The pellet was vortexed at maximum speed for 15 sec with 200 µl of CERI reagent from the Pierce NE-PER fractionation kit (Pierce Biotech) with Complete™ mini protease inhibitor cocktail, then incubated on ice for 10 min. This was followed by addition of 11 µl of CERII, vortexing for 5 sec and incubation on ice for 1 min. The mixture was spun at 13,000 rpm for 5 min and the supernatant collected as the cytosolic fraction. The nuclei in the pellet were suspended in extraction buffer (15 mM Tris-HCl pH 7.3, 1 mM EDTA, 0.4 M NaCl, 1 mM $MgCl_2$, 10% glycerol, 10 mM β -mercaptoethanol and Complete™ mini protease inhibitor cocktail), mixed for 1 hr at 4°C and spun down at 13,000 rpm for 10 min. The supernatant was collected as the soluble nuclear fraction.

3.4.6 Subcellular localization of XPF-YFP in Chinese hamster Ovary (CHO) cells

XPF cDNA was cloned into pYFP-N1 (BD Biosciences Clontech, Palo Alto, CA) such that YFP was expressed as fusion protein at the C-terminus of XPF. This construct, pXPF-YFP-N1, was then used to create XPF^{R153P}-YFP by QuickChange^{R} Site-Directed Mutagenesis Kit (Stratagene, Cedar Creek, TX) according to the manufacturer's instructions. The wild type and mutant constructs were transfected in XPF-deficient CHO cell lines UV41 or UV47 using

lipofectamine^{TM} 2000 (Invitrogen, Carlsbad, CA) following the manufacturer's instructions. Cells expressing YFP were flow sorted using Dako Cytomation MoFLo high-speed cell sorter (Dako North America, Carpinteria, CA) 24-48 hrs after transfection.

To study the subcellular localization of XPF, YFP-positive CHO cells were plated on glass coverslips and grown to 95% confluency. The next day, the samples were fixed with 2% paraformaldehyde in sodium phosphate buffer, pH 7.4, for 15 min. The cells were permeabilized with 0.1% Triton X-100 in phosphate-buffered and nuclei were stained with Dapi-vector shield (Vector Laboratories, Inc. Burlingame, CA). XPF-YFP was visualized using an Olympus BX51 fluorescent 4 microscope at 60-100X magnification.

3.4.7 Clonogenic survival assays of wild type and mutant CHO cells

Wild type (AA8), XPF-deficient (UV41), XPF-YFP and XPF^{R153P}-YFP cells were seeded in 6 cm dishes in triplicate at 10^3-10^4 cells per plate, depending on the dose of genotoxin. After 16 hr, the cells were irradiated with UV-C or exposed to mitomycin C (MMC). After approximately one week, the cultures were fixed and stained with 50% methanol, 7% acetic acid and 0.1% Coomassie blue. Colonies, consisting of at least 10 cells, were counted using a Nikon SMZ 2B 15 stereomicroscope microscope with 10X eyepiece. The data were plotted as the number of colonies that grew on the treated plates relative to untreated plates ± the standard error of the mean for 2-3 independent experiments.

3.4.8 Immunoblotting of XPF in Wt and mutant CHO cells

Whole cell extracts were prepared from C5RO and UV41 cells transfected with vectors expressing YFP, XPF-YFP or XPF^{R153P}-YFP. Proteins were separated by SDS PAGE using a 10% gel. XPF was detected using a human XPF monoclonal antibody (clone 219; Neomarker, Fremont, CA) at a dilution of 1:1000. YFP was detected using a GFP monoclonal antibody (Clones 7.1 and 13.1; Roche, Indianapolis, IN) at a dilution of 1:1000.

3.4.9 Correction of *XPF* mutant cell UV sensitivity by micro-injection of recombinant XPF-ERCC1

Microinjection of purified proteins was performed as previously described (de Jonge *et al.*, 1983; Weeda *et al.*, 1990). Briefly, primary human fibroblasts from XP51RO were fused by treating cultures with inactivated Sendai virus and then plated on glass coverslips. Subsequently, purified, recombinant XPF-ERCC1 protein complex (wild type or containing the R799W or R153P mutation in XPF) was injected into the nuclei of homopolykaryons. The cultures were irradiated with 10 J/m^2 UV-C and pulse labeled for 3 hrs with ^{3}H-thymidine. Unscheduled DNA synthesis (UDS) was detected by autoradiography.

4.0 IMMUNODETECTION OF DNA REPAIR ENDONUCLEASE ERCC1-XPF IN HUMAN TISSUE

This chapter was published in Cancer Research:

Bhagwat, N.R., Roginskaya, V.Y., Acquafondata, M.B., Dhir, R., Wood, R.D., and Niedernhofer, L.J. (2009b). Immunodetection of DNA repair endonuclease ERCC1-XPF in human tissue. Cancer research *69*, 6831-6838.

4.1 INTRODUCTION

It is important to identify molecular markers that help guide cancer treatment decisions to improve patient survival and quality of life in advanced stage disease. Non-small cell lung carcinoma (NSCLC), accounting for ~85% of all lung cancers in the United States, is a prime example. The overall five-year survival rate is only 17%, largely because NSCLC is rarely detected prior to dissemination and current methods of screening are ineffective (Patz *et al.*, 2000; Ries LAG, 2008). Platinum-based chemotherapy can improve survival when used as adjuvant therapy after surgical resection of NSCLC (Arriagada *et al.*, 2004; Winton *et al.*, 2005). For patients with stage IIIB or IV disease, platinum-based combination chemotherapy is the first line of treatment (Bulzebruck *et al.*, 1992; Bunn and Kelly, 1998). However, this is effective in

only a subset of patients. Prediction of which patients are mostly likely to respond to platinum-based chemotherapy is therefore imperative.

Cisplatin [*cis*-diamminedichloroplatinum(II)] and related platinum-based drugs inhibit cell proliferation because they cause DNA damage, including adducts on single bases, intrastrand crosslinks between two bases, and interstrand crosslinks (ICLs) between DNA strands (Eastman, 1987). The monoadducts and intrastrand crosslinks are repaired by nucleotide excision repair (NER), a DNA repair mechanism that excises helix-distorting lesions affecting one DNA strand. ICLs are repaired by mechanisms that remain poorly defined, but involve proteins from multiple DNA repair pathways including homologous recombination (De Silva *et al.*, 2000), Fanconi anemia (Friedberg, 2006; Niedernhofer *et al.*, 2005), translesion polymerases and NER (Collins, 1993). ERCC1-XPF is a structure-specific nuclease, that acts both in NER (Sijbers *et al.*, 1996a) and the repair of ICLs (De Silva *et al.*, 2000). Thus, ERCC1-XPF is uniquely important for protection against the cytotoxicity caused by cisplatin-induced DNA damage. If ERCC1-XPF levels vary between tumors, it would be an attractive target for use as a predictor of the efficacy of platinum-based chemotherapy.

XPF harbors the catalytic domain in the heterodimeric nuclease, (Enzlin and Scharer, 2002) and ERCC1 is required for DNA binding (Tsodikov *et al.*, 2005). The levels of ERCC1 are reduced in XPF-deficient mammalian cells and vice versa, suggesting that the proteins stabilize one another in vivo (Biggerstaff *et al.*, 1993). Due to the obligate nature of this partnership, it follows that cellular levels of the two proteins should be closely correlated and that either could potentially be a good biomarker of the response to platinum-based therapy.

There has been increasing interest in measuring the levels of ERCC1 in NSCLC specimens by immunohistochemistry (IHC) (Hwang *et al.*, 2008; Lee *et al.*, 2008; Olaussen *et*

al., 2006; Zheng *et al.*, 2007). ERCC1 expression, as measured by IHC, was reported to correlate with poor response to cisplatin chemotherapy and significantly decreased survival (Olaussen *et al.*, 2006). On the other hand, it has also been reported that increased ERCC1 in tumours was associated with longer survival after surgical treatment of NSCLC (Lee *et al.*, 2008; Zheng *et al.*, 2007). Unfortunately, the antibody (8F1) used in almost all studies is not specific for ERCC1 (Niedernhofer *et al.*, 2007). It recognizes human ERCC1, but also a second major nuclear antigen of unknown identity, and the antibody is unable to discriminate between cells expressing ERCC1-XPF and cells that do not (Niedernhofer *et al.*, 2007).

To determine if ERCC1-XPF is a biomarker for prognosis and making therapeutic decisions in NSCLC or other types of cancer, the specificity of relevant antibodies must be critically evaluated. Here we examine a collection of antibodies raised against each subunit of the nuclease for their ability to specifically detect their respective antigens in several applications. This not only provides reliable tools for the detection of ERCC1 and XPF in clinical specimens, but also illustrates a strategy for the validation of other antibodies against other potential biomarkers that could stratify patients according to cancer risk, response to therapy and prognosis.

4.2 MATERIAL AND METHODS

4.2.1 Cell lines, recombinant proteins and whole cell extract preparation

Primary human fibroblast cell lines C5RO (normal), XP51RO (*XPF* mutant) (Niedernhofer *et al.*, 2006), 165TOR (*ERCC1* mutant) (Jaspers *et al.*, 2007) and XP25RO (*XPA* mutant) were cultured in Ham's F-10 with 10% fetal bovine serum (FBS), antibiotics and non-essential amino acids. Transformed human fibroblasts XP2YO (XP-F) (Yagi *et al.*, 1991) were cultured in RPMI with 10% FBS, antibiotics and non-essential amino acids. CHO cell lines AA8 (wild-type) (Thompson *et al.*, 1980), UV47 (*Xpf* mutant) and 43-3B (*Ercc1* mutant) (Wood and Burki, 1982) were cultured in D-MEM with 10% FBS, antibiotics and non-essential amino acids. Mouse embryonic stem (ES) cell lines IB10 (wild-type) and clone 49 ($Ercc1^{-/-}$) (Niedernhofer *et al.*, 2001) were cultured in a 1:1 mixture of DMEM and Buffalo rat liver (BRL) cell conditioned media with 10% FBS, antibiotics, non-essential amino acids, 0.1 mM 2-mercaptoethanol and leukemic inhibitory factor (1000 units/ml, Gibco).

Recombinant XPF with an N-terminal His tag and ERCC1 with a C-terminal His tag were expressed from a dicistronic construct in *E. coli* and purified, as previously described (Kuraoka *et al.*, 2000). For preparation of whole cell extracts (WCEs), cells were grown to 80-90% confluence in 10 cm dishes or 75 cm^2 flasks, trypsinized and washed with PBS, and then lysed at 4ºC for 30 min with NP-40 lysis buffer (1% NP-40, 10% Glycerol, 20 mM Tris, pH 7.4, 137 mM NaCl, 2 mM Na_3V0_4 and protease inhibitor cocktail set III (Calbiochem).

4.2.2 Immunoblotting and immunoprecipitation

For immunoblotting, 50 µg of total protein from each WCE and 20 ng of recombinant HIS-tagged ERCC1 and XPF were boiled in 4X loading buffer (0.25 M Tris-HCl, pH 8.5, 8% SDS, 1.6 mM EDTA, 0.1 M DTT, 0.04% bromophenol blue and 40% glycerol), separated by SDS-PAGE (10% polyacrylamide gel), and transferred to a nitrocellulose membrane. Anti-ERCC1 and anti-XPF antibodies (listed in Table 4-1) were tested for their ability to specifically detect the respective proteins.

For immunoprecipitation, WCEs of C5RO cells were pre-cleared for 30 min by incubation with protein A+G agarose beads (Calbiochem) and incubated at 4ºC with 10 µl of each of the primary antibodies and 25 µl protein A+G beads with continuous mixing for 12 hr. The beads were collected by centrifugation at maximum speed (15 min), washed three times each with the NP-40 lysis buffer and PBS, boiled for 10 min in protein loading buffer, and eluted proteins separated by SDS-PAGE. Immunoprecipitated XPF was detected with anti-XPF antibody (Ab-1, Neomarkers, 1:1000) and AP conjugated goat anti-mouse secondary antibody (1:7500, Promega).

4.2.3 Immunofluorescence and UV-C-induced local damage

C5RO and XP2YO cells were plated at 75-80% confluence and labeled with 0.6 µm and 3 µm diameter latex beads (Sigma-Aldrich) respectively, as described (Botta *et al.*, 2002; Vermeulen *et al.*, 2000). After 24 hr, cells were washed three times with PBS, trypsinized and co-plated on coverslips. Twelve hr later, the cells were fixed with 2% paraformaldehyde (ICN Biomedicals) at 37ºC for 15 min. Triton-X-100 (0.2% in PBS) was used to permeabilize the cells and 5% BSA in

PBS was used for blocking. Primary antibodies were used as described in Supplemental Table 2. Goat anti-mouse IgG (1:1000), chicken anti-rabbit IgG (1:1000), goat anti-mouse IgG2b (1:500) or goat anti-mouse IgG1 (1:500) secondary antibodies conjugated either with Alexa fluor 488 or Alexa fluor 594 (Invitrogen) were used for visualization.

For co-localization of ERCC1-XPF with UVC radiation-induced cyclobutane pyrimidine dimers (CPD), experiments were performed as described (Mone *et al.*, 2001; Volker *et al.*, 2001) with minor modifications. C5RO cells grown on glass coverslips were irradiated with 60 J/m^2 UV through Isopore™ membrane filters (Millipore) with 8 μm pores to induce subnuclear domains of DNA damage. The cultures were then incubated in medium for 45 min to allow initiation of DNA repair, and then fixed with 2% paraformaldehyde with 0.15% Triton-X-100 for 15 min on ice. Samples were blocked with 5% BSA in PBS for 20 min at RT and incubated with anti-ERCC1 or anti-XPF antibodies at the same dilution as for immunofluorescence (Table 4-2) for 90 min at RT. Secondary antibodies were used as described above. This was followed by fixation with 2% paraformaldehyde for 10 min, denaturation with 2N HCl for 5 sec and blocking with 5% BSA in PBS for 20 min, all at RT. Cells were stained secondarily for CPDs using mouse anti-thymine dimer antibody (1:200, Kamiya Biomedical) for 90 min at RT and either Alexa fluor 488 or Alexa fluor 594 conjugated goat anti-mouse secondary antibodies (1:500, Invitrogen).

Table 4-1: Results of the antibody screen

Antigen	Antibody	Source	Origin	Clonality	WB			IP	IF	Local damage	IHC
					Human	Hamster	Mouse	Human	Human		
ERCC1	FL297	Santa Cruz	Rabbit	poly	+	-	-	+	+	+	+
	D-10	Santa Cruz	Mouse	mono	+	+	+	+	+	+	-
	3H11[1]	Cancer Research UK	Mouse	mono	+	-	-	+	-	-	-
	8F1[2]	Neomarkers	Mouse	mono	-	-	-	+	-	-	-
	RW018	Cancer Research UK	Rabbit	poly	+	-	-	+	-	-	-
	RW017	Cancer Research UK	Rabbit	poly	+	+	+/-	+	-	-	-
XPF	Ab-1	Neomarkers	Mouse	mono	+	-	-	+	+	+	-
	4H4	Cancer Research UK	Mouse	mono	+	-	-	+	+	+	+
	3F2	Cancer Research UK	Mouse	mono	+	-	-	+	+	+	+
	9A2	Cancer Research UK	Mouse	mono	+	+/-	+/-	+	-	-	-
	RA-1	Cancer Research UK	Rabbit	poly	+	+	+/-	+	-	-	-

[1]Available from several commercial vendors including Neomarkers (ERCC1 Ab-1).
[2]Stocks from Cancer Research UK were also tested. Available from several commercial vendors under other names including Neomarkers (ERCC1 Ab-2), Spring Biosciences (SPM243) and Santa Cruz.
Abbreviations: WB = immunoblot; IP = immunoprecipitation; IF = immunofluorescence; Local damage = Co-localization with UV-induced DNA damage; IHC = immunohistochemistry on paraffin embedded material.

4.2.4 Immunohistochemistry

C5RO, HeLa, XP42RO, XP51RO, 165TOR and XP2YO cells were grown to 75-80% confluence, fixed at room temperature with 10% neutral-buffered formalin for 15 min, and then collected by scraping. Cells were stored in neutral-buffered formalin at 4ºC for at least 3 hr, then pelleted by centrifugation (1,200 rpm, 5 min) and washed twice with PBS. Cells were resuspended in 500 µl of 80% ethanol, transferred to Eppendorf tubes containing 300 µl of solidified 1% low melting point agarose in PBS, and re-pelleted. The ethanol was aspirated and the bottoms of the tubes cut off. The agarose plugs containing the cells were pushed and molded into the caps of Eppendorf tubes and snap frozen on dry ice. The solidified pellets were extruded from the caps and paraffin embedded according to standard methods for tissue.

For immunohistochemical staining of the cell plug and paraffin embedded tissue sections, antigen retrieval was carried out at pH 6 (Dako Target retrieval solution, Dako) at 95°C for 20 min. Samples were blocked with 20% swine serum for 30 min and then incubated with either FL297 (anti-ERCC1, rabbit polyclonal, 1:250) or 3F2 (anti-XPF, mouse monoclonal, 1:1000) for 60 min at room temperature. Primary antibody signal was then detected using biotinylated anti-rabbit or anti-mouse secondary antibody for 30 min and DAB+ for 5 min at room temperature (Vectastain ABC kit; Vector Laboratories). Haematoxylin was used for counterstaining.

Table 4-2: Optimal antibody concentrations for immunoblots and immunofluorescence

Antibody	Dilution	
	Immunoblot	Immunofluorescence
FL297	1:1000	1:200
D-10	1:100	1:100
3H11	1:500	-
8F1	1:100	-
RW018	1:1500	-
RW017	1:1500	-
Ab-1	1:100	1:200
4H4	1:500	1:400
3F2	1:500	1:100
9A2	1:10000	-
RA-1	1:5000	-

4.3 RESULTS

A panel of antibodies against human ERCC1 and XPF, including commercially available reagents and those from our laboratory (Table 4-1), were tested for their specificity in immunoblotting, immunoprecipitation, immunofluorescence and IHC.

4.3.1 Immunoblotting and Immunoprecipitation

Antibodies were first screened for their specificity for ERCC1 or XPF by immunoblotting. Normal and ERCC1-XPF deficient human fibroblasts were lysed and immunoblotted along with recombinant His-tagged ERCC1 and XPF proteins (Figure 4-1A). Antibodies were categorized as specific for their target protein if they: 1) detected a band of the appropriate molecular weight (~116 kDa for XPF and 37 kDa for ERCC1) in normal cells (C5RO) and in *XPA* mutant cells (XP25RO), 2) detected the recombinant protein (slightly retarded in its migration due to the HIS-tag), 3) showed significantly reduced or no signal in *ERCC1* (165TOR) and *XPF* (XP2YO and XP51RO) mutant cell lines, and 4) did not detect additional bands of the incorrect molecular weight in both normal and mutant cells (results summarized in Table 4-1). All of the antibodies screened were specific for ERCC1 or XPF on immunoblotting (e.g., 3H11 and D-10 for ERCC1; 4H4 and 3F2 for XPF in Figure 4-1A) except for 8F1, which detected ERCC1 and an additional, spurious band of approximately 45 kDa. The spurious band is of equal intensity in normal and ERCC1-XPF deficient cells (Figure 4-1A, bottom, left panel and (Niedernhofer *et al.*, 2007)). Importantly, the spurious band picked-up by 8F1 is detected in extracts from fibroblast cell lines,

but not HeLa cell extracts (Figure 4-1B, indicated with a "?"), which were used previously as a negative control for immunodetection of ERCC1 (Olaussen *et al.*, 2007). All of the antibodies also detected degradation products of XPF or ERCC1 in cell lines with abundant ERCC1-XPF expression (Figure 4-1 A-C, bands marked by "*"). The optimal dilution of each antibody for immunoblotting was determined (Table 4-2).

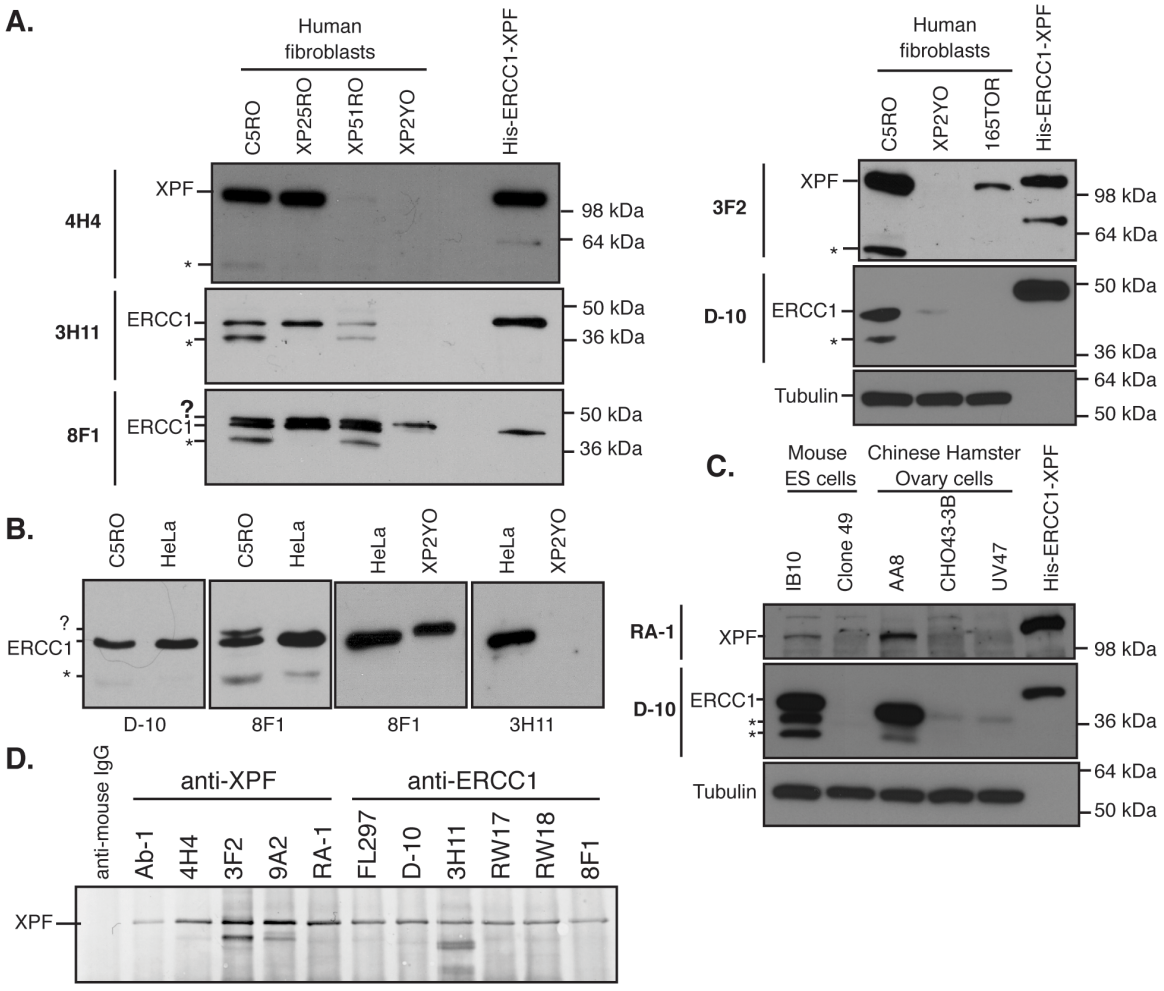

Figure 4-1: Immunodetection of ERCC1-XPF in whole cell extracts

***A*, Examples of how each of the test antibodies was screened for specificity for ERCC1 or XPF by immunoblot. WCEs were prepared from normal (C5RO), *XPA* mutant (XP25RO), *XPF* mutants (XP51RO and XP2YO) or *ERCC1* mutant (165TOR) human fibroblasts. Proteins were separated by SDS-PAGE and identified on the blot by loading recombinant His-tagged ERCC1-XPF. Blots were immunostained with each**

of the test antibodies (e.g., anti-XPF: 4H4 and 3F2, and anti-ERCC1: 3H11, D-10 and 8F1). Tubulin was used as a loading control. An asterisk (*) is used to denote degradation products of ERCC1 or XPF detected by all antibodies and a question mark (?) is used to denote an unidentified spurious band detected only by the 8F1 antibody. *B,* 8F1, but not D-10 or 3H11, detects a band that migrates more slowly than ERCC1 (denoted ?). This antigen is found in fibroblasts (C5RO and XP2YO), but not HeLa cells. *C,* Two examples of screening the test antibodies for their ability to detect ERCC1 or XPF in mouse or hamster cell extracts. Lysates were prepared from wild-type (IB10) and *Ercc1*$^{-/-}$ mouse embryonic stem cells (clone 49) as well as wild-type (AA8), *Ercc1* mutant (43-3B) and *Xpf* mutant (UV47) Chinese hamster ovary cells. These were run on SDS-PAGE along with recombinant His-tagged ERCC1-XPF. Blots were immunostained with each of the test antibodies (e.g., anti-XPF RA-1 and anti-ERCC1 D-10). Tubulin was used as a loading control. *D,* Immunoprecipitation of ERCC1-XPF from WCEs from normal human fibroblasts with each of the test antibodies. Precipitates were separated by SDS-PAGE, blotted and immunostained with antibody Ab-1 to detect XPF protein.

To further test the utility of these antibodies, WCE from wild-type and ERCC1-XPF deficient mouse embryonic stem cells (IB10 and clone 49, respectively) and Chinese hamster ovary cells (AA8, CHO43-3B [*Ercc1* mutant] and UV47 [*Xpf* mutant]) were also immunoblotted (Figure 4-1C). In general, cross-reactivity for mouse and hamster proteins was poor (Table 4-1). The only commercially available antibody that detected rodent ERCC1 was D-10 (Figure 4-1C).

Each of the ERCC1 and XPF antibodies were screened for their ability to immunoprecipitate their respective antigen from WCEs of normal cells (Figure 4-1D). The precipitates were all probed for XPF using antibody Ab-1. XPF was detected in all samples precipitated with antibodies against XPF, as well as antibodies against its obligate binding partner ERCC1, as expected (Niedernhofer *et al.*, 2007). Immunoblotting for XPF showed that all antibodies tested were able to immunoprecipitate the ERCC1-XPF nuclease, indicating that each is appropriate for this application (Table 4-1).

4.3.2 Immunofluorescence

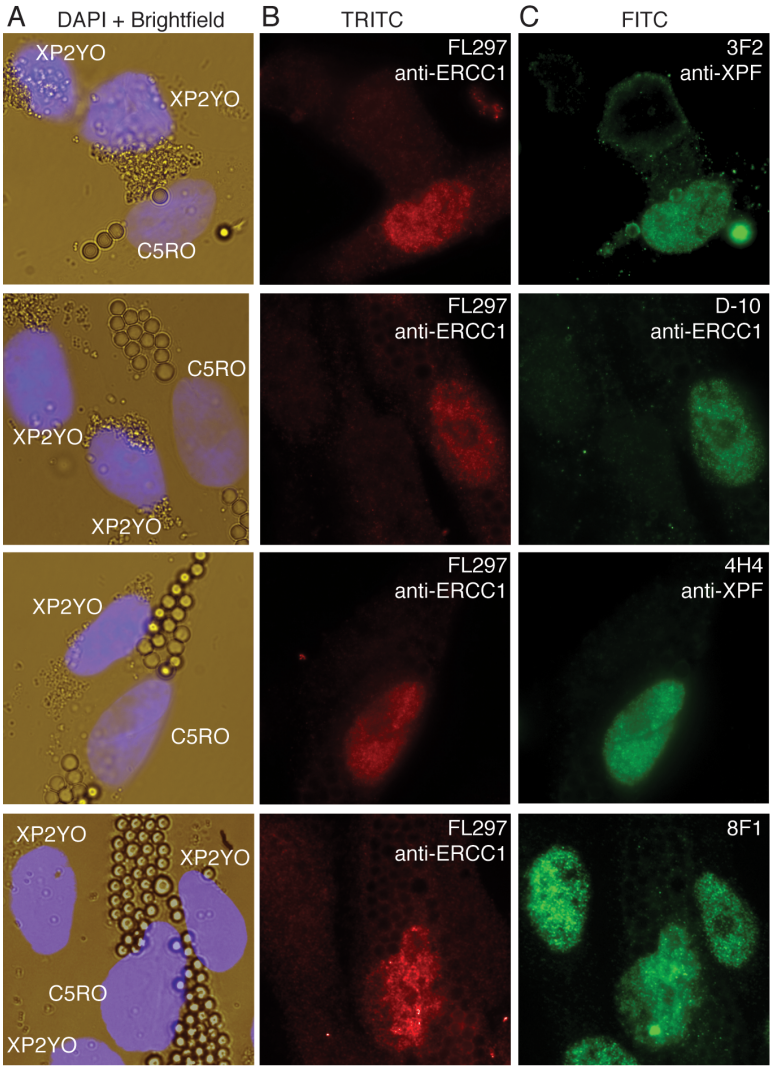

Figure 4-2: Immunofluorescence detection of ERCC1-XPF in cells

The cytoplasm of normal (C5RO) and ERCC1-XPF deficient *XPF* mutant human fibroblasts (XP2YO) was labeled with large and small latex beads, respectively. Then the cells were co-cultured on glass coverslips, fixed and stained. *A,* Brightfield images reveal both cell types in a single field. The nuclei are stained with DAPI. *B,* Immunostaining with antibody FL297 against ERCC1 distinguishes between the normal and ERCC1-XPF deficient cells. Nuclei of C5RO, but not XP2YO cells stain positively (red, Alexa-594). *C,* Co-immunostaining with each of the test antibodies (3F2, D-10, 4H4 and 8F1; secondary antibody

Alexa 488, in green) reveals which are specific for ERCC1-XPF. Only those nuclei that stain positively with FL-297 (red nuclei in B) should show green signal.

Antibodies that recognize denatured protein in immunoblots do not always detect their antigen in cells or tissues fixed with formaldehyde. Thus, each of the ERCC1 and XPF antibodies were screened for their ability to detect their respective antigen by immunofluorescence (IF) and immunohistochemistry (IHC). For IF, normal (C5RO) and *XPF* mutant human fibroblasts (XP2YO) were labeled with large (3 μm) and small (0.6 μm) latex beads, respectively, then co-cultured on glass coverslips to create a sample with an internal negative control (XP2YO cells). The coverslips were simultaneously immunostained with two antibodies (Figure 4-2): the test antibody against ERCC1 or XPF, and FL297 an antibody against ERCC1, which we previously established specifically recognizes ERCC1-XPF positive cells in immunofluorescence (Niedernhofer *et al.*, 2007). For the test antibody to be appropriate for IF application, it must stain the nuclei of normal cells only (those with large beads) and the same nuclei as FL297. Anti-XPF antibodies Ab-1, 4H4 and 3F2 and anti-ERCC1 antibody D-10 showed nuclear staining in normal cells (C5RO) and no staining in *XPF* mutant cells (XP2YO). Antibody 8F1 stained the nuclei of both cell types equally and therefore was unable to distinguish between normal and ERCC1-XPF deficient cells (Figure 4-2, bottom panels and (Niedernhofer *et al.*, 2007)). These data indicate that there are several commercially available antibodies (ERCC1: FL297 and D-10; XPF: Ab-1) appropriate for detecting ERCC1-XPF in human cells. Potential applications include fine needle aspirates and tumour biopsies.

4.3.3 UV-C induced local damage

When cells are irradiated with UV-C through a polypropylene micropore filter, DNA damage is induced in regions of the nucleus corresponding to the filter pores (Volker *et al.*, 2001). The sites of DNA damage can be identified with an antibody against UV radiation-induced cyclopyrimidine dimers (CPD) (Volker *et al.*, 2001). ERCC1-XPF localizes to these sites of damage during NER and thus co-localizes with CPDs by immunofluorescence (Volker *et al.*, 2001). Co-immunostaining of UV-C irradiated fibroblasts with anti-CPD antibody and test antibodies against ERCC1 or XPF revealed that the antibodies which discriminated between normal and ERCC1-XPF-deficient cells in IF also detected functional ERCC1-XPF in this local damage assay (Figure 4-3). Antibody 8F1, which was unable to discriminate between normal and ERCC1-XPF deficient cells in IF, did not yield a signal that co-localized with CPDs (Figure 4-3, bottom row). These results reinforce the IF data and indicate that several commercially available antibodies can be used to specifically detect ERCC1-XPF in fixed cells.

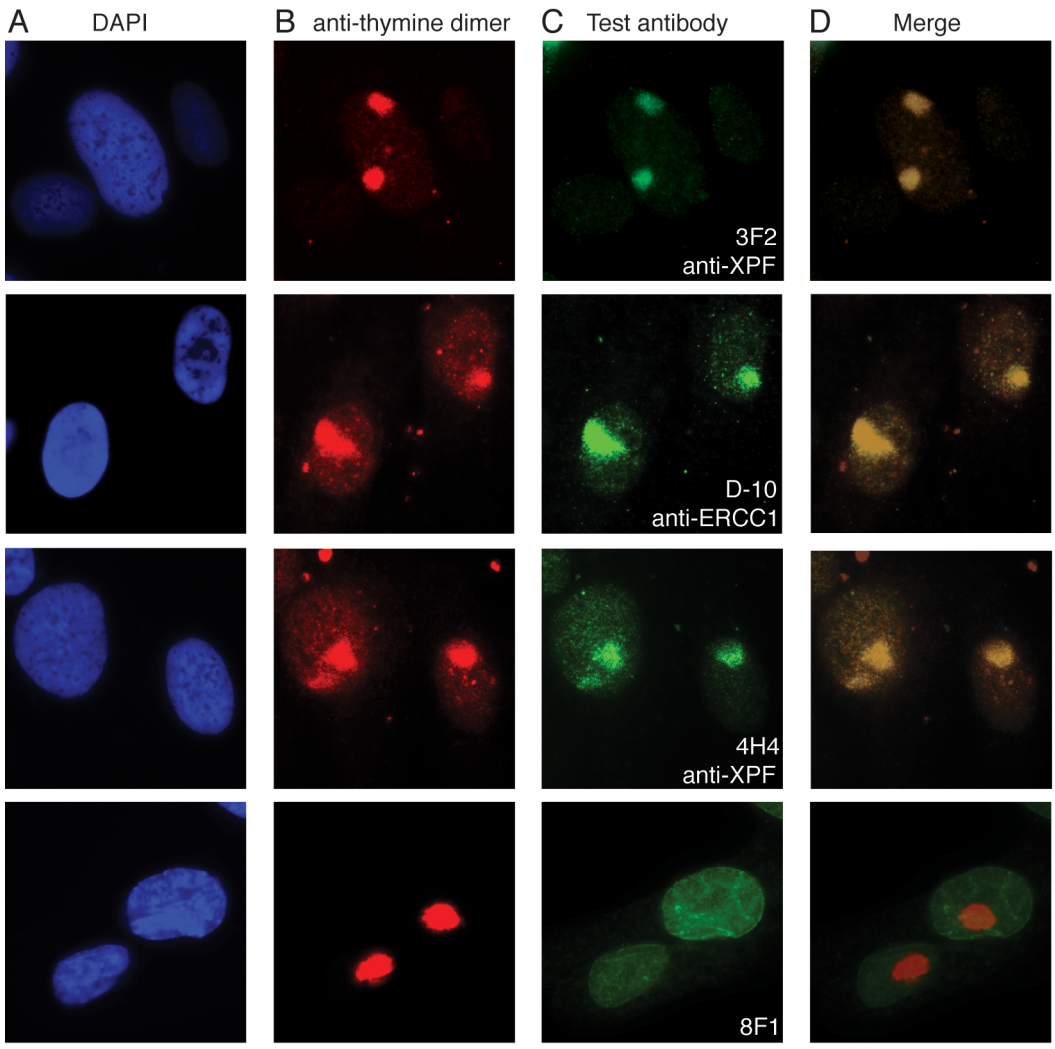

Figure 4-3: Immunofluorescence detection of ERCC1-XPF at sites of UV-C induced DNA damage

C5RO fibroblasts were irradiated with UV-C through a filter to induce sub-nuclear domains of DNA damage. The cells were stained with *A*, DAPI to identify the nuclei; *B*, anti-CPD to identify the sites of DNA damage and *C*, each of the test antibodies against ERCC1 or XPF. The merged images *D*, reveal which antibodies give a signal that co-localizes with UV-induced DNA damage, indicating their specificity for ERCC1-XPF DNA repair endonuclease.

4.3.4 Immunohistochemistry

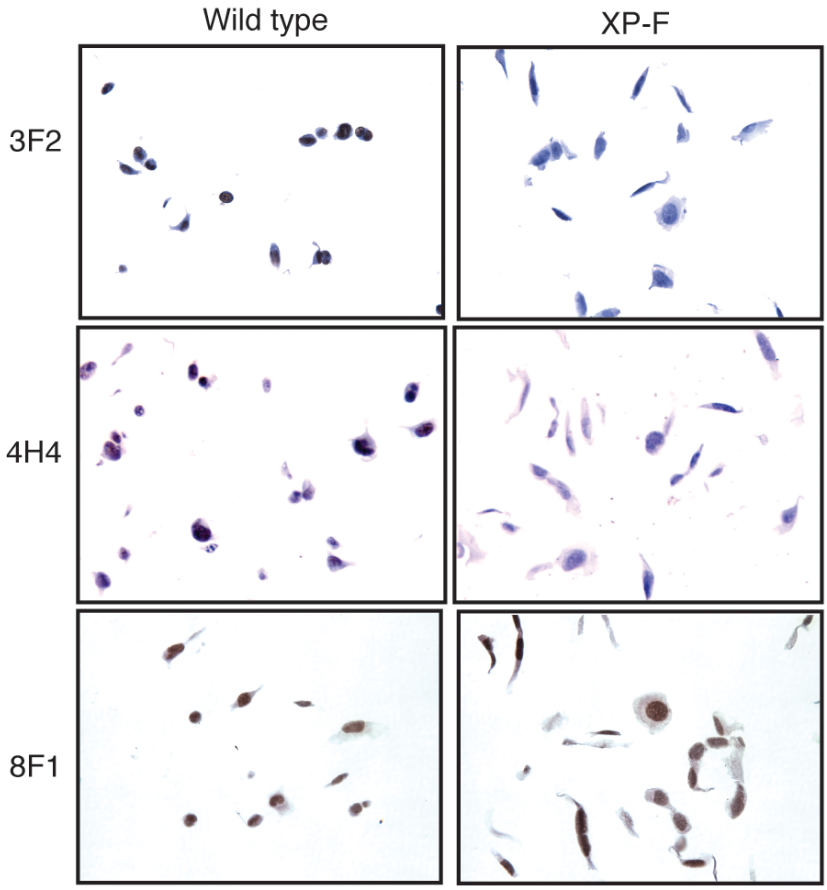

Figure 4-4: Immunohistochemical detection of ERCC1-XPF

Normal or ERCC1-XPF deficient human fibroblasts (XP2YO) were fixed in paraformaldehyde, pelleted in agarose, paraffin embedded, sectioned and stained as positive and negative controls, respectively, for IHC with antibodies against XPF (3F2 and 4H4) and ERCC1 (8F1). Notably, 8F1 was unable to discriminate between the normal and ERCC1-XPF deficient fibroblasts.

The most commonly used approach for measuring protein in tumors in clinical studies is IHC. However, for many essential proteins that are of interest as potential biomarkers in cancer prognosis, such as ERCC1 and XPF, true negative controls are not available. To circumvent this problem, we created paraffin-embedded blocks of normal and ERCC1-XPF deficient cell pellets for use as positive and negative controls to screen the test antibodies for their specificity in IHC.

Normal and *XPF* mutant human fibroblasts were fixed in paraformaldehyde, pelleted in agarose, embedded in paraffin, sectioned and immunostained, according to the method used for solid tumors. Antibody 3F2, against XPF, stained the nuclei of paraffin-embedded normal but not ERCC1-XPF deficient cells by IHC (Figure 4-4, first row). Similarly, antibody 4H4 against XPF (Figure 4-4, second row) was able to discriminate between normal and ERCC1-XPF deficient cells, indicating that both of these antibodies are appropriate for detection of XPF by IHC (Table 4-1). In contrast, antibody 8F1 against ERCC1 stained the nuclei of normal and ERCC1-XPF deficient cells equally (Figure 4-4, third row), demonstrating its inability to discriminate between ERCC1 positive and negative specimens by IHC, as previously observed for other applications (Niedernhofer *et al.*, 2007). Like 8F1, the other test antibodies were unable to discriminate between normal and ERCC1-XPF deficient cells by IHC (data not shown), with the exception of FL297. Antibody FL297 against ERCC1 was tested on six cell lines: two ERCC1-XPF proficient (C5RO and HeLa) and four ERCC1-XPF deficient (XP2YO, XP42RO, XP51RO and 165TOR). FL297 stained nuclei of both repair proficient cell lines (Figure 4-5, C5RO and HeLa). All ERCC1-XPF deficient cells (Figure 4-5, XP2YO, XP42RO, XP51RO and 165TOR) did not have nuclear staining, although there was a variable level of cytoplasmic staining in all cell lines. ERCC1-XPF functions exclusively as a nuclear complex. Thus the absence of nuclear staining indicates a negative result on IHC, as expected for these ERCC1-XPF deficient cell lines. HeLa cells showed a more intense nuclear staining than C5RO cells. This correlates with the relative expression of ERCC1 in these cell lines, indicating that FL297 can distinguish between different levels of ERCC1 on IHC. Therefore FL297 (anti-ERCC1), 4H4 (anti-XPF) and 3F2 (anti-XPF) are the only antibodies against ERCC1-XPF demonstrated to specifically detect this DNA repair nuclease by IHC.

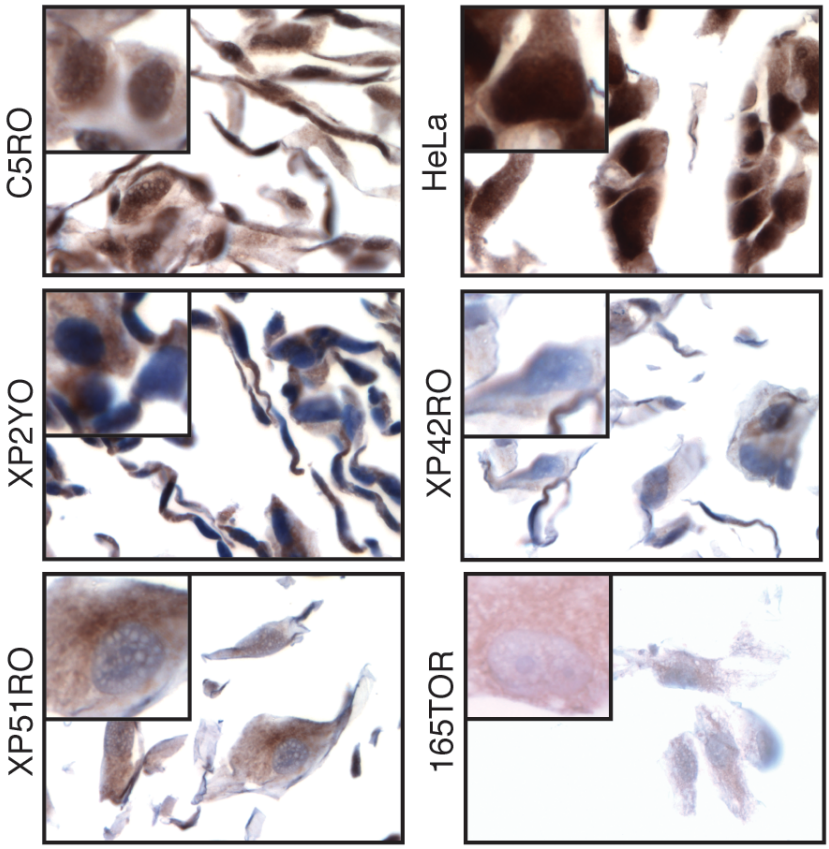

Figure 4-5: Immunohistochemical detection of ERCC1 by antibody FL297

Six human cell lines were paraffin-embedded, sectioned and stained with FL297. Two were ERCC1-XPF proficient: C5RO and HeLa, and four were ERCC1-XPF deficient: XP2YO, XP42RO, XP51RO and 165TOR.

Lung tumor sections stained with antibody 3F2 display highly variable nuclear staining in different NSCLC samples (Figure 4-6A), suggesting that expression of XPF may vary in tumors. Sections from the same NSCLC tumor were immunostained with FL297 (anti-ERCC1) and 3F2 (anti-XPF) to determine if both proteins are detected in the same cells as expected (Figure 4-6B). Both antibodies stained the same cell types with approximately the same intensity, confirming that ERCC1-XPF are co-expressed and both FL297 and 3F2 antibodies are appropriate for immunodetection of this repair complex in clinical specimens.

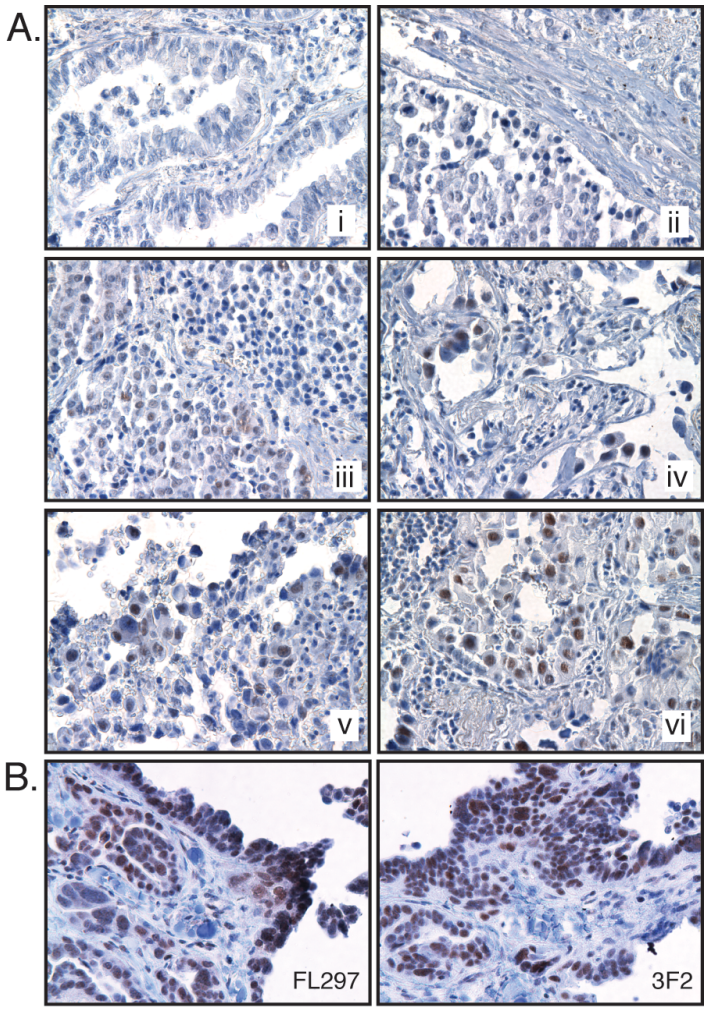

Figure 4-6: Immunohistochemical staining of lung tumors for ERCC1-XPF

***A*, Lung tumor sections were immunostained with 3F2. Representative sections have been arranged in increasing order of staining intensity (i-vi) showing the range of staining variability. *B*, Cross-sections of the same tumor stained alternately with FL297 (anti-ERCC1) and 3F2 (ant-XPF) showing similarities in staining patterns.**

4.4 DISCUSSION

For several types of common cancers, e.g., lung cancer, patient survival rates have not improved in the last decade (Jemal *et al.*, 2008). Response to therapy is highly variable, and in some cases, e.g., ovarian cancer, does not improve overall survival (Armstrong, 2002; Jemal *et al.*, 2008; McGuire *et al.*, 2002). This is particularly true for platinum-based therapies to which patients frequently become refractory (Modesitt and Jazaeri, 2007). Therefore, a major goal in oncology is to define biomarkers that can stratify cancer patients according to their likelihood of responding to chemotherapy. A highly active current focus of this effort is to measure expression of ERCC1 in tumors as a potential biomarker of DNA repair and therefore, resistance to genotoxic therapeutic agents (Rosell *et al.*, 2007; Simon *et al.*, 2007; Vilmar and Sorensen, 2008). To infer conclusions about the mechanism of therapy failure, it is imperative to rigorously standardize methods to accurately measure biomarker expression.

Immunohistochemistry (IHC) is an extremely valuable method for measuring tumor biomarkers. Unlike other immunological methods, IHC is applied to fixed specimens, which are the most abundantly available from surgical resections of tumors, allowing the large-scale screens necessary to validate the biological significance of novel biomarkers. Small amounts of tumor tissue, such as those obtained by needle biopsy, are sufficient for a semi-quantitative measurement of the antigen of interest. IHC is therefore used in decisions regarding diagnosis, prognosis and therapy of malignancies. However, there are multiple variables in the processing of samples in IHC and data analysis that need to be addressed prior to the widespread use of IHC as a quantitative immunoassay (Taylor and Levenson, 2006). The staining intensity is affected

significantly by the choice of fixative, the time of fixation (Grube, 2004), the extent of deparaffinization (Taylor, 1992), thickness of the tissue section (Grube, 2004), the antigen retrieval technique (Shi *et al.*, 1995), sensitivity and specificity of antibodies, and inter-observer inconsistencies in sample analysis (Taylor and Levenson, 2006). Furthermore, scoring of samples as positive or negative for a particular biomarker can be based on a subjective scale of staining intensity or percent of positively staining cells. Therefore, the importance of validating and standardizing every IHC protocol used in clinical trials cannot be overstated. In this manuscript we have critically analyzed the reagents available for measuring ERCC1 expression in tissue samples and developed a standardized method for ERCC1 IHC that could be applied to tumors.

In order to develop an IHC protocol, the first step is to identify an antibody that is specific for the target antigen. This is accomplished by immunoblotting using protein extracts from human cells or tissue and demonstrating that the antibody detects a single band of the appropriate molecular weight (Holmseth *et al.*, 2006; Pradidarcheep *et al.*, 2008). It is imperative to include positive and negative controls in which the antigen is known to be expressed or depleted (either genetically or by shRNA), respectively (Figure 4-1). Another excellent positive control is recombinant tagged protein included as a molecular weight control on immunoblot or overexpressed in a cell line (Figure 4-1). Of eleven screened antibodies that detect ERCC1-XPF, ten were specific for the repair complex (Table 4-1).

The second step in developing an IHC protocol is to validate that an antibody retains its specificity for an antigen in fixed samples (Holmseth *et al.*, 2006). This can be accomplished directly in tissue samples only if negative controls (tissues in which the antigen is not expressed) are available. For many of the tumor biomarkers this is not feasible because the antigens of

interest are key regulators of cell cycle control and genome maintenance, and thus are ubiquitously expressed. Alternatively, the specificity of an antibody to detect a biomarker in fixed material can be validated using positive and negative control cell lines processed according to the IHC protocol (Figure 4-4) (Holmseth *et al.*, 2006; Rhodes *et al.*, 2002). In our experiments, normal human fibroblasts (C5RO) were used as a positive control and XP-F patient fibroblasts (XP2YO), deficient in ERCC1-XPF, were used as a negative control due to the absence of human tissue samples missing this protein (Figure 4-4). Such internal controls must be included in every IHC analysis (Grube, 2004; Pradidarcheep *et al.*, 2008) (Leong, 2004). One important step in validating proper controls is establishing that the antigen staining has a proper subcellular localization, for example, ERCC1-XPF is a nuclear antigen (Figure 4-2). A second step that can provide internal validation of an immunostaining protocol is to differentially label the positive and negative control cell lines and co-culture them, creating a sample with both immunoreactive and unreactive cells (Figure 4-2).

Using the above methods with stringent controls, we discovered that antibody 8F1 is not suitable for measurement of ERCC1 expression because it detects a second antigen (Niedernhofer *et al.*, 2007). It has been reported that 8F1 could discriminate between HeLa cells and an isogenic strain in which ERCC1 expression was knocked down by siRNA (Olaussen *et al.*, 2007). Based on this, it was argued that 8F1 is suitable for measurement of ERCC1 by IHC. However, HeLa cells do not have appreciable amount of the non-specific antigen (Figure 4-1D) and are thus inappropriate for use as either positive or negative control for validating this antibody. In the present work, using formalin-fixed paraffin-embedded normal and ERCC1-XPF deficient cell lines, it was confirmed that 8F1 is unable to differentiate between normal and ERCC1 deficient cells by IHC (Figure 4-4). Since antibody 8F1 is the most widely used antibody

for IHC (Hwang *et al.*, 2008; Kim *et al.*, 2008b; Kwon *et al.*, 2007; Lee *et al.*, 2008; Olaussen *et al.*, 2006; Steffensen *et al.*, 2007), it is important to emphasize that it is not specific for ERCC1 and that validated alternative antibodies exist to reliably measure ERCC1 by IHC. The extensive literature on 8F1-IHC does however indicate that the antibody may have prognostic value. This warrants further investigation to identify the unknown antigen recognized by 8F1.

After testing a panel of antibodies raised against ERCC1 and XPF, antibodies suitable for a variety of immunodetection techniques were identified (Table 4-1). Most of these are unsuitable for IHC, primarily because they do not discriminate between positive and negative controls in fixed material. Those that do work (FL297, 4H4, 3F2) should facilitate the intense interest in measuring ERCC1 expression in tumor samples by IHC. These are validated alternatives to 8F1 that can be used to reliably measure ERCC1 and XPF by IHC. FL297 and 3F2 were used to measure ERCC1 and XPF, respectively, in lung tumor sections (Figure 4-6). Variable levels of cytoplasmic staining were seen in paraffin embedded cell lines (Figure 4-5). This staining does not correlate with the level of ERCC1-XPF in cells, nor their sensitivity to genotoxic stress. It should therefore be noted that when using these antibodies, grading of expression levels should be based on the extent of nuclear staining only. The levels of both proteins vary between specimens, ranging from intense staining to virtually no staining, but parallel one another (Figure 4-6). This indicates that either ERCC1 or XPF might serve as a biomarker of DNA repair in tumors. There was also differential expression within a tumor depending on the cell type. These results indicate that measuring ERCC1-XPF may be of value for stratifying patients for responsiveness to therapy.

5.0 MEASUREMENT OF ERCC1-XPF EXPRESSION IN OVARIAN CARCINOMA

5.1 INTRODUCTION

Ovarian carcinoma is the fifth most common cause of cancer deaths in women in the US. The death rate from ovarian carcinoma has remained relatively unchanged for last five decades. More than two-thirds of patients have advanced stage disease at the time of diagnosis (Jemal *et al.*, 2008). Primary therapy for these patients consists of debulking surgery followed by platinum-based chemotherapy (Vergote *et al.*, 2008). Of these women, approximately 25% are either refractory to chemotherapy or recur within 6 months of therapy, and usually die within 18 months (McGuire *et al.*, 1996; Ozols *et al.*, 2003; Piccart *et al.*, 2000). In effect these patients receive ineffective therapy that contributes further to their morbidity, lowering their quality of life. There is no way to predict the resistance to chemotherapy in these patients.

The cytotoxicity of platinum-based compounds is mediated through DNA monoadducts, and intrastrand and interstrand crosslinks (Rabik and Dolan, 2007). ERCC1-XPF functions in both DNA repair pathways required to repair this DNA damage, NER (Sijbers *et al.*, 1996a) and ICL repair (De Silva *et al.*, 2000). It is logical to hypothesize that ERCC1-XPF levels are predictive of resistance to platinum-based chemotherapy and by extension, treatment outcome.

Measurement of the levels of ERCC1 and XPF mRNA and protein in ovarian carcinoma specimens showed a wide range of expression among tumors. It was found that expression of

ERCC1 and XPF mRNA is closely correlated, as is that of the respective proteins. However, for both proteins, the levels of mRNA do not correlate to the levels of protein. This suggests that the protein levels are regulated at translational and/or post-translational levels.

5.2 RESULTS AND CONCLUSIONS

5.2.1 Levels of ERCC1 and XPF mRNA show wide variation

Measurement of mRNA levels from tumor samples revealed a wide range of expression. The median level of *ERCC1* mRNA was 6.02 (range: 0.91 – 79.89; 25th – 75th percentile: 2.58 – 11.55) (Figure 5-1) and the median level of *XPF* mRNA was 1.27 (range: 0.27 – 5.98; 25th – 75th percentile: 0.81 – 2.64) (Figure 5-2).

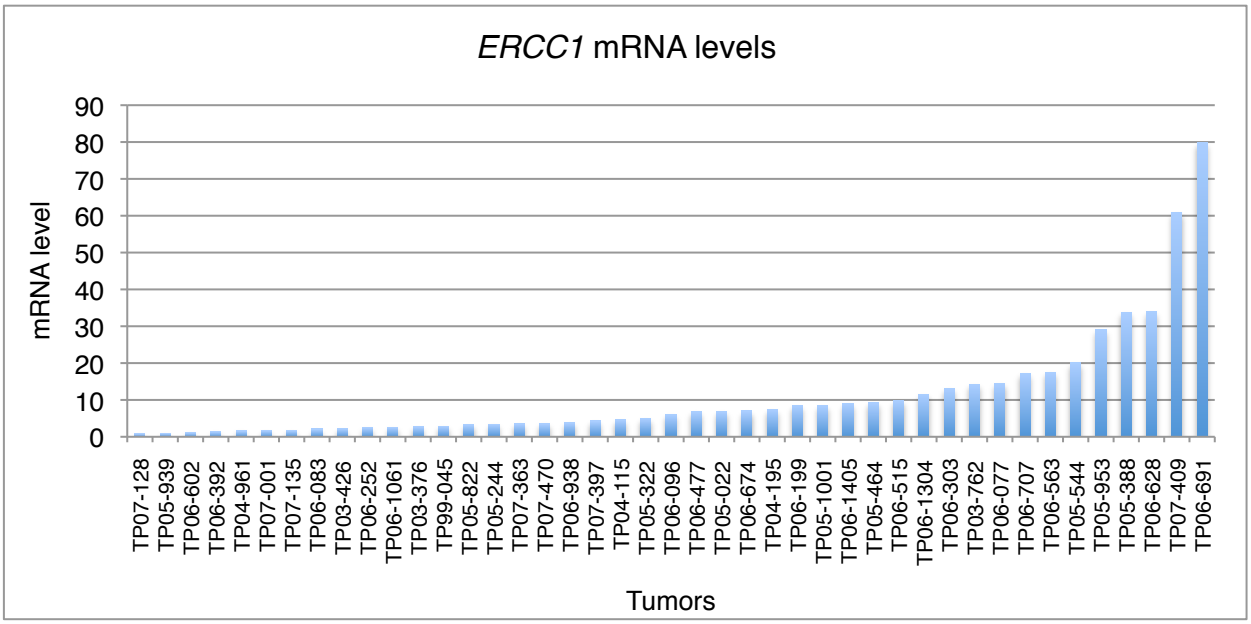

Figure 5-1: Tumor *ERCC1* mRNA levels

***ERCC1* mRNA levels in tumors were measured by qPCR. *ERCC1* mRNA levels are plotted on the Y-axis and the tumor identifiers are arranged on the X-axis in an increasing order of the levels of mRNA expression.**

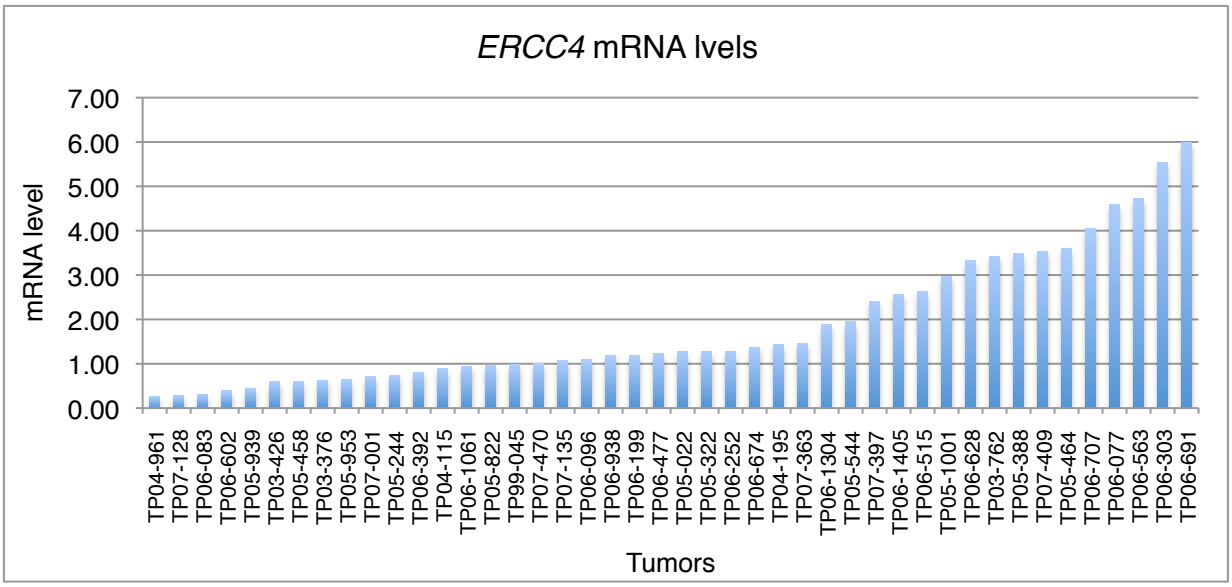

Figure 5-2: Tumor *XPF* mRNA levels

***XPF* mRNA levels in tumors were measured by qPCR. *XPF* mRNA levels are plotted on the Y-axis and the tumor identifiers are arranged on the X-axis in an increasing order of the levels of mRNA expression.**

5.2.2 ERCC1 and XPF mRNA levels are correlated

The levels of ERCC1 and XPF mRNA show strong positive correlation (Figure 5-3). Statistical analysis shows a Pearson r = 0.661 (p<0.001) and Spearman r = 0.827 (p<0.001).

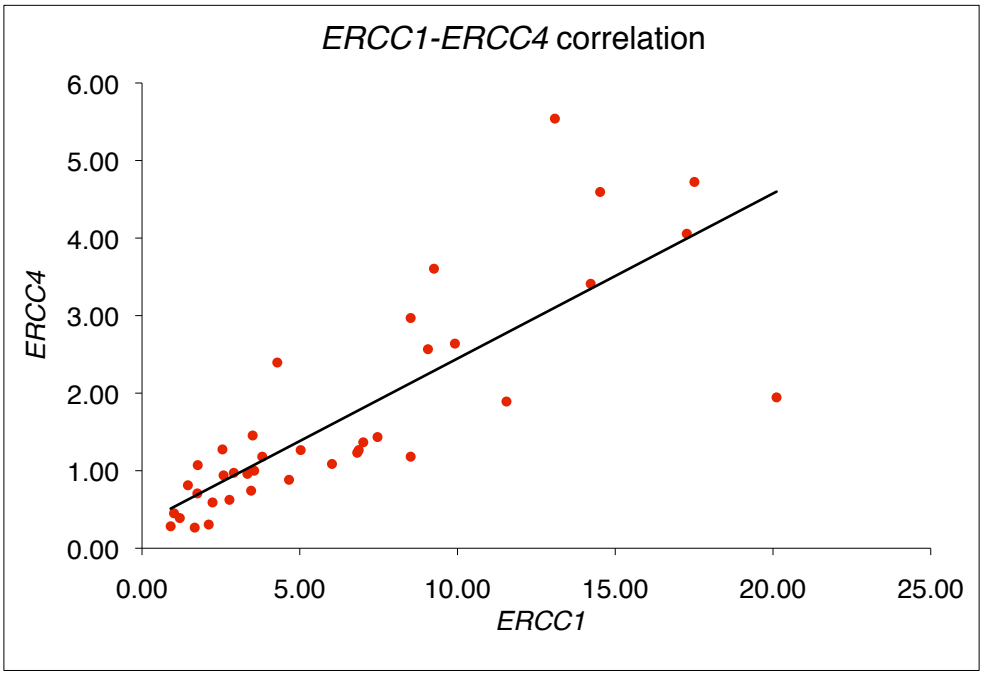

Figure 5-3: Correlation between *ERCC1* and *XPF* mRNA levels

Levels of *ERCC1* and *XPF* mRNA show strong correlation. *XPF* mRNA levels are plotted on the Y axis and *ERCC1* mRNA levels are on the X-axis.

ERCC1 and XPF protein levels vary widely

Immunoblots of proteins extracted from the ovarian tumor samples showed a large variation in levels of ERCC1 and XPF protein levels among tumors (Figure 5-4). The band intensity anaysis revealed more than 12-fold difference in XPF between tumors with the lowest and the highest XPF levels, and more than 5-fold difference ERCC1 between tumors with the lowest and the highest ERCC1 levels (Figure 5-5). The ratio of ERCC1 to XPF however, remained relatively constant (Figure 5-5). The levels of ERCC1 and XPF proteins showed a strong positive correlation (Figure 5-6) further showing that ERCC1 and XPF exist as a tightly bound heterodimer *in vivo*.

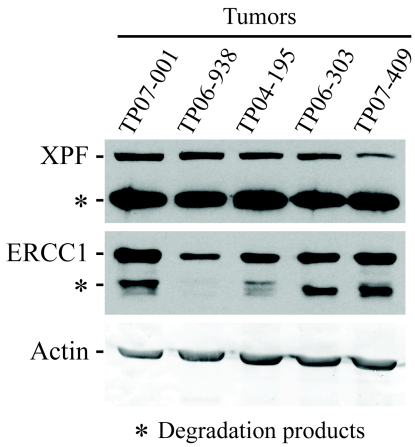

Figure 5-4: Immunoblot for ERCC1 and XPF

Ovarian tumor lysates were blotted for ERCC1 and XPF. Actin is the loading control. A selection of samples showing a range of protein expressions is shown.

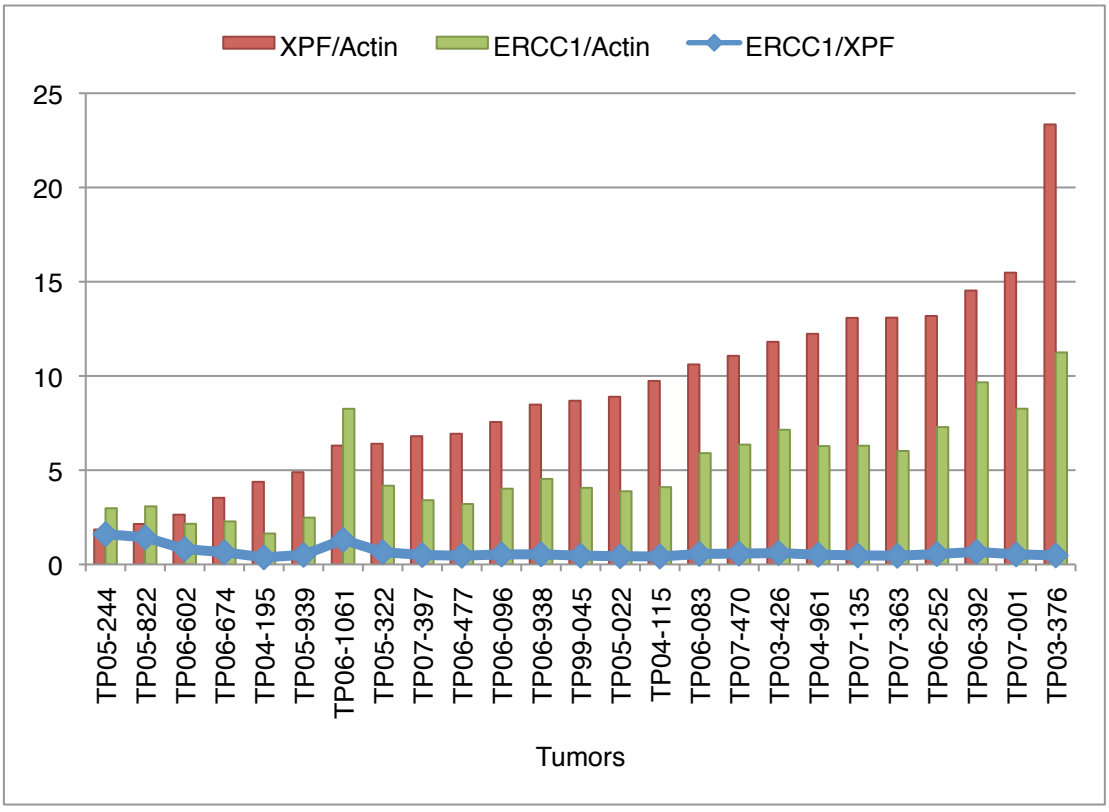

Figure 5-5: Levels of ERCC1 and XPF protein expression in ovarian tumors

Immunoblot band intensities of ERCC1 and XPF proteins were corrected with actin loading control and plotted on the Y-axis with tumor identifiers on the X-axis. The blue line represents the ratio between ERCC1 and XPF levels.

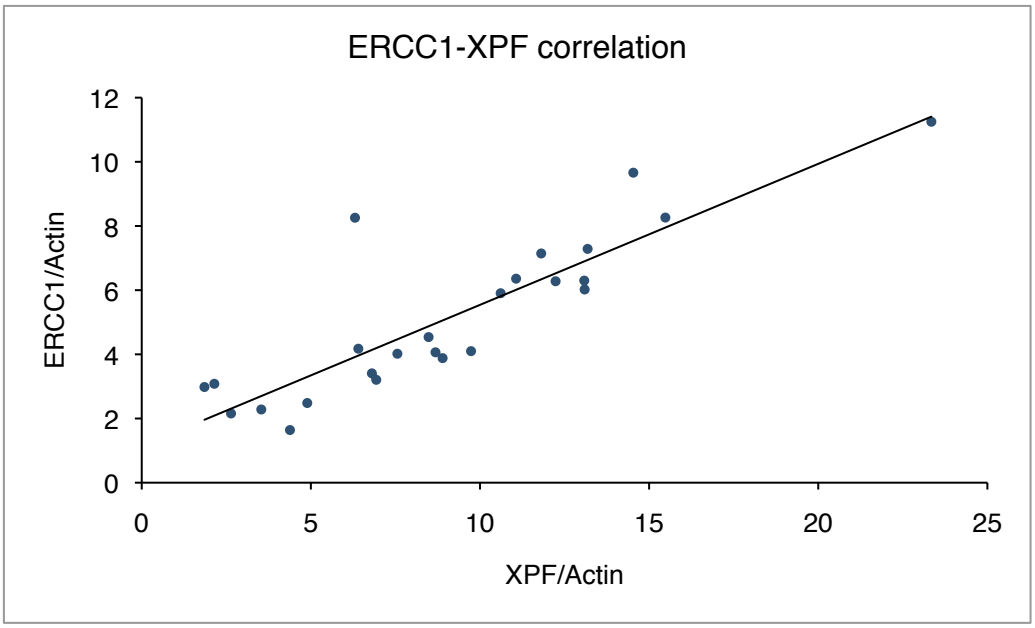

Figure 5-6: Correlation between levels ERCC1 and XPF in ovarian tumors

Levels of ERCC1 and XPF proteins show strong positive correlation. Actin-corrected ERCC1 protein levels are plotted on the Y-axis and corrected XPF protein levels are on the X-axis.

5.2.3 Protein levels do not correlate with mRNA levels

Tumors were charted in increasing order of the *ERCC1* mRNA expression. Corresponding ERCC1 protein levels did not show a pattern matching that of the mRNA levels (Figure 5-7). Charting the XPF mRNA and protein levels in a similar fashion failed to reveal any correlation between the two (Figure 5-8). This shows that a change in mRNA levels does not translate into a protein level change for either of these proteins. It is likely that ERCC1-XPF protein levels are not regulated at a transcriptional level.

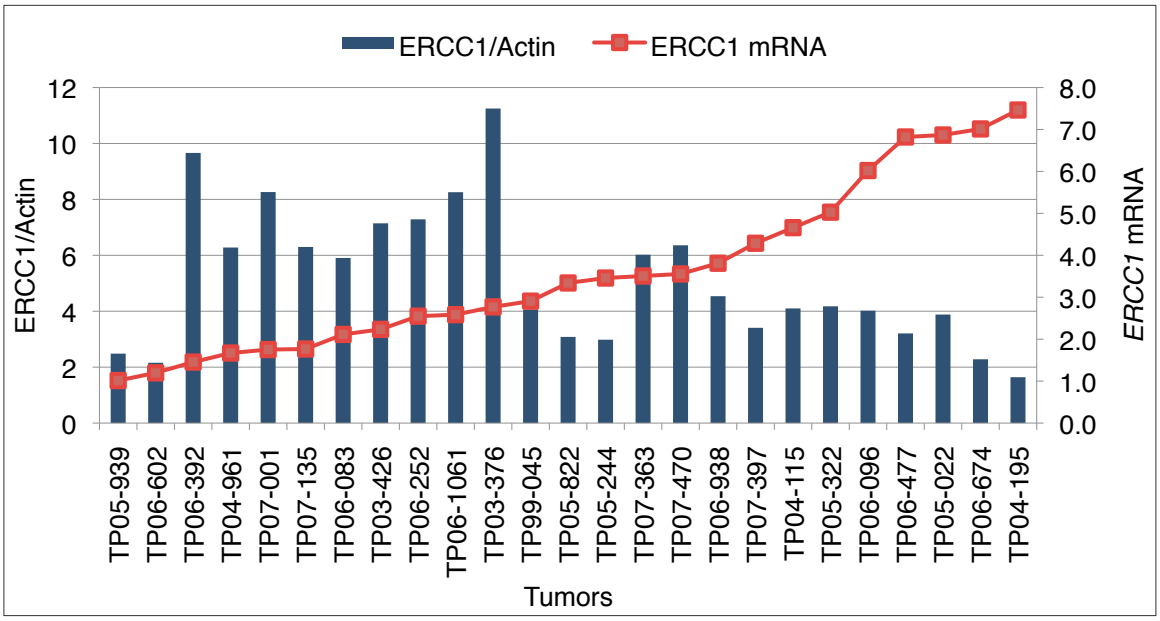

Figure 5-7: Correlation between ERCC1 protein and mRNA levels

ERCC1 protein and mRNA levels show no correlation. Actin-corrected ERCC1 protein levels are charted on the primary vertical axis, whereas *ERCC1* mRNA levels are charted on the secondary vertical axis.

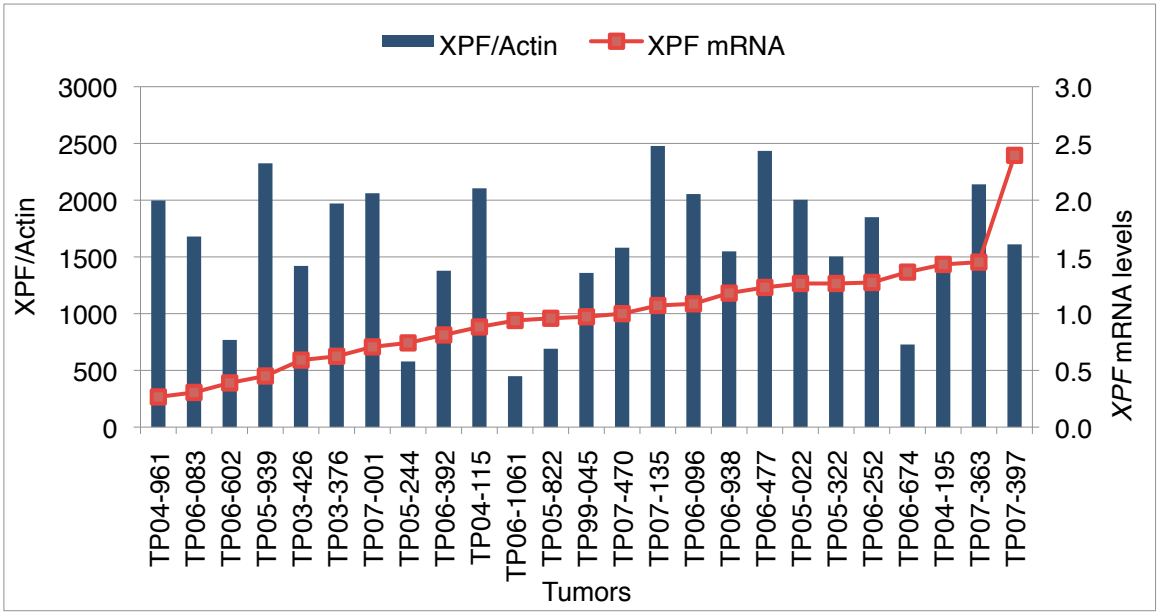

Figure 5-8: Correlation between XPF protein and mRNA levels

XPF protein and mRNA levels show no correlation. Actin-corrected XPF protein levels are charted on the primary vertical axis, whereas *XPF* mRNA levels are charted on the secondary vertical axis.

In conclusion, for both ERCC1 and XPF, the mRNA levels do not reflect the protein levels. Therefore, mRNA levels cannot be used as an indicator of protein expression of either ERCC1 or XPF. The expression of ERCC1 and XPF is closely correlated and therefore one can be used as a surrogate for the other.

It remains to be known if the levels of either protein or mRNA have any effect on the patient outcome and survival. This will be done by categorizing the tumors according to clinical outcome and drug resistance.

6.0 CONCLUSIONS

ERCC1 and XPF form a stable complex that acts as a structure-specific endonuclease (Sijbers *et al.*, 1996a). *Ercc1* and *Xpf* mutant mice and patients have a phenotype of premature aging that differs significantly from other NER-deficient counterparts (Niedernhofer *et al.*, 2006; Tian *et al.*, 2004). This difference in phenotypes is explained by the role of ERCC1-XPF in DNA repair mechanisms distinct from NER, such as ICL repair (Niedernhofer *et al.*, 2004).

Although it is known that ERCC1-XPF is required for crosslink repair, it was not known whether or how it interacts with another group of proteins that is very important for crosslink repair, the FA proteins. All FA proteins except FANCM-FAAP24 and FANCJ lack the ability to manipulate DNA. FANCM-FAAP24 and FANCJ do not possess nuclease activity required to excise the crosslink from the DNA (Ali *et al.*, 2009). It followed therefore that some nuclease, potentially ERCC1-XPF had to play a role in this pathway. As it is shown here, that was indeed the case (Bhagwat *et al.*, 2009a). This is an important finding, because it explains how nuclease processing of ICL occurs in the FA pathway. In addition, the FANCD2 monoubiquitination and chromatin localization events, which were thought to be simultaneous could be dissected and shown to be separate, which explains why without ERCC1-XPF, the DSBs produced during ICL repair cannot be resolved even though HRR-mediating proteins, such as RAD51 begin to localize to the site of damage (Al-Minawi *et al.*, 2009). This work also provides a clear evidence that the activation of the FA pathway by FANCD2 monoubiquitination can occur in the absence of both

ERCC1-XPF and EME1-MUS81, and therefore is independent of both DSB formation and ICL unhooking. This also means that blocked replication forks are probably sufficient for activation of ATR and the subsequent phosphorylation of proteins in the FA pathway. The mammalian ICL repair pathway has remained elusive due to the involvement of a wide array of DNA repair proteins, confounding the picture. By linking the nuclease component with the signaling and homologous recombination component of the mechanism, the model has made a definite forward progress. It is very important to elucidate this pathway as it has important contribution to the processes of cancer and aging.

Although we know that ERCC1-XPF deficiency causes a deficit in a variety of DNA repair pathways, the pleiotropy of these genes makes it difficult to interpret the phenotypes they present. It was found that XPF with mutations seen in some severe cases of XP-F and XFE still retained some amount of nuclease activity. This did not explain the severity of phenotype seen in the patients. It was found by cellular fractionation and immunofluorescence that these mutant proteins are unable to enter the nucleus. The mutant proteins are probably misfolded and therefore mislocalize to the cytoplasm. Indeed, microinjection of mutant proteins directly into the nucleus of ERCC1-XPF deficient cells corrected the phenotype of reduced UV-UDS in these cells. This revealed the role of proper folding and localization of proteins in the ERCC1-XPF deficiency phenotype. This also means that other genes such as those involved in protein folding and nuclear transport can affect the end result of an *XPF* mutation. This would explain the variation in disease severity in patients harboring the same mutation of *XPF*.

XP is a rare disease, with a 1 in 250,000 incidence in the US and Europe (Robbins *et al.*, 1974). This shows the importance of NER proteins to normal cell physiology. Due to the role of these proteins in prevention of mutagenesis and genomic instability, it is likely that they are

important for both the causation and progression of cancers. One may hypothesize that people with lower levels of NER and other DNA repair pathways would be more susceptible to oncogenesis through both endogenous and exogenous genotoxic stress. Also, tumors that express higher levels of DNA repair factors may be more resistant to genotoxic agents used to treat cancers, than tumors expressing lower levels of the same. If that were true, measurement of the levels of DNA repair proteins in tumors could be an invaluable tool in our battle against cancer. With the ability to predict whether or not a certain patient will respond to a specific treatment, it would be possible to devise personally tailored therapies that would improve survival outcome and quality of life for cancer patients. To test these hypotheses, it is of paramount importance that we develop tools for accurate measurement of DNA repair proteins. Immunohistochemistry has been traditionally used as a semi-quantitative method for measurement of biomarkers in tumors. However, this methodology is plagued with multiple variables that need to be carefully addressed before applying IHC to any study as a quantitative technique (Taylor and Levenson, 2006).

We have elaborated a rigorous approach to standardizing measurement of ERCC1 and XPF in tumors. Antibodies that could specifically detect ERCC1 and XPF in tumors with the ability to discriminate between different levels of these proteins have been found. Studies are now in progress to evaluate the possibility that ERCC1 and/or XPF may be predictive of tumor resistance or outcome. These studies will cover types of cancers that are treated with platinum-based chemotherapy including ovarian carcinoma, lung carcinoma and squamous cell carcinoma of head and neck. It remains to be seen if these proteins are indeed the useful tumor biomarkers they were hypothesized to be.

APPENDIX

LIST OF COMMON ABBREVIATIONS

AP site	Apurinic/apyrimidinic site
COFS	Cerebro-occulo-facio-skeletal syndrome
DSB	Double strand break
ERCC1	Excision repair cross-complementing rodent repair deficiency group 1
FA	Fanconi anemia
HN2	Nitrogen mustard
HRR	Homologous recombination repair
ICL	Interstrand crosslink
IR	Ionizing radiation
MMC	Mitomycin C

MMEJ	Microhomology-mediated end joining
NER	Nucleotide excision repair
NHEJ	Non-homologous end joining
NSCLC	Non-small cell lung carninoma
SNP	Single nucleotide polymorphism
SSA	Single strand annealing
XFE	XPF-ERCC1 progeroid syndrome
XP	Xeroderma pigmentosum
XP-F	Xeroderma pigmentosum complementation group F
XPF	Protein defective in XP-F

BIBLIOGRAPHY

Abraham, J., Lemmers, B., Hande, M.P., Moynahan, M.E., Chahwan, C., Ciccia, A., Essers, J., Hanada, K., Chahwan, R., Khaw, A.K., *et al.* (2003). Eme1 is involved in DNA damage processing and maintenance of genomic stability in mammalian cells. The EMBO journal *22*, 6137-6147.

Ahmad, A., Robinson, A.R., Duensing, A., van Drunen, E., Beverloo, H.B., Weisberg, D.B., Hasty, P., Hoeijmakers, J.H., and Niedernhofer, L.J. (2008). ERCC1-XPF endonuclease facilitates DNA double-strand break repair. Mol Cell Biol *28*, 5082-5092.

Al-Minawi, A.Z., Lee, Y.F., Hakansson, D., Johansson, F., Lundin, C., Saleh-Gohari, N., Schultz, N., Jenssen, D., Bryant, H.E., Meuth, M., *et al.* (2009). The ERCC1/XPF endonuclease is required for completion of homologous recombination at DNA replication forks stalled by inter-strand cross-links. Nucleic acids research.

Al-Minawi, A.Z., Saleh-Gohari, N., and Helleday, T. (2008). The ERCC1/XPF endonuclease is required for efficient single-strand annealing and gene conversion in mammalian cells. Nucleic acids research *36*, 1-9.

Ali, A.M., Singh, T.R., and Meetei, A.R. (2009). FANCM-FAAP24 and FANCJ: FA proteins that metabolize DNA. Mutation research *668*, 20-26.

Altaha, R., Liang, X., Yu, J.J., and Reed, E. (2004). Excision repair cross complementing-group 1: gene expression and platinum resistance. International journal of molecular medicine *14*, 959-970.

Andreassen, P.R., D'Andrea, A.D., and Taniguchi, T. (2004). ATR couples FANCD2 monoubiquitination to the DNA-damage response. Genes & development *18*, 1958-1963.

Araki, M., Masutani, C., Takemura, M., Uchida, A., Sugasawa, K., Kondoh, J., Ohkuma, Y., and Hanaoka, F. (2001). Centrosome protein centrin 2/caltractin 1 is part of the xeroderma pigmentosum group C complex that initiates global genome nucleotide excision repair. The Journal of biological chemistry *276*, 18665-18672.

Arase, S., Kozuka, T., Tanaka, K., Ikenaga, M., and Takebe, H. (1979). A sixth complementation group in xeroderma pigmentosum. Mutat Res *59*, 143-146.

Aravind, L., Walker, D.R., and Koonin, E.V. (1999). Conserved domains in DNA repair proteins and evolution of repair systems. Nucleic acids research *27*, 1223-1242.

Armstrong, D.K. (2002). Relapsed ovarian cancer: challenges and management strategies for a chronic disease. Oncologist *7 Suppl 5*, 20-28.

Arriagada, R., Bergman, B., Dunant, A., Le Chevalier, T., Pignon, J.P., and Vansteenkiste, J. (2004). Cisplatin-based adjuvant chemotherapy in patients with completely resected non-small-cell lung cancer. N Engl J Med *350*, 351-360.

Auerbach, A.D., and Wolman, S.R. (1976). Susceptibility of Fanconi's anaemia fibroblasts to chromosome damage by carcinogens. Nature *261*, 494-496.

Bae, J.B., Mukhopadhyay, S.S., Liu, L., Zhang, N., Tan, J., Akhter, S., Liu, X., Shen, X., Li, L., and Legerski, R.J. (2008). Snm1B/Apollo mediates replication fork collapse and S Phase checkpoint activation in response to DNA interstrand cross-links. Oncogene *27*, 5045-5056.

Bailly, V., Sommers, C.H., Sung, P., Prakash, L., and Prakash, S. (1992). Specific complex formation between proteins encoded by the yeast DNA repair and recombination genes RAD1 and RAD10. Proceedings of the National Academy of Sciences of the United States of America *89*, 8273-8277.

Baker, B.S., Carpenter, A.T., and Ripoll, P. (1978). The Utilization during Mitotic Cell Division of Loci Controlling Meiotic Recombination and Disjunction in DROSOPHILA MELANOGASTER. Genetics *90*, 531-578.

Bardwell, A.J., Bardwell, L., Tomkinson, A.E., and Friedberg, E.C. (1994). Specific cleavage of model recombination and repair intermediates by the yeast Rad1-Rad10 DNA endonuclease. Science (New York, NY *265*, 2082-2085.

Bardwell, L., Cooper, A.J., and Friedberg, E.C. (1992). Stable and specific association between the yeast recombination and DNA repair proteins RAD1 and RAD10 in vitro. Mol Cell Biol *12*, 3041-3049.

Bastin-Shanower, S.A., Fricke, W.M., Mullen, J.R., and Brill, S.J. (2003). The mechanism of Mus81-Mms4 cleavage site selection distinguishes it from the homologous endonuclease Rad1-Rad10. Mol Cell Biol *23*, 3487-3496.

Berardini, M., Foster, P.L., and Loechler, E.L. (1999). DNA polymerase II (polB) is involved in a new DNA repair pathway for DNA interstrand cross-links in Escherichia coli. Journal of bacteriology *181*, 2878-2882.

Berneburg, M., Clingen, P.H., Harcourt, S.A., Lowe, J.E., Taylor, E.M., Green, M.H., Krutmann, J., Arlett, C.F., and Lehmann, A.R. (2000). The cancer-free phenotype in trichothiodystrophy is unrelated to its repair defect. Cancer Res *60*, 431-438.

Bhagwat, N., Olsen, A.L., Wang, A.T., Hanada, K., Stuckert, P., Kanaar, R., D'Andrea, A., Niedernhofer, L.J., and McHugh, P.J. (2009a). XPF-ERCC1 participates in the Fanconi anemia pathway of crosslink repair. Mol Cell Biol, MCB.00086-00009.

Bhagwat, N.R., Roginskaya, V.Y., Acquafondata, M.B., Dhir, R., Wood, R.D., and Niedernhofer, L.J. (2009b). Immunodetection of DNA repair endonuclease ERCC1-XPF in human tissue. Cancer research *69*, 6831-6838.

Biggerstaff, M., Szymkowski, D.E., and Wood, R.D. (1993). Co-correction of the ERCC1, ERCC4 and xeroderma pigmentosum group F DNA repair defects in vitro. The EMBO journal *12*, 3685-3692.

Blais, V., Gao, H., Elwell, C.A., Boddy, M.N., Gaillard, P.H., Russell, P., and McGowan, C.H. (2004). RNA interference inhibition of Mus81 reduces mitotic recombination in human cells. Molecular biology of the cell *15*, 552-562.

Boddy, M.N., Gaillard, P.H., McDonald, W.H., Shanahan, P., Yates, J.R., 3rd, and Russell, P. (2001). Mus81-Eme1 are essential components of a Holliday junction resolvase. Cell *107*, 537-548.

Boddy, M.N., Lopez-Girona, A., Shanahan, P., Interthal, H., Heyer, W.D., and Russell, P. (2000). Damage tolerance protein Mus81 associates with the FHA1 domain of checkpoint kinase Cds1. Mol Cell Biol *20*, 8758-8766.

Bohr, V.A., Smith, C.A., Okumoto, D.S., and Hanawalt, P.C. (1985). DNA repair in an active gene: removal of pyrimidine dimers from the DHFR gene of CHO cells is much more efficient than in the genome overall. Cell *40*, 359-369.

Boiteux, S., and Guillet, M. (2004). Abasic sites in DNA: repair and biological consequences in Saccharomyces cerevisiae. DNA repair *3*, 1-12.

Botta, E., Nardo, T., Lehmann, A.R., Egly, J.M., Pedrini, A.M., and Stefanini, M. (2002). Reduced level of the repair/transcription factor TFIIH in trichothiodystrophy. Human molecular genetics *11*, 2919-2928.

Brookman, K.W., Lamerdin, J.E., Thelen, M.P., Hwang, M., Reardon, J.T., Sancar, A., Zhou, Z.Q., Walter, C.A., Parris, C.N., and Thompson, L.H. (1996). ERCC4 (XPF) encodes a human nucleotide excision repair protein with eukaryotic recombination homologs. Mol Cell Biol *16*, 6553-6562.

Brooks, P.J. (2008). The 8,5'-cyclopurine-2'-deoxynucleosides: candidate neurodegenerative DNA lesions in xeroderma pigmentosum, and unique probes of transcription and nucleotide excision repair. DNA repair *7*, 1168-1179.

Bulzebruck, H., Bopp, R., Drings, P., Bauer, E., Krysa, S., Probst, G., van Kaick, G., Muller, K.M., and Vogt-Moykopf, I. (1992). New aspects in the staging of lung cancer. Prospective validation of the International Union Against Cancer TNM classification. Cancer *70*, 1102-1110.

Bunn, P.A., Jr., and Kelly, K. (1998). New chemotherapeutic agents prolong survival and improve quality of life in non-small cell lung cancer: a review of the literature and future directions. Clin Cancer Res *4*, 1087-1100.

Carpenter, A.T., and Baker, B.S. (1982). On the Control of the Distribution of Meiotic Exchange in DROSOPHILA MELANOGASTER. Genetics *101*, 81-89.

Carr, A.M., Schmidt, H., Kirchhoff, S., Muriel, W.J., Sheldrick, K.S., Griffiths, D.J., Basmacioglu, C.N., Subramani, S., Clegg, M., Nasim, A.*, et al.* (1994). The rad16 gene of Schizosaccharomyces pombe: a homolog of the RAD1 gene of Saccharomyces cerevisiae. Mol Cell Biol *14*, 2029-2040.

Champoux, J.J. (2001). DNA topoisomerases: structure, function, and mechanism. Annu Rev Biochem *70*, 369-413.

Chen, H., Shao, C., Shi, H., Mu, Y., Sai, K., and Chen, Z. (2007). Single nucleotide polymorphisms and expression of ERCC1 and ERCC2 vis-a-vis chemotherapy drug cytotoxicity in human glioma. Journal of neuro-oncology *82*, 257-262.

Cheng, S., Sancar, A., and Hearst, J.E. (1991). RecA-dependent incision of psoralen-crosslinked DNA by (A)BC excinuclease. Nucleic acids research *19*, 657-663.

Chung, H.H., Kim, M.K., Kim, J.W., Park, N.H., Song, Y.S., Kang, S.B., and Lee, H.P. (2006). XRCC1 R399Q polymorphism is associated with response to platinum-based neoadjuvant chemotherapy in bulky cervical cancer. Gynecologic oncology *103*, 1031-1037.

Ciccia, A., Constantinou, A., and West, S.C. (2003). Identification and characterization of the human mus81-eme1 endonuclease. The Journal of biological chemistry *278*, 25172-25178.

Ciccia, A., Ling, C., Coulthard, R., Yan, Z., Xue, Y., Meetei, A.R., Laghmani el, H., Joenje, H., McDonald, N., de Winter, J.P.*, et al.* (2007). Identification of FAAP24, a Fanconi anemia core complex protein that interacts with FANCM. Molecular cell *25*, 331-343.

Clarkson, S.G. (2003). The XPG story. Biochimie *85*, 1113-1121.

Cobo, M., Isla, D., Massuti, B., Montes, A., Sanchez, J.M., Provencio, M., Vinolas, N., Paz-Ares, L., Lopez-Vivanco, G., Munoz, M.A.*, et al.* (2007). Customizing cisplatin based on quantitative excision repair cross-complementing 1 mRNA expression: a phase III trial in non-small-cell lung cancer. J Clin Oncol *25*, 2747-2754.

Cole, R.S. (1973). Repair of DNA containing interstrand crosslinks in Escherichia coli: sequential excision and recombination. Proceedings of the National Academy of Sciences of the United States of America *70*, 1064-1068.

Collins, A.R. (1993). Mutant rodent cell lines sensitive to ultraviolet light, ionizing radiation and cross-linking agents: a comprehensive survey of genetic and biochemical characteristics. Mutation research *293*, 99-118.

Collins, N.B., Wilson, J.B., Bush, T., Thomashevski, A., Roberts, K.J., Jones, N.J., and Kupfer, G.M. (2009). ATR-dependent phosphorylation of FANCA on serine 1449 after DNA damage is important for FA pathway function. Blood *113*, 2181-2190.

D'Andrea, A.D., and Grompe, M. (2003). The Fanconi anaemia/BRCA pathway. Nature reviews *3*, 23-34.

Dabholkar, M., Bostick-Bruton, F., Weber, C., Bohr, V.A., Egwuagu, C., and Reed, E. (1992). ERCC1 and ERCC2 expression in malignant tissues from ovarian cancer patients. Journal of the National Cancer Institute *84*, 1512-1517.

Dabholkar, M., Vionnet, J., Bostick-Bruton, F., Yu, J.J., and Reed, E. (1994). Messenger RNA levels of XPAC and ERCC1 in ovarian cancer tissue correlate with response to platinum-based chemotherapy. The Journal of clinical investigation *94*, 703-708.

Davies, A.A., Friedberg, E.C., Tomkinson, A.E., Wood, R.D., and West, S.C. (1995). Role of the Rad1 and Rad10 proteins in nucleotide excision repair and recombination. The Journal of biological chemistry *270*, 24638-24641.

de Boer, J., Andressoo, J.O., de Wit, J., Huijmans, J., Beems, R.B., van Steeg, H., Weeda, G., van der Horst, G.T., van Leeuwen, W., Themmen, A.P.*, et al.* (2002). Premature aging in mice deficient in DNA repair and transcription. Science *296*, 1276-1279.

de Jonge, A.J., Vermeulen, W., Klein, B., and Hoeijmakers, J.H. (1983). Microinjection of human cell extracts corrects xeroderma pigmentosum defect. Embo J *2*, 637-641.

de Laat, W.L., Appeldoorn, E., Jaspers, N.G., and Hoeijmakers, J.H. (1998a). DNA structural elements required for ERCC1-XPF endonuclease activity. The Journal of biological chemistry *273*, 7835-7842.

de Laat, W.L., Jaspers, N.G., and Hoeijmakers, J.H. (1999). Molecular mechanism of nucleotide excision repair. Genes & development *13*, 768-785.

de Laat, W.L., Sijbers, A.M., Odijk, H., Jaspers, N.G., and Hoeijmakers, J.H. (1998b). Mapping of interaction domains between human repair proteins ERCC1 and XPF. Nucleic Acids Res *26*, 4146-4152.

de los Santos, T., Hunter, N., Lee, C., Larkin, B., Loidl, J., and Hollingsworth, N.M. (2003). The Mus81/Mms4 endonuclease acts independently of double-Holliday junction resolution to promote a distinct subset of crossovers during meiosis in budding yeast. Genetics *164*, 81-94.

de los Santos, T., Loidl, J., Larkin, B., and Hollingsworth, N.M. (2001). A role for MMS4 in the processing of recombination intermediates during meiosis in Saccharomyces cerevisiae. Genetics *159*, 1511-1525.

De Silva, I.U., McHugh, P.J., Clingen, P.H., and Hartley, J.A. (2000). Defining the roles of nucleotide excision repair and recombination in the repair of DNA interstrand cross-links in mammalian cells. Molecular and cellular biology *20*, 7980-7990.

de Vries, A., van Oostrom, C.T., Hofhuis, F.M., Dortant, P.M., Berg, R.J., de Gruijl, F.R., Wester, P.W., van Kreijl, C.F., Capel, P.J., van Steeg, H.*, et al.* (1995). Increased susceptibility to ultraviolet-B and carcinogens of mice lacking the DNA excision repair gene XPA. Nature *377*, 169-173.

Decottignies, A. (2007). Microhomology-mediated end joining in fission yeast is repressed by pku70 and relies on genes involved in homologous recombination. Genetics *176*, 1403-1415.

Digweed, M., Rothe, S., Demuth, I., Scholz, R., Schindler, D., Stumm, M., Grompe, M., Jordan, A., and Sperling, K. (2002). Attenuation of the formation of DNA-repair foci containing RAD51 in Fanconi anaemia. Carcinogenesis *23*, 1121-1126.

Doe, C.L., Ahn, J.S., Dixon, J., and Whitby, M.C. (2002). Mus81-Eme1 and Rqh1 involvement in processing stalled and collapsed replication forks. The Journal of biological chemistry *277*, 32753-32759.

Doecke, J., Zhao, Z.Z., Pandeya, N., Sadeghi, S., Stark, M., Green, A.C., Hayward, N.K., Webb, P.M., and Whiteman, D.C. (2008). Polymorphisms in MGMT and DNA repair genes and the risk of esophageal adenocarcinoma. International journal of cancer *123*, 174-180.

Doig, J., Anderson, C., Lawrence, N.J., Selfridge, J., Brownstein, D.G., and Melton, D.W. (2006). Mice with skin-specific DNA repair gene (Ercc1) inactivation are hypersensitive to ultraviolet irradiation-induced skin cancer and show more rapid actinic progression. Oncogene *25*, 6229-6238.

Dolle, M.E., Busuttil, R.A., Garcia, A.M., Wijnhoven, S., van Drunen, E., Niedernhofer, L.J., van der Horst, G., Hoeijmakers, J.H., van Steeg, H., and Vijg, J. (2006). Increased genomic instability is not a prerequisite for shortened lifespan in DNA repair deficient mice. Mutation research *596*, 22-35.

Dronkert, M.L., de Wit, J., Boeve, M., Vasconcelos, M.L., van Steeg, H., Tan, T.L., Hoeijmakers, J.H., and Kanaar, R. (2000). Disruption of mouse SNM1 causes increased sensitivity to the DNA interstrand cross-linking agent mitomycin C. Molecular and cellular biology *20*, 4553-4561.

Dubaele, S., Proietti De Santis, L., Bienstock, R.J., Keriel, A., Stefanini, M., Van Houten, B., and Egly, J.M. (2003). Basal transcription defect discriminates between xeroderma pigmentosum and trichothiodystrophy in XPD patients. Mol Cell *11*, 1635-1646.

Duncan, J., Hamilton, L., and Friedberg, E.C. (1976). Enzymatic degradation of uracil-containing DNA. II. Evidence for N-glycosidase and nuclease activities in unfractionated extracts of Bacillus subtilis. Journal of virology *19*, 338-345.

Durant, S.T., Morris, M.M., Illand, M., McKay, H.J., McCormick, C., Hirst, G.L., Borts, R.H., and Brown, R. (1999). Dependence on RAD52 and RAD1 for anticancer drug resistance mediated by inactivation of mismatch repair genes. Curr Biol *9*, 51-54.

Eastman, A. (1987). The formation, isolation and characterization of DNA adducts produced by anticancer platinum complexes. Pharmacol Ther *34*, 155-166.

Edwards, S.W., Tan, C.M., and Limbird, L.E. (2000). Localization of G-protein-coupled receptors in health and disease. Trends Pharmacol Sci *21*, 304-308.

Enzlin, J.H., and Scharer, O.D. (2002). The active site of the DNA repair endonuclease XPF-ERCC1 forms a highly conserved nuclease motif. The EMBO journal *21*, 2045-2053.

Evans, E., Moggs, J.G., Hwang, J.R., Egly, J.M., and Wood, R.D. (1997). Mechanism of open complex and dual incision formation by human nucleotide excision repair factors. Embo J *16*, 6559-6573.

Fabbro, M., Rodriguez, J.A., Baer, R., and Henderson, B.R. (2002). BARD1 induces BRCA1 intranuclear foci formation by increasing RING-dependent BRCA1 nuclear import and inhibiting BRCA1 nuclear export. J Biol Chem *277*, 21315-21324.

Fekairi, S., Scaglione, S., Chahwan, C., Taylor, E.R., Tissier, A., Coulon, S., Dong, M.Q., Ruse, C., Yates, J.R., 3rd, Russell, P.*, et al.* (2009). Human SLX4 is a Holliday junction resolvase subunit that binds multiple DNA repair/recombination endonucleases. Cell *138*, 78-89.

Finkel, T. (2005). Radical medicine: treating ageing to cure disease. Nat Rev Mol Cell Biol *6*, 971-976.

Fishman-Lobell, J., and Haber, J.E. (1992). Removal of nonhomologous DNA ends in double-strand break recombination: the role of the yeast ultraviolet repair gene RAD1. Science (New York, NY *258*, 480-484.

Friedberg, E.C. (2006). DNA repair and mutagenesis, 2nd edn (Washington, D.C., ASM Press).

Fujiwara, Y., and Tatsumi, M. (1977). Cross-link repair in human cells and its possible defect in Fanconi's anemia cells. Journal of molecular biology *113*, 635-649.

Gaillard, P.H., Noguchi, E., Shanahan, P., and Russell, P. (2003). The endogenous Mus81-Eme1 complex resolves Holliday junctions by a nick and counternick mechanism. Molecular cell *12*, 747-759.

Gaillard, P.H., and Wood, R.D. (2001). Activity of individual ERCC1 and XPF subunits in DNA nucleotide excision repair. Nucleic acids research *29*, 872-879.

Garcia-Closas, M., Malats, N., Real, F.X., Welch, R., Kogevinas, M., Chatterjee, N., Pfeiffer, R., Silverman, D., Dosemeci, M., Tardon, A.*, et al.* (2006). Genetic variation in the nucleotide excision repair pathway and bladder cancer risk. Cancer Epidemiol Biomarkers Prev *15*, 536-542.

Garcia-Higuera, I., Kuang, Y., Naf, D., Wasik, J., and D'Andrea, A.D. (1999). Fanconi anemia proteins FANCA, FANCC, and FANCG/XRCC9 interact in a functional nuclear complex. Mol Cell Biol *19*, 4866-4873.

Garcia-Higuera, I., Taniguchi, T., Ganesan, S., Meyn, M.S., Timmers, C., Hejna, J., Grompe, M., and D'Andrea, A.D. (2001). Interaction of the Fanconi anemia proteins and BRCA1 in a common pathway. Molecular cell *7*, 249-262.

Gillet, L.C., and Scharer, O.D. (2006). Molecular mechanisms of mammalian global genome nucleotide excision repair. Chem Rev *106*, 253-276.

Graham, J.M., Jr., Anyane-Yeboa, K., Raams, A., Appeldoorn, E., Kleijer, W.J., Garritsen, V.H., Busch, D., Edersheim, T.G., and Jaspers, N.G. (2001). Cerebro-oculo-facio-skeletal syndrome with a nucleotide excision-repair defect and a mutated XPD gene, with prenatal diagnosis in a triplet pregnancy. American journal of human genetics *69*, 291-300.

Greenberg, S. (2008). A Profile of Older Americans: 2008, U.S.D.o.H.a.H.S. Administration on Aging, ed.

Gregory, R.C., Taniguchi, T., and D'Andrea, A.D. (2003). Regulation of the Fanconi anemia pathway by monoubiquitination. Seminars in cancer biology *13*, 77-82.

Grube, D. (2004). Constants and variables in immunohistochemistry. Arch Histol Cytol *67*, 115-134.

Guillet, M., and Boiteux, S. (2002). Endogenous DNA abasic sites cause cell death in the absence of Apn1, Apn2 and Rad1/Rad10 in Saccharomyces cerevisiae. The EMBO journal *21*, 2833-2841.

Guillet, M., and Boiteux, S. (2003). Origin of endogenous DNA abasic sites in Saccharomyces cerevisiae. Mol Cell Biol *23*, 8386-8394.

Haber, J.E. (2006). Transpositions and translocations induced by site-specific double-strand breaks in budding yeast. DNA repair *5*, 998-1009.

Hanada, K., Budzowska, M., Davies, S.L., van Drunen, E., Onizawa, H., Beverloo, H.B., Maas, A., Essers, J., Hickson, I.D., and Kanaar, R. (2007). The structure-specific endonuclease Mus81 contributes to replication restart by generating double-strand DNA breaks. Nat Struct Mol Biol *14*, 1096-1104.

Hanada, K., Budzowska, M., Modesti, M., Maas, A., Wyman, C., Essers, J., and Kanaar, R. (2006). The structure-specific endonuclease Mus81-Eme1 promotes conversion of

interstrand DNA crosslinks into double-strands breaks. The EMBO journal *25*, 4921-4932.

Hanawalt, P.C. (2002). Subpathways of nucleotide excision repair and their regulation. Oncogene *21*, 8949-8956.

Hanawalt, P.C., and Spivak, G. (2008). Transcription-coupled DNA repair: two decades of progress and surprises. Nat Rev Mol Cell Biol *9*, 958-970.

Hansen, R.D., Sorensen, M., Tjonneland, A., Overvad, K., Wallin, H., Raaschou-Nielsen, O., and Vogel, U. (2008). A haplotype of polymorphisms in ASE-1, RAI and ERCC1 and the effects of tobacco smoking and alcohol consumption on risk of colorectal cancer: a Danish prospective case-cohort study. BMC cancer *8*, 54.

Hazrati, A., Ramis-Castelltort, M., Sarkar, S., Barber, L.J., Schofield, C.J., Hartley, J.A., and McHugh, P.J. (2008). Human SNM1A suppresses the DNA repair defects of yeast pso2 mutants. DNA repair *7*, 230-238.

Hefner, E., Preuss, S.B., and Britt, A.B. (2003). Arabidopsis mutants sensitive to gamma radiation include the homologue of the human repair gene ERCC1. Journal of experimental botany *54*, 669-680.

Henning, K.A., Li, L., Iyer, N., McDaniel, L.D., Reagan, M.S., Legerski, R., Schultz, R.A., Stefanini, M., Lehmann, A.R., Mayne, L.V.*, et al.* (1995). The Cockayne syndrome group A gene encodes a WD repeat protein that interacts with CSB protein and a subunit of RNA polymerase II TFIIH. Cell *82*, 555-564.

Henriques, J.A., and Moustacchi, E. (1980). Isolation and characterization of pso mutants sensitive to photo-addition of psoralen derivatives in Saccharomyces cerevisiae. Genetics *95*, 273-288.

Henriques, J.A., Vicente, E.J., Leandro da Silva, K.V., and Schenberg, A.C. (1989). PSO4: a novel gene involved in error-prone repair in Saccharomyces cerevisiae. Mutation research *218*, 111-124.

Hirata, H., Hinoda, Y., Matsuyama, H., Tanaka, Y., Okayama, N., Suehiro, Y., Zhao, H., Urakami, S., Kawamoto, K., Kawakami, T.*, et al.* (2006). Polymorphisms of DNA repair genes are associated with renal cell carcinoma. Biochemical and biophysical research communications *342*, 1058-1062.

Hoeijmakers, J.H., Eker, A.P., Wood, R.D., and Robins, P. (1990). Use of in vivo and in vitro assays for the characterization of mammalian excision repair and isolation of repair proteins. Mutat Res *236*, 223-238.

Hohl, M., Dunand-Sauthier, I., Staresincic, L., Jaquier-Gubler, P., Thorel, F., Modesti, M., Clarkson, S.G., and Scharer, O.D. (2007). Domain swapping between FEN-1 and XPG defines regions in XPG that mediate nucleotide excision repair activity and substrate specificity. Nucleic Acids Res *35*, 3053-3063.

Holmseth, S., Lehre, K.P., and Danbolt, N.C. (2006). Specificity controls for immunocytochemistry. Anat Embryol (Berl) *211*, 257-266.

Hooker, S., Bonilla, C., Akereyeni, F., Ahaghotu, C., and Kittles, R.A. (2008). NAT2 and NER genetic variants and sporadic prostate cancer susceptibility in African Americans. Prostate Cancer Prostatic Dis *11*, 349-356.

Houtsmuller, A.B., Rademakers, S., Nigg, A.L., Hoogstraten, D., Hoeijmakers, J.H., and Vermeulen, W. (1999). Action of DNA repair endonuclease ERCC1/XPF in living cells. Science (New York, NY *284*, 958-961.

Howlett, N.G., Taniguchi, T., Olson, S., Cox, B., Waisfisz, Q., De Die-Smulders, C., Persky, N., Grompe, M., Joenje, H., Pals, G.*, et al.* (2002). Biallelic inactivation of BRCA2 in Fanconi anemia. Science (New York, NY *297*, 606-609.

Hoy, C.A., Thompson, L.H., Mooney, C.L., and Salazar, E.P. (1985). Defective DNA cross-link removal in Chinese hamster cell mutants hypersensitive to bifunctional alkylating agents. Cancer research *45*, 1737-1743.

Hsia, K.T., Millar, M.R., King, S., Selfridge, J., Redhead, N.J., Melton, D.W., and Saunders, P.T. (2003). DNA repair gene Ercc1 is essential for normal spermatogenesis and oogenesis and for functional integrity of germ cell DNA in the mouse. Development (Cambridge, England) *130*, 369-378.

Hsiang, Y.H., Lihou, M.G., and Liu, L.F. (1989). Arrest of replication forks by drug-stabilized topoisomerase I-DNA cleavable complexes as a mechanism of cell killing by camptothecin. Cancer research *49*, 5077-5082.

Hussain, S., Wilson, J.B., Blom, E., Thompson, L.H., Sung, P., Gordon, S.M., Kupfer, G.M., Joenje, H., Mathew, C.G., and Jones, N.J. (2006). Tetratricopeptide-motif-mediated interaction of FANCG with recombination proteins XRCC3 and BRCA2. DNA repair *5*, 629-640.

Hwang, I.G., Ahn, M.J., Park, B.B., Ahn, Y.C., Han, J., Lee, S., Kim, J., Shim, Y.M., Ahn, J.S., and Park, K. (2008). ERCC1 expression as a prognostic marker in N2(+) nonsmall-cell lung cancer patients treated with platinum-based neoadjuvant concurrent chemoradiotherapy. Cancer.

Ishiai, M., Kimura, M., Namikoshi, K., Yamazoe, M., Yamamoto, K., Arakawa, H., Agematsu, K., Matsushita, N., Takeda, S., Buerstedde, J.M.*, et al.* (2004). DNA cross-link repair protein SNM1A interacts with PIAS1 in nuclear focus formation. Molecular and cellular biology *24*, 10733-10741.

Isla, D., Sarries, C., Rosell, R., Alonso, G., Domine, M., Taron, M., Lopez-Vivanco, G., Camps, C., Botia, M., Nunez, L.*, et al.* (2004). Single nucleotide polymorphisms and outcome in docetaxel-cisplatin-treated advanced non-small-cell lung cancer. Ann Oncol *15*, 1194-1203.

Ito, S., Kuraoka, I., Chymkowitch, P., Compe, E., Takedachi, A., Ishigami, C., Coin, F., Egly, J.M., and Tanaka, K. (2007). XPG stabilizes TFIIH, allowing transactivation of nuclear receptors: implications for Cockayne syndrome in XP-G/CS patients. Mol Cell *26*, 231-243.

Ivanov, E.L., and Haber, J.E. (1995). RAD1 and RAD10, but not other excision repair genes, are required for double-strand break-induced recombination in Saccharomyces cerevisiae. Mol Cell Biol *15*, 2245-2251.

Iyer, V.N., and Szybalski, W. (1963). A Molecular Mechanism of Mitomycin Action: Linking of Complementary DNA Strands. Proceedings of the National Academy of Sciences of the United States of America *50*, 355-362.

Jachymczyk, W.J., von Borstel, R.C., Mowat, M.R., and Hastings, P.J. (1981). Repair of interstrand cross-links in DNA of Saccharomyces cerevisiae requires two systems for DNA repair: the RAD3 system and the RAD51 system. Mol Gen Genet *182*, 196-205.

Jaspers, N.G., Raams, A., Silengo, M.C., Wijgers, N., Niedernhofer, L.J., Robinson, A.R., Giglia-Mari, G., Hoogstraten, D., Kleijer, W.J., Hoeijmakers, J.H.*, et al.* (2007). First reported patient with human ERCC1 deficiency has cerebro-oculo-facio-skeletal syndrome with a mild defect in nucleotide excision repair and severe developmental failure. American journal of human genetics *80*, 457-466.

Jemal, A., Siegel, R., Ward, E., Hao, Y., Xu, J., Murray, T., and Thun, M.J. (2008). Cancer statistics, 2008. CA Cancer J Clin *58*, 71-96.

Jemal, A., Siegel, R., Ward, E., Hao, Y., Xu, J., and Thun, M.J. (2009). Cancer statistics, 2009. CA Cancer J Clin *59*, 225-249.

Joenje, H., and Patel, K.J. (2001). The emerging genetic and molecular basis of Fanconi anaemia. Nature reviews *2*, 446-457.

Joshi, M.B., Shirota, Y., Danenberg, K.D., Conlon, D.H., Salonga, D.S., Herndon, J.E., 2nd, Danenberg, P.V., and Harpole, D.H., Jr. (2005). High gene expression of TS1, GSTP1, and ERCC1 are risk factors for survival in patients treated with trimodality therapy for esophageal cancer. Clin Cancer Res *11*, 2215-2221.

Joyce, E.F., Tanneti, S.N., and McKim, K.S. (2009). Drosophila hold'em is required for a subset of meiotic crossovers and interacts with the dna repair endonuclease complex subunits MEI-9 and ERCC1. Genetics *181*, 335-340.

Kabotyanski, E.B., Gomelsky, L., Han, J.O., Stamato, T.D., and Roth, D.B. (1998). Double-strand break repair in Ku86- and XRCC4-deficient cells. Nucleic acids research *26*, 5333-5342.

Kalikaki, A., Kanaki, M., Vassalou, H., Souglakos, J., Voutsina, A., Georgoulias, V., and Mavroudis, D. (2009). DNA repair gene polymorphisms predict favorable clinical outcome in advanced non-small-cell lung cancer. Clinical lung cancer *10*, 118-123.

Kapetanaki, M.G., Guerrero-Santoro, J., Bisi, D.C., Hsieh, C.L., Rapic-Otrin, V., and Levine, A.S. (2006). The DDB1-CUL4ADDB2 ubiquitin ligase is deficient in xeroderma pigmentosum group E and targets histone H2A at UV-damaged DNA sites. Proc Natl Acad Sci U S A *103*, 2588-2593.

Karin, M., Cao, Y., Greten, F.R., and Li, Z.W. (2002). NF-kappaB in cancer: from innocent bystander to major culprit. Nat Rev Cancer *2*, 301-310.

Kau, T.R., Way, J.C., and Silver, P.A. (2004). Nuclear transport and cancer: from mechanism to intervention. Nat Rev Cancer *4*, 106-117.

Kim, J.M., Kee, Y., Gurtan, A., and D'Andrea, A.D. (2008a). Cell cycle dependent chromatin loading of the fanconi anemia core complex by FANCM/FAAP24. Blood.

Kim, M.K., Cho, K.J., Kwon, G.Y., Park, S.I., Kim, Y.H., Kim, J.H., Song, H.Y., Shin, J.H., Jung, H.Y., Lee, G.H.*, et al.* (2008b). Patients with ERCC1-negative locally advanced esophageal cancers may benefit from preoperative chemoradiotherapy. Clin Cancer Res *14*, 4225-4231.

Kirkwood, T.B. (2005). Understanding the odd science of aging. Cell *120*, 437-447.

Kiyohara, C., and Yoshimasu, K. (2007). Genetic polymorphisms in the nucleotide excision repair pathway and lung cancer risk: a meta-analysis. International journal of medical sciences *4*, 59-71.

Klein, H.L. (1988). Different types of recombination events are controlled by the RAD1 and RAD52 genes of Saccharomyces cerevisiae. Genetics *120*, 367-377.

Kohn, K.W., Spears, C.L., and Doty, P. (1966). Inter-strand crosslinking of DNA by nitrogen mustard. Journal of molecular biology *19*, 266-288.

Komori, K., Fujikane, R., Shinagawa, H., and Ishino, Y. (2002). Novel endonuclease in Archaea cleaving DNA with various branched structure. Genes Genet Syst *77*, 227-241.

Kraemer, K.H., Lee, M.M., and Scotto, J. (1987). Xeroderma pigmentosum. Cutaneous, ocular, and neurologic abnormalities in 830 published cases. Arch Dermatol *123*, 241-250.

Kraemer, K.H., Patronas, N.J., Schiffmann, R., Brooks, B.P., Tamura, D., and DiGiovanna, J.J. (2007). Xeroderma pigmentosum, trichothiodystrophy and Cockayne syndrome: a complex genotype-phenotype relationship. Neuroscience *145*, 1388-1396.

Kuraoka, I., Kobertz, W.R., Ariza, R.R., Biggerstaff, M., Essigmann, J.M., and Wood, R.D. (2000). Repair of an interstrand DNA cross-link initiated by ERCC1-XPF repair/recombination nuclease. The Journal of biological chemistry *275*, 26632-26636.

Kwon, H.C., Roh, M.S., Oh, S.Y., Kim, S.H., Kim, M.C., Kim, J.S., and Kim, H.J. (2007). Prognostic value of expression of ERCC1, thymidylate synthase, and glutathione S-

transferase P1 for 5-fluorouracil/oxaliplatin chemotherapy in advanced gastric cancer. Ann Oncol *18*, 504-509.

Laine, J.P., and Egly, J.M. (2006). When transcription and repair meet: a complex system. Trends Genet *22*, 430-436.

Lan, L., Hayashi, T., Rabeya, R.M., Nakajima, S., Kanno, S., Takao, M., Matsunaga, T., Yoshino, M., Ichikawa, M., Riele, H.*, et al.* (2004). Functional and physical interactions between ERCC1 and MSH2 complexes for resistance to cis-diamminedichloroplatinum(II) in mammalian cells. DNA repair *3*, 135-143.

Langer, R., Specht, K., Becker, K., Ewald, P., Bekesch, M., Sarbia, M., Busch, R., Feith, M., Stein, H.J., Siewert, J.R.*, et al.* (2005). Association of pretherapeutic expression of chemotherapy-related genes with response to neoadjuvant chemotherapy in Barrett carcinoma. Clin Cancer Res *11*, 7462-7469.

Lawrence, N.J., Sacco, J.J., Brownstein, D.G., Gillingwater, T.H., and Melton, D.W. (2008). A neurological phenotype in mice with DNA repair gene Ercc1 deficiency. DNA repair *7*, 281-291.

Leadon, S.A., and Lawrence, D.A. (1991). Preferential repair of DNA damage on the transcribed strand of the human metallothionein genes requires RNA polymerase II. Mutation research *255*, 67-78.

Lee, K., and Lee, S.E. (2007). Saccharomyces cerevisiae Sae2- and Tel1-dependent single-strand DNA formation at DNA break promotes microhomology-mediated end joining. Genetics *176*, 2003-2014.

Lee, K.H., Min, H.S., Han, S.W., Oh, D.Y., Lee, S.H., Kim, D.W., Im, S.A., Chung, D.H., Kim, Y.T., Kim, T.Y.*, et al.* (2008). ERCC1 expression by immunohistochemistry and EGFR mutations in resected non-small cell lung cancer. Lung Cancer *60*, 401-407.

Leong, A.S. (2004). Quantitation in immunohistology: fact or fiction? A discussion of variables that influence results. Appl Immunohistochem Mol Morphol *12*, 1-7.

Li, L., Elledge, S.J., Peterson, C.A., Bales, E.S., and Legerski, R.J. (1994). Specific association between the human DNA repair proteins XPA and ERCC1. Proc Natl Acad Sci U S A *91*, 5012-5016.

Li, L., Peterson, C.A., Lu, X., and Legerski, R.J. (1995). Mutations in XPA that prevent association with ERCC1 are defective in nucleotide excision repair. Mol Cell Biol *15*, 1993-1998.

Li, L., Peterson, C.A., Zhang, X., and Legerski, R.J. (2000). Requirement for PCNA and RPA in interstrand crosslink-induced DNA synthesis. Nucleic acids research *28*, 1424-1427.

Lindahl, T. (1976). New class of enzymes acting on damaged DNA. Nature *259*, 64-66.

Lindahl, T. (1979). DNA glycosylases, endonucleases for apurinic/apyrimidinic sites, and base excision-repair. Progress in nucleic acid research and molecular biology *22*, 135-192.

Lindahl, T., and Karlstrom, O. (1973). Heat-induced depyrimidination of deoxyribonucleic acid in neutral solution. Biochemistry *12*, 5151-5154.

Ling, C., Ishiai, M., Ali, A.M., Medhurst, A.L., Neveling, K., Kalb, R., Yan, Z., Xue, Y., Oostra, A.B., Auerbach, A.D.*, et al.* (2007). FAAP100 is essential for activation of the Fanconi anemia-associated DNA damage response pathway. The EMBO journal *26*, 2104-2114.

Liu, C., Pouliot, J.J., and Nash, H.A. (2002). Repair of topoisomerase I covalent complexes in the absence of the tyrosyl-DNA phosphodiesterase Tdp1. Proceedings of the National Academy of Sciences of the United States of America *99*, 14970-14975.

Liu, N., Lamerdin, J.E., Tebbs, R.S., Schild, D., Tucker, J.D., Shen, M.R., Brookman, K.W., Siciliano, M.J., Walter, C.A., Fan, W.*, et al.* (1998). XRCC2 and XRCC3, new human Rad51-family members, promote chromosome stability and protect against DNA cross-links and other damages. Molecular cell *1*, 783-793.

Lord, R.V., Brabender, J., Gandara, D., Alberola, V., Camps, C., Domine, M., Cardenal, F., Sanchez, J.M., Gumerlock, P.H., Taron, M.*, et al.* (2002). Low ERCC1 expression correlates with prolonged survival after cisplatin plus gemcitabine chemotherapy in non-small cell lung cancer. Clin Cancer Res *8*, 2286-2291.

Marmorstein, L.Y., Ouchi, T., and Aaronson, S.A. (1998). The BRCA2 gene product functionally interacts with p53 and RAD51. Proceedings of the National Academy of Sciences of the United States of America *95*, 13869-13874.

Matsumura, Y., Nishigori, C., Yagi, T., Imamura, S., and Takebe, H. (1998). Characterization of molecular defects in xeroderma pigmentosum group F in relation to its clinically mild symptoms. Hum Mol Genet *7*, 969-974.

Matsuoka, S., Ballif, B.A., Smogorzewska, A., McDonald, E.R., 3rd, Hurov, K.E., Luo, J., Bakalarski, C.E., Zhao, Z., Solimini, N., Lerenthal, Y.*, et al.* (2007). ATM and ATR substrate analysis reveals extensive protein networks responsive to DNA damage. Science (New York, NY *316*, 1160-1166.

McCabe, K.M., Hemphill, A., Akkari, Y., Jakobs, P.M., Pauw, D., Olson, S.B., Moses, R.E., and Grompe, M. (2008). ERCC1 is required for FANCD2 focus formation. Mol Genet Metab *95*, 66-73.

McGuire, V., Jesser, C.A., and Whittemore, A.S. (2002). Survival among U.S. women with invasive epithelial ovarian cancer. Gynecol Oncol *84*, 399-403.

McGuire, W.P., Hoskins, W.J., Brady, M.F., Kucera, P.R., Partridge, E.E., Look, K.Y., Clarke-Pearson, D.L., and Davidson, M. (1996). Cyclophosphamide and cisplatin compared with paclitaxel and cisplatin in patients with stage III and stage IV ovarian cancer. N Engl J Med *334*, 1-6.

McHugh, P.J., Gill, R.D., Waters, R., and Hartley, J.A. (1999). Excision repair of nitrogen mustard-DNA adducts in Saccharomyces cerevisiae. Nucleic acids research *27*, 3259-3266.

McHugh, P.J., Spanswick, V.J., and Hartley, J.A. (2001). Repair of DNA interstrand crosslinks: molecular mechanisms and clinical relevance. The lancet oncology *2*, 483-490.

McPherson, J.P., Lemmers, B., Chahwan, R., Pamidi, A., Migon, E., Matysiak-Zablocki, E., Moynahan, M.E., Essers, J., Hanada, K., Poonepalli, A.*, et al.* (2004). Involvement of mammalian Mus81 in genome integrity and tumor suppression. Science (New York, NY *304*, 1822-1826.

McWhir, J., Selfridge, J., Harrison, D.J., Squires, S., and Melton, D.W. (1993). Mice with DNA repair gene (ERCC-1) deficiency have elevated levels of p53, liver nuclear abnormalities and die before weaning. Nature genetics *5*, 217-224.

McWilliams, R.R., Bamlet, W.R., Cunningham, J.M., Goode, E.L., de Andrade, M., Boardman, L.A., and Petersen, G.M. (2008). Polymorphisms in DNA repair genes, smoking, and pancreatic adenocarcinoma risk. Cancer research *68*, 4928-4935.

Medhurst, A.L., Huber, P.A., Waisfisz, Q., de Winter, J.P., and Mathew, C.G. (2001). Direct interactions of the five known Fanconi anaemia proteins suggest a common functional pathway. Human molecular genetics *10*, 423-429.

Meetei, A.R., de Winter, J.P., Medhurst, A.L., Wallisch, M., Waisfisz, Q., van de Vrugt, H.J., Oostra, A.B., Yan, Z., Ling, C., Bishop, C.E.*, et al.* (2003). A novel ubiquitin ligase is deficient in Fanconi anemia. Nature genetics *35*, 165-170.

Meetei, A.R., Levitus, M., Xue, Y., Medhurst, A.L., Zwaan, M., Ling, C., Rooimans, M.A., Bier, P., Hoatlin, M., Pals, G.*, et al.* (2004). X-linked inheritance of Fanconi anemia complementation group B. Nature genetics *36*, 1219-1224.

Meetei, A.R., Medhurst, A.L., Ling, C., Xue, Y., Singh, T.R., Bier, P., Steltenpool, J., Stone, S., Dokal, I., Mathew, C.G.*, et al.* (2005). A human ortholog of archaeal DNA repair protein Hef is defective in Fanconi anemia complementation group M. Nature genetics *37*, 958-963.

Meira, L.B., Graham, J.M., Jr., Greenberg, C.R., Busch, D.B., Doughty, A.T., Ziffer, D.W., Coleman, D.M., Savre-Train, I., and Friedberg, E.C. (2000). Manitoba aboriginal kindred with original cerebro-oculo- facio-skeletal syndrome has a mutation in the Cockayne syndrome group B (CSB) gene. American journal of human genetics *66*, 1221-1228.

Mellon, I., and Hanawalt, P.C. (1989). Induction of the Escherichia coli lactose operon selectively increases repair of its transcribed DNA strand. Nature *342*, 95-98.

Mellon, I., Spivak, G., and Hanawalt, P.C. (1987). Selective removal of transcription-blocking DNA damage from the transcribed strand of the mammalian DHFR gene. Cell *51*, 241-249.

Metzger, R., Leichman, C.G., Danenberg, K.D., Danenberg, P.V., Lenz, H.J., Hayashi, K., Groshen, S., Salonga, D., Cohen, H., Laine, L.*, et al.* (1998). ERCC1 mRNA levels complement thymidylate synthase mRNA levels in predicting response and survival for gastric cancer patients receiving combination cisplatin and fluorouracil chemotherapy. J Clin Oncol *16*, 309-316.

Min, Y.H., Cheong, J.W., Kim, J.Y., Eom, J.I., Lee, S.T., Hahn, J.S., Ko, Y.W., and Lee, M.H. (2004). Cytoplasmic mislocalization of p27Kip1 protein is associated with constitutive phosphorylation of Akt or protein kinase B and poor prognosis in acute myelogenous leukemia. Cancer Res *64*, 5225-5231.

Mocquet, V., Laine, J.P., Riedl, T., Yajin, Z., Lee, M.Y., and Egly, J.M. (2008). Sequential recruitment of the repair factors during NER: the role of XPG in initiating the resynthesis step. The EMBO journal *27*, 155-167.

Modesitt, S.C., and Jazaeri, A.A. (2007). Recurrent epithelial ovarian cancer: pharmacotherapy and novel therapeutics. Expert Opin Pharmacother *8*, 2293-2305.

Moggs, J.G., Yarema, K.J., Essigmann, J.M., and Wood, R.D. (1996). Analysis of incision sites produced by human cell extracts and purified proteins during nucleotide excision repair of a 1,3-intrastrand d(GpTpG)-cisplatin adduct. J Biol Chem *271*, 7177-7186.

Moll, U.M., Riou, G., and Levine, A.J. (1992). Two distinct mechanisms alter p53 in breast cancer: mutation and nuclear exclusion. Proc Natl Acad Sci U S A *89*, 7262-7266.

Mone, M.J., Volker, M., Nikaido, O., Mullenders, L.H., van Zeeland, A.A., Verschure, P.J., Manders, E.M., and van Driel, R. (2001). Local UV-induced DNA damage in cell nuclei results in local transcription inhibition. EMBO Rep *2*, 1013-1017.

Montes de Oca, R., Andreassen, P.R., Margossian, S.P., Gregory, R.C., Taniguchi, T., Wang, X., Houghtaling, S., Grompe, M., and D'Andrea, A.D. (2005). Regulated interaction of the Fanconi anemia protein, FANCD2, with chromatin. Blood *105*, 1003-1009.

Monzo, M., Moreno, I., Navarro, A., Ibeas, R., Artells, R., Gel, B., Martinez, F., Moreno, J., Hernandez, R., and Navarro-Vigo, M. (2007). Single nucleotide polymorphisms in nucleotide excision repair genes XPA, XPD, XPG and ERCC1 in advanced colorectal cancer patients treated with first-line oxaliplatin/fluoropyrimidine. Oncology *72*, 364-370.

Moriwaki, S., and Kraemer, K.H. (2001). Xeroderma pigmentosum--bridging a gap between clinic and laboratory. Photodermatol Photoimmunol Photomed *17*, 47-54.

Mortensen, U.H., Bendixen, C., Sunjevaric, I., and Rothstein, R. (1996). DNA strand annealing is promoted by the yeast Rad52 protein. Proceedings of the National Academy of Sciences of the United States of America *93*, 10729-10734.

Moser, J., Kool, H., Giakzidis, I., Caldecott, K., Mullenders, L.H., and Fousteri, M.I. (2007). Sealing of chromosomal DNA nicks during nucleotide excision repair requires XRCC1 and DNA ligase III alpha in a cell-cycle-specific manner. Mol Cell *27*, 311-323.

Motycka, T.A., Bessho, T., Post, S.M., Sung, P., and Tomkinson, A.E. (2004). Physical and functional interaction between the XPF/ERCC1 endonuclease and hRad52. The Journal of biological chemistry *279*, 13634-13639.

Mu, D., Wakasugi, M., Hsu, D.S., and Sancar, A. (1997). Characterization of reaction intermediates of human excision repair nuclease. The Journal of biological chemistry *272*, 28971-28979.

Munoz, P., Blanco, R., de Carcer, G., Schoeftner, S., Benetti, R., Flores, J.M., Malumbres, M., and Blasco, M.A. (2009). TRF1 controls telomere length and mitotic fidelity in epithelial homeostasis. Mol Cell Biol *29*, 1608-1625.

Munoz, P., Blanco, R., Flores, J.M., and Blasco, M.A. (2005). XPF nuclease-dependent telomere loss and increased DNA damage in mice overexpressing TRF2 result in premature aging and cancer. Nature genetics *37*, 1063-1071.

Murai, M., Enokido, Y., Inamura, N., Yoshino, M., Nakatsu, Y., van der Horst, G.T., Hoeijmakers, J.H., Tanaka, K., and Hatanaka, H. (2001). Early postnatal ataxia and abnormal cerebellar development in mice lacking Xeroderma pigmentosum Group A and Cockayne syndrome Group B DNA repair genes. Proceedings of the National Academy of Sciences of the United States of America *98*, 13379-13384.

Murray, D., Macann, A., Hanson, J., and Rosenberg, E. (1996). ERCC1/ERCC4 5'-endonuclease activity as a determinant of hypoxic cell radiosensitivity. International journal of radiation biology *69*, 319-327.

Murray, D., and Rosenberg, E. (1996). The importance of the ERCC1/ERCC4[XPF] complex for hypoxic-cell radioresistance does not appear to derive from its participation in the nucleotide excision repair pathway. Mutation research *364*, 217-226.

Nakatsu, Y., Asahina, H., Citterio, E., Rademakers, S., Vermeulen, W., Kamiuchi, S., Yeo, J.P., Khaw, M.C., Saijo, M., Kodo, N*., et al.* (2000). XAB2, a novel tetratricopeptide repeat protein involved in transcription-coupled DNA repair and transcription. J Biol Chem *275*, 34931-34937.

Niedernhofer, L.J., Bhagwat, N., and Wood, R.D. (2007). ERCC1 and non-small-cell lung cancer. The New England journal of medicine *356*, 2538-2540; author reply 2540-2531.

Niedernhofer, L.J., Essers, J., Weeda, G., Beverloo, B., de Wit, J., Muijtjens, M., Odijk, H., Hoeijmakers, J.H., and Kanaar, R. (2001). The structure-specific endonuclease Ercc1-Xpf is required for targeted gene replacement in embryonic stem cells. The EMBO journal *20*, 6540-6549.

Niedernhofer, L.J., Garinis, G.A., Raams, A., Lalai, A.S., Robinson, A.R., Appeldoorn, E., Odijk, H., Oostendorp, R., Ahmad, A., van Leeuwen, W.*, et al.* (2006). A new progeroid syndrome reveals that genotoxic stress suppresses the somatotroph axis. Nature *444*, 1038-1043.

Niedernhofer, L.J., Lalai, A.S., and Hoeijmakers, J.H. (2005). Fanconi anemia (cross)linked to DNA repair. Cell *123*, 1191-1198.

Niedernhofer, L.J., Odijk, H., Budzowska, M., van Drunen, E., Maas, A., Theil, A.F., de Wit, J., Jaspers, N.G., Beverloo, H.B., Hoeijmakers, J.H.*, et al.* (2004). The structure-specific endonuclease Ercc1-Xpf is required to resolve DNA interstrand cross-link-induced double-strand breaks. Mol Cell Biol *24*, 5776-5787.

Niedzwiedz, W., Mosedale, G., Johnson, M., Ong, C.Y., Pace, P., and Patel, K.J. (2004). The Fanconi anaemia gene FANCC promotes homologous recombination and error-prone DNA repair. Molecular cell *15*, 607-620.

Nijman, S.M., Huang, T.T., Dirac, A.M., Brummelkamp, T.R., Kerkhoven, R.M., D'Andrea, A.D., and Bernards, R. (2005). The deubiquitinating enzyme USP1 regulates the Fanconi anemia pathway. Molecular cell *17*, 331-339.

Nishino, T., Komori, K., Ishino, Y., and Morikawa, K. (2003). X-ray and biochemical anatomy of an archaeal XPF/Rad1/Mus81 family nuclease: similarity between its endonuclease domain and restriction enzymes. Structure *11*, 445-457.

Nomura, Y., Adachi, N., and Koyama, H. (2007). Human Mus81 and FANCB independently contribute to repair of DNA damage during replication. Genes Cells *12*, 1111-1122.

Nouspikel, T. (2008). Nucleotide excision repair and neurological diseases. DNA Repair (Amst) *7*, 1155-1167.

Nouspikel, T., Lalle, P., Leadon, S.A., Cooper, P.K., and Clarkson, S.G. (1997). A common mutational pattern in Cockayne syndrome patients from xeroderma pigmentosum group G: implications for a second XPG function. Proc Natl Acad Sci U S A *94*, 3116-3121.

Nunez, F., Chipchase, M.D., Clarke, A.R., and Melton, D.W. (2000). Nucleotide excision repair gene (ERCC1) deficiency causes G(2) arrest in hepatocytes and a reduction in liver binucleation: the role of p53 and p21. Faseb J *14*, 1073-1082.

O'Connor, P.M., and Kohn, K.W. (1990). Comparative pharmacokinetics of DNA lesion formation and removal following treatment of L1210 cells with nitrogen mustards. Cancer communications *2*, 387-394.

O'Donovan, A., Davies, A.A., Moggs, J.G., West, S.C., and Wood, R.D. (1994). XPG endonuclease makes the 3' incision in human DNA nucleotide excision repair. Nature *371*, 432-435.

Oestergaard, V.H., Langevin, F., Kuiken, H.J., Pace, P., Niedzwiedz, W., Simpson, L.J., Ohzeki, M., Takata, M., Sale, J.E., and Patel, K.J. (2007). Deubiquitination of FANCD2 is required for DNA crosslink repair. Molecular cell *28*, 798-809.

Ogi, T., and Lehmann, A.R. (2006). The Y-family DNA polymerase kappa (pol kappa) functions in mammalian nucleotide-excision repair. Nat Cell Biol *8*, 640-642.

Olaussen, K.A., Dunant, A., Fouret, P., Brambilla, E., Andre, F., Haddad, V., Taranchon, E., Filipits, M., Pirker, R., Popper, H.H.*, et al.* (2006). DNA repair by ERCC1 in non-small-cell lung cancer and cisplatin-based adjuvant chemotherapy. The New England journal of medicine *355*, 983-991.

Olaussen, K.A., Fouret, P., and Kroemer, G. (2007). ERCC1-specific immunostaining in non-small-cell lung cancer. The New England journal of medicine *357*, 1559-1561.

Osman, F., Dixon, J., Doe, C.L., and Whitby, M.C. (2003). Generating crossovers by resolution of nicked Holliday junctions: a role for Mus81-Eme1 in meiosis. Molecular cell *12*, 761-774.

Ozols, R.F., Bundy, B.N., Greer, B.E., Fowler, J.M., Clarke-Pearson, D., Burger, R.A., Mannel, R.S., DeGeest, K., Hartenbach, E.M., and Baergen, R. (2003). Phase III trial of carboplatin and paclitaxel compared with cisplatin and paclitaxel in patients with optimally resected stage III ovarian cancer: a Gynecologic Oncology Group study. J Clin Oncol *21*, 3194-3200.

Palom, Y., Suresh Kumar, G., Tang, L.Q., Paz, M.M., Musser, S.M., Rockwell, S., and Tomasz, M. (2002). Relative toxicities of DNA cross-links and monoadducts: new insights from studies of decarbamoyl mitomycin C and mitomycin C. Chem Res Toxicol *15*, 1398-1406.

Pan, J., Lin, J., Izzo, J., Liu, Y., Xing, J., Huang, M., Ajani, J., and Wu, X. (2009). Genetic Susceptibility to Esophageal Cancer: The Role of the Nucleotide Excision Repair Pathway. Carcinogenesis.

Paques, F., and Haber, J.E. (1997). Two pathways for removal of nonhomologous DNA ends during double-strand break repair in Saccharomyces cerevisiae. Mol Cell Biol *17*, 6765-6771.

Park, C.H., and Sancar, A. (1994). Formation of a ternary complex by human XPA, ERCC1, and ERCC4(XPF) excision repair proteins. Proceedings of the National Academy of Sciences of the United States of America *91*, 5017-5021.

Park, S.Y., Hong, Y.C., Kim, J.H., Kwak, S.M., Cho, J.H., Lee, H.L., and Ryu, J.S. (2006). Effect of ERCC1 polymorphisms and the modification by smoking on the survival of non-small cell lung cancer patients. Medical oncology (Northwood, London, England) *23*, 489-498.

Parmar, K., D'Andrea, A., and Niedernhofer, L.J. (2009). Mouse models of Fanconi anemia. Mutation research *668*, 133-140.

Patz, E.F., Jr., Goodman, P.C., and Bepler, G. (2000). Screening for lung cancer. N Engl J Med *343*, 1627-1633.

Paulsen, R.D., and Cimprich, K.A. (2007). The ATR pathway: fine-tuning the fork. DNA repair *6*, 953-966.

Pena, S.D., and Shokeir, M.H. (1974). Autosomal recessive cerebro-oculo-facio-skeletal (COFS) syndrome. Clin Genet *5*, 285-293.

Piccart, M.J., Bertelsen, K., James, K., Cassidy, J., Mangioni, C., Simonsen, E., Stuart, G., Kaye, S., Vergote, I., Blom, R.*, et al.* (2000). Randomized intergroup trial of cisplatin-paclitaxel versus cisplatin-cyclophosphamide in women with advanced epithelial ovarian cancer: three-year results. J Natl Cancer Inst *92*, 699-708.

Pichierri, P., and Rosselli, F. (2004). The DNA crosslink-induced S-phase checkpoint depends on ATR-CHK1 and ATR-NBS1-FANCD2 pathways. The EMBO journal *23*, 1178-1187.

Poot, M., Verkerk, A., Koster, J.F., Esterbauer, H., and Jongkind, J.F. (1987). Influence of cumene hydroperoxide and 4-hydroxynonenal on the glutathione metabolism during in vitro ageing of human skin fibroblasts. Eur J Biochem *162*, 287-291.

Pouliot, J.J., Yao, K.C., Robertson, C.A., and Nash, H.A. (1999). Yeast gene for a Tyr-DNA phosphodiesterase that repairs topoisomerase I complexes. Science (New York, NY *286*, 552-555.

Pradidarcheep, W., Labruyere, W.T., Dabhoiwala, N.F., and Lamers, W.H. (2008). Lack of Specificity of Commercially Available Antisera: Better Specifications Needed. J Histochem Cytochem.

Prasher, J.M., Lalai, A.S., Heijmans-Antonissen, C., Ploemacher, R.E., Hoeijmakers, J.H., Touw, I.P., and Niedernhofer, L.J. (2005). Reduced hematopoietic reserves in DNA interstrand crosslink repair-deficient Ercc1-/- mice. The EMBO journal *24*, 861-871.

Qiao, F., Mi, J., Wilson, J.B., Zhi, G., Bucheimer, N.R., Jones, N.J., and Kupfer, G.M. (2004). Phosphorylation of fanconi anemia (FA) complementation group G protein, FANCG, at serine 7 is important for function of the FA pathway. The Journal of biological chemistry *279*, 46035-46045.

Qiao, F., Moss, A., and Kupfer, G.M. (2001). Fanconi anemia proteins localize to chromatin and the nuclear matrix in a DNA damage- and cell cycle-regulated manner. The Journal of biological chemistry *276*, 23391-23396.

Quintela-Fandino, M., Hitt, R., Medina, P.P., Gamarra, S., Manso, L., Cortes-Funes, H., and Sanchez-Cespedes, M. (2006). DNA-repair gene polymorphisms predict favorable

clinical outcome among patients with advanced squamous cell carcinoma of the head and neck treated with cisplatin-based induction chemotherapy. J Clin Oncol *24*, 4333-4339.

Rabik, C.A., and Dolan, M.E. (2007). Molecular mechanisms of resistance and toxicity associated with platinating agents. Cancer treatment reviews *33*, 9-23.

Raschle, M., Knipscheer, P., Enoiu, M., Angelov, T., Sun, J., Griffith, J.D., Ellenberger, T.E., Scharer, O.D., and Walter, J.C. (2008). Mechanism of replication-coupled DNA interstrand crosslink repair. Cell *134*, 969-980.

Reed, E., Dabholkar, M., Thornton, K., Thompson, C., Yu, J.J., and Bostick-Bruton, F. (2000). Evidence for in the appearance of mRNAs of nucleotide excision repair genes, in human ovarian cancer tissues. Oncology reports *7*, 1123-1128.

Reynolds, R.J., Love, J.D., and Friedberg, E.C. (1981). Molecular mechanisms of pyrimidine dimer excision in Saccharomyces cerevisiae: excision of dimers in cell extracts. J Bacteriol *147*, 705-708.

Rhodes, A., Jasani, B., Couturier, J., McKinley, M.J., Morgan, J.M., Dodson, A.R., Navabi, H., Miller, K.D., and Balaton, A.J. (2002). A formalin-fixed, paraffin-processed cell line standard for quality control of immunohistochemical assay of HER-2/neu expression in breast cancer. Am J Clin Pathol *117*, 81-89.

Riedl, T., Hanaoka, F., and Egly, J.M. (2003). The comings and goings of nucleotide excision repair factors on damaged DNA. The EMBO journal *22*, 5293-5303.

Ries LAG, M.D., Krapcho M, Stinchcomb DG, Howlader N, Horner MJ, Mariotto A, Miller BA, Feuer EJ, Altekruse SF, Lewis DR, Clegg L, Eisner MP, Reichman M, Edwards BK (eds) (2008). SEER Cancer Statistics Review, 1975-2005 (Bethesda, MD, National Cancer Institute).

Robbins, J.H., Brumback, R.A., Mendiones, M., Barrett, S.F., Carl, J.R., Cho, S., Denckla, M.B., Ganges, M.B., Gerber, L.H., Guthrie, R.A*., et al.* (1991). Neurological disease in xeroderma pigmentosum. Documentation of a late onset type of the juvenile onset form. Brain *114 (Pt 3)*, 1335-1361.

Robbins, J.H., Kraemer, K.H., Lutzner, M.A., Festoff, B.W., and Coon, H.G. (1974). Xeroderma pigmentosum. An inherited diseases with sun sensitivity, multiple cutaneous neoplasms, and abnormal DNA repair. Ann Intern Med *80*, 221-248.

Rosell, R., Felip, E., and Paz-Ares, L. (2007). How could pharmacogenomics help improve patient survival? Lung Cancer *57 Suppl 2*, S35-41.

Rosell, R., Lord, R.V., Taron, M., and Reguart, N. (2002). DNA repair and cisplatin resistance in non-small-cell lung cancer. Lung Cancer *38*, 217-227.

Rosin-Arbesfeld, R., Cliffe, A., Brabletz, T., and Bienz, M. (2003). Nuclear export of the APC tumour suppressor controls beta-catenin function in transcription. Embo J *22*, 1101-1113.

Ruhland, A., Kircher, M., Wilborn, F., and Brendel, M. (1981). A yeast mutant specifically sensitive to bifunctional alkylation. Mutation research *91*, 457-462.

Saijo, M., Kuraoka, I., Masutani, C., Hanaoka, F., and Tanaka, K. (1996). Sequential binding of DNA repair proteins RPA and ERCC1 to XPA in vitro. Nucleic acids research *24*, 4719-4724.

Sargent, R.G., Meservy, J.L., Perkins, B.D., Kilburn, A.E., Intody, Z., Adair, G.M., Nairn, R.S., and Wilson, J.H. (2000). Role of the nucleotide excision repair gene ERCC1 in formation of recombination-dependent rearrangements in mammalian cells. Nucleic acids research *28*, 3771-3778.

Sargent, R.G., Rolig, R.L., Kilburn, A.E., Adair, G.M., Wilson, J.H., and Nairn, R.S. (1997). Recombination-dependent deletion formation in mammalian cells deficient in the nucleotide excision repair gene ERCC1. Proceedings of the National Academy of Sciences of the United States of America *94*, 13122-13127.

Sarkar, S., Davies, A.A., Ulrich, H.D., and McHugh, P.J. (2006). DNA interstrand crosslink repair during G1 involves nucleotide excision repair and DNA polymerase zeta. The EMBO journal *25*, 1285-1294.

Sasaki, M.S., and Tonomura, A. (1973). A high susceptibility of Fanconi's anemia to chromosome breakage by DNA cross-linking agents. Cancer research *33*, 1829-1836.

Schaeffer, L., Moncollin, V., Roy, R., Staub, A., Mezzina, M., Sarasin, A., Weeda, G., Hoeijmakers, J.H., and Egly, J.M. (1994). The ERCC2/DNA repair protein is associated with the class II BTF2/TFIIH transcription factor. The EMBO journal *13*, 2388-2392.

Schaeffer, L., Roy, R., Humbert, S., Moncollin, V., Vermeulen, W., Hoeijmakers, J.H., Chambon, P., and Egly, J.M. (1993). DNA repair helicase: a component of BTF2 (TFIIH) basic transcription factor. Science (New York, NY *260*, 58-63.

Schiestl, R.H., and Prakash, S. (1988). RAD1, an excision repair gene of Saccharomyces cerevisiae, is also involved in recombination. Mol Cell Biol *8*, 3619-3626.

Schiestl, R.H., and Prakash, S. (1990). RAD10, an excision repair gene of Saccharomyces cerevisiae, is involved in the RAD1 pathway of mitotic recombination. Mol Cell Biol *10*, 2485-2491.

Schmidt, H., Kapitza-Fecke, P., Stephen, E.R., and Gutz, H. (1989). Some of the swi genes of Schizosaccharomyces pombe also have a function in the repair of radiation damage. Curr Genet *16*, 89-94.

Selfridge, J., Hsia, K.T., Redhead, N.J., and Melton, D.W. (2001). Correction of liver dysfunction in DNA repair-deficient mice with an ERCC1 transgene. Nucleic acids research *29*, 4541-4550.

Selfridge, J., Pow, A.M., McWhir, J., Magin, T.M., and Melton, D.W. (1992). Gene targeting using a mouse HPRT minigene/HPRT-deficient embryonic stem cell system: inactivation of the mouse ERCC-1 gene. Somatic cell and molecular genetics *18*, 325-336.

Sgouros, J., Gaillard, P.H., and Wood, R.D. (1999). A relationship betweena DNA-repair/recombination nuclease family and archaeal helicases. Trends in biochemical sciences *24*, 95-97.

Shannon, M., Lamerdin, J.E., Richardson, L., McCutchen-Maloney, S.L., Hwang, M.H., Handel, M.A., Stubbs, L., and Thelen, M.P. (1999). Characterization of the mouse Xpf DNA repair gene and differential expression during spermatogenesis. Genomics *62*, 427-435.

Shen, M.R., Jones, I.M., and Mohrenweiser, H. (1998). Nonconservative amino acid substitution variants exist at polymorphic frequency in DNA repair genes in healthy humans. Cancer research *58*, 604-608.

Shi, S.R., Imam, S.A., Young, L., Cote, R.J., and Taylor, C.R. (1995). Antigen retrieval immunohistochemistry under the influence of pH using monoclonal antibodies. J Histochem Cytochem *43*, 193-201.

Shirota, Y., Stoehlmacher, J., Brabender, J., Xiong, Y.P., Uetake, H., Danenberg, K.D., Groshen, S., Tsao-Wei, D.D., Danenberg, P.V., and Lenz, H.J. (2001). ERCC1 and thymidylate synthase mRNA levels predict survival for colorectal cancer patients receiving combination oxaliplatin and fluorouracil chemotherapy. J Clin Oncol *19*, 4298-4304.

Shivji, M.K., Moggs, J.G., Kuraoka, I., and Wood, R.D. (1999). Dual-incision assays for nucleotide excision repair using DNA with a lesion at a specific site. Methods Mol Biol *113*, 373-392.

Shivji, M.K., Podust, V.N., Hubscher, U., and Wood, R.D. (1995). Nucleotide excision repair DNA synthesis by DNA polymerase epsilon in the presence of PCNA, RFC, and RPA. Biochemistry *34*, 5011-5017.

Sijbers, A.M., de Laat, W.L., Ariza, R.R., Biggerstaff, M., Wei, Y.F., Moggs, J.G., Carter, K.C., Shell, B.K., Evans, E., de Jong, M.C*., et al.* (1996a). Xeroderma pigmentosum group F caused by a defect in a structure-specific DNA repair endonuclease. Cell *86*, 811-822.

Sijbers, A.M., van der Spek, P.J., Odijk, H., van den Berg, J., van Duin, M., Westerveld, A., Jaspers, N.G., Bootsma, D., and Hoeijmakers, J.H. (1996b). Mutational analysis of the human nucleotide excision repair gene ERCC1. Nucleic acids research *24*, 3370-3380.

Sijbers, A.M., van Voorst Vader, P.C., Snoek, J.W., Raams, A., Jaspers, N.G., and Kleijer, W.J. (1998). Homozygous R788W point mutation in the XPF gene of a patient with xeroderma pigmentosum and late-onset neurologic disease. J Invest Dermatol *110*, 832-836.

Simon, G.R., Ismail-Khan, R., and Bepler, G. (2007). Nuclear excision repair-based personalized therapy for non-small cell lung cancer: From hypothesis to reality. Int J Biochem Cell Biol.

Smith, G.R., Boddy, M.N., Shanahan, P., and Russell, P. (2003). Fission yeast Mus81.Eme1 Holliday junction resolvase is required for meiotic crossing over but not for gene conversion. Genetics *165*, 2289-2293.

Smogorzewska, A., Matsuoka, S., Vinciguerra, P., McDonald, E.R., 3rd, Hurov, K.E., Luo, J., Ballif, B.A., Gygi, S.P., Hofmann, K., D'Andrea, A.D*., et al.* (2007). Identification of the FANCI Protein, a Monoubiquitinated FANCD2 Paralog Required for DNA Repair. Cell.

Staresincic, L., Fagbemi, A.F., Enzlin, J.H., Gourdin, A.M., Wijgers, N., Dunand-Sauthier, I., Giglia-Mari, G., Clarkson, S.G., Vermeulen, W., and Scharer, O.D. (2009). Coordination of dual incision and repair synthesis in human nucleotide excision repair. The EMBO journal.

Steffensen, K.D., Waldstrom, M., Jeppesen, U., Brandslund, I., and Jakobsen, A. (2007). Prediction of response to chemotherapy by ERCC1 immunohistochemistry and ERCC1 polymorphism in ovarian cancer. Int J Gynecol Cancer.

Steffensen, K.D., Waldstrom, M., Jeppesen, U., Brandslund, I., and Jakobsen, A. (2008). Prediction of response to chemotherapy by ERCC1 immunohistochemistry and ERCC1 polymorphism in ovarian cancer. Int J Gynecol Cancer *18*, 702-710.

Stiff, T., Walker, S.A., Cerosaletti, K., Goodarzi, A.A., Petermann, E., Concannon, P., O'Driscoll, M., and Jeggo, P.A. (2006). ATR-dependent phosphorylation and activation of ATM in response to UV treatment or replication fork stalling. The EMBO journal *25*, 5775-5782.

Su, D., Ma, S., Liu, P., Jiang, Z., Lv, W., Zhang, Y., Deng, Q., Smith, S., and Yu, H. (2007). Genetic polymorphisms and treatment response in advanced non-small cell lung cancer. Lung Cancer *56*, 281-288.

Sugasawa, K. (2006). UV-induced ubiquitylation of XPC complex, the UV-DDB-ubiquitin ligase complex, and DNA repair. J Mol Histol *37*, 189-202.

Sugasawa, K., Ng, J.M., Masutani, C., Iwai, S., van der Spek, P.J., Eker, A.P., Hanaoka, F., Bootsma, D., and Hoeijmakers, J.H. (1998). Xeroderma pigmentosum group C protein complex is the initiator of global genome nucleotide excision repair. Molecular cell *2*, 223-232.

Sugawara, N., Paques, F., Colaiacovo, M., and Haber, J.E. (1997). Role of Saccharomyces cerevisiae Msh2 and Msh3 repair proteins in double-strand break-induced recombination. Proceedings of the National Academy of Sciences of the United States of America *94*, 9214-9219.

Svendsen, J.M., Smogorzewska, A., Sowa, M.E., O'Connell, B.C., Gygi, S.P., Elledge, S.J., and Harper, J.W. (2009). Mammalian BTBD12/SLX4 assembles a Holliday junction resolvase and is required for DNA repair. Cell *138*, 63-77.

Swanson, R.L., Morey, N.J., Doetsch, P.W., and Jinks-Robertson, S. (1999). Overlapping specificities of base excision repair, nucleotide excision repair, recombination, and translesion synthesis pathways for DNA base damage in Saccharomyces cerevisiae. Mol Cell Biol *19*, 2929-2935.

Takayama, K., Salazar, E.P., Broughton, B.C., Lehmann, A.R., Sarasin, A., Thompson, L.H., and Weber, C.A. (1996). Defects in the DNA repair and transcription gene ERCC2(XPD) in trichothiodystrophy. Am J Hum Genet *58*, 263-270.

Takenaka, T., Yano, T., Kiyohara, C., Miura, N., Kouso, H., Ohba, T., Kometani, T., Shoji, F., Yoshino, I., and Maehara, Y. (2009). Effects of excision repair cross-complementation group 1 (ERCC1) single nucleotide polymorphisms on the prognosis of non-small cell lung cancer patients. Lung Cancer.

Taniguchi, T., Garcia-Higuera, I., Andreassen, P.R., Gregory, R.C., Grompe, M., and D'Andrea, A.D. (2002). S-phase-specific interaction of the Fanconi anemia protein, FANCD2, with BRCA1 and RAD51. Blood *100*, 2414-2420.

Tapias, A., Auriol, J., Forget, D., Enzlin, J.H., Scharer, O.D., Coin, F., Coulombe, B., and Egly, J.M. (2004). Ordered conformational changes in damaged DNA induced by nucleotide excision repair factors. The Journal of biological chemistry *279*, 19074-19083.

Taylor, C.R. (1992). Quality assurance and standardization in immunohistochemistry. A proposal for the annual meeting of the Biological Stain Commission, June, 1991. Biotech Histochem *67*, 110-117.

Taylor, C.R., and Levenson, R.M. (2006). Quantification of immunohistochemistry--issues concerning methods, utility and semiquantitative assessment II. Histopathology *49*, 411-424.

Taylor, E.M., Broughton, B.C., Botta, E., Stefanini, M., Sarasin, A., Jaspers, N.G., Fawcett, H., Harcourt, S.A., Arlett, C.F., and Lehmann, A.R. (1997). Xeroderma pigmentosum and trichothiodystrophy are associated with different mutations in the XPD (ERCC2) repair/transcription gene. Proc Natl Acad Sci U S A *94*, 8658-8663.

Thompson, L.H., Fong, S., and Brookman, K. (1980). Validation of conditions for efficient detection of HPRT and APRT mutations in suspension-cultured Chinese hamster ovary cells. Mutation research *74*, 21-36.

Thompson, L.H., and Hinz, J.M. (2009). Cellular and molecular consequences of defective Fanconi anemia proteins in replication-coupled DNA repair: Mechanistic insights. Mutation research *668*, 54-72.

Tian, M., Shinkura, R., Shinkura, N., and Alt, F.W. (2004). Growth retardation, early death, and DNA repair defects in mice deficient for the nucleotide excision repair enzyme XPF. Mol Cell Biol *24*, 1200-1205.

Torres-Ramos, C.A., Johnson, R.E., Prakash, L., and Prakash, S. (2000). Evidence for the involvement of nucleotide excision repair in the removal of abasic sites in yeast. Mol Cell Biol *20*, 3522-3528.

Troelstra, C., van Gool, A., de Wit, J., Vermeulen, W., Bootsma, D., and Hoeijmakers, J.H. (1992). ERCC6, a member of a subfamily of putative helicases, is involved in Cockayne's syndrome and preferential repair of active genes. Cell *71*, 939-953.

Tsodikov, O.V., Enzlin, J.H., Scharer, O.D., and Ellenberger, T. (2005). Crystal structure and DNA binding functions of ERCC1, a subunit of the DNA structure-specific endonuclease XPF-ERCC1. Proc Natl Acad Sci U S A *102*, 11236-11241.

Tsodikov, O.V., Ivanov, D., Orelli, B., Staresincic, L., Shoshani, I., Oberman, R., Scharer, O.D., Wagner, G., and Ellenberger, T. (2007). Structural basis for the recruitment of ERCC1-XPF to nucleotide excision repair complexes by XPA. EMBO J *26*, 4768-4776.

van Duin, M., de Wit, J., Odijk, H., Westerveld, A., Yasui, A., Koken, H.M., Hoeijmakers, J.H., and Bootsma, D. (1986). Molecular characterization of the human excision repair gene ERCC-1: cDNA cloning and amino acid homology with the yeast DNA repair gene RAD10. Cell *44*, 913-923.

van Gool, A.J., Citterio, E., Rademakers, S., van Os, R., Vermeulen, W., Constantinou, A., Egly, J.M., Bootsma, D., and Hoeijmakers, J.H. (1997). The Cockayne syndrome B protein, involved in transcription-coupled DNA repair, resides in an RNA polymerase II-containing complex. Embo J *16*, 5955-5965.

Van Houten, B., Gamper, H., Holbrook, S.R., Hearst, J.E., and Sancar, A. (1986). Action mechanism of ABC excision nuclease on a DNA substrate containing a psoralen crosslink at a defined position. Proceedings of the National Academy of Sciences of the United States of America *83*, 8077-8081.

van Vuuren, A.J., Appeldoorn, E., Odijk, H., Humbert, S., Moncollin, V., Eker, A.P., Jaspers, N.G., Egly, J.M., and Hoeijmakers, J.H. (1995). Partial characterization of the DNA repair protein complex, containing the ERCC1, ERCC4, ERCC11 and XPF correcting activities. Mutat Res *337*, 25-39.

Vance, J.R., and Wilson, T.E. (2001). Repair of DNA strand breaks by the overlapping functions of lesion-specific and non-lesion-specific DNA 3' phosphatases. Mol Cell Biol *21*, 7191-7198.

Vance, J.R., and Wilson, T.E. (2002). Yeast Tdp1 and Rad1-Rad10 function as redundant pathways for repairing Top1 replicative damage. Proceedings of the National Academy of Sciences of the United States of America *99*, 13669-13674.

Vannier, J.B., Depeiges, A., White, C., and Gallego, M.E. (2009). ERCC1/XPF protects short telomeres from homologous recombination in Arabidopsis thaliana. PLoS Genet *5*, e1000380.

Venema, J., Bartosova, Z., Natarajan, A.T., van Zeeland, A.A., and Mullenders, L.H. (1992). Transcription affects the rate but not the extent of repair of cyclobutane pyrimidine dimers in the human adenosine deaminase gene. The Journal of biological chemistry *267*, 8852-8856.

Vergote, I., van Gorp, T., Amant, F., Leunen, K., Neven, P., and Berteloot, P. (2008). Timing of debulking surgery in advanced ovarian cancer. Int J Gynecol Cancer *18 Suppl 1*, 11-19.

Vermeulen, W., Bergmann, E., Auriol, J., Rademakers, S., Frit, P., Appeldoorn, E., Hoeijmakers, J.H., and Egly, J.M. (2000). Sublimiting concentration of TFIIH transcription/DNA repair factor causes TTD-A trichothiodystrophy disorder. Nat Genet *26*, 307-313.

Vermeulen, W., Scott, R.J., Rodgers, S., Muller, H.J., Cole, J., Arlett, C.F., Kleijer, W.J., Bootsma, D., Hoeijmakers, J.H., and Weeda, G. (1994). Clinical heterogeneity within xeroderma pigmentosum associated with mutations in the DNA repair and transcription gene ERCC3. Am J Hum Genet *54*, 191-200.

Vilmar, A., and Sorensen, J.B. (2008). Excision repair cross-complementation group 1 (ERCC1) in platinum-based treatment of non-small cell lung cancer with special emphasis on carboplatin: A review of current literature. Lung Cancer.

Volker, M., Mone, M.J., Karmakar, P., van Hoffen, A., Schul, W., Vermeulen, W., Hoeijmakers, J.H., van Driel, R., van Zeeland, A.A., and Mullenders, L.H. (2001). Sequential assembly of the nucleotide excision repair factors in vivo. Molecular cell *8*, 213-224.

Wakasugi, M., Reardon, J.T., and Sancar, A. (1997). The non-catalytic function of XPG protein during dual incision in human nucleotide excision repair. The Journal of biological chemistry *272*, 16030-16034.

Wakasugi, M., and Sancar, A. (1998). Assembly, subunit composition, and footprint of human DNA repair excision nuclease. Proceedings of the National Academy of Sciences of the United States of America *95*, 6669-6674.

Wang, X., Andreassen, P.R., and D'Andrea, A.D. (2004). Functional interaction of monoubiquitinated FANCD2 and BRCA2/FANCD1 in chromatin. Mol Cell Biol *24*, 5850-5862.

Wang, X., Kennedy, R., Ray, K., Stuckert, P., Ellenberger, T., and D'Andrea, A.D. (2007). Chk1-mediated Phosphorylation of FANCE is Required for the Fanconi Anemia/BRCA Pathway. Mol Cell Biol.

Ward, I.M., and Chen, J. (2001). Histone H2AX is phosphorylated in an ATR-dependent manner in response to replicational stress. The Journal of biological chemistry *276*, 47759-47762.

Ward, J.F. (1988). DNA damage produced by ionizing radiation in mammalian cells: identities, mechanisms of formation, and reparability. Progress in nucleic acid research and molecular biology *35*, 95-125.

Warnecke-Eberz, U., Metzger, R., Miyazono, F., Baldus, S.E., Neiss, S., Brabender, J., Schaefer, H., Doerfler, W., Bollschweiler, E., Dienes, H.P*., et al.* (2004). High specificity of quantitative excision repair cross-complementing 1 messenger RNA expression for prediction of minor histopathological response to neoadjuvant radiochemotherapy in esophageal cancer. Clin Cancer Res *10*, 3794-3799.

Weeda, G., Donker, I., de Wit, J., Morreau, H., Janssens, R., Vissers, C.J., Nigg, A., van Steeg, H., Bootsma, D., and Hoeijmakers, J.H. (1997). Disruption of mouse ERCC1 results in a novel repair syndrome with growth failure, nuclear abnormalities and senescence. Curr Biol *7*, 427-439.

Weeda, G., van Ham, R.C., Vermeulen, W., Bootsma, D., van der Eb, A.J., and Hoeijmakers, J.H. (1990). A presumed DNA helicase encoded by ERCC-3 is involved in the human repair disorders xeroderma pigmentosum and Cockayne's syndrome. Cell *62*, 777-791.

Welsh, M.J., and Smith, A.E. (1993). Molecular mechanisms of CFTR chloride channel dysfunction in cystic fibrosis. Cell *73*, 1251-1254.

Wilcox, D.R., and Prakash, L. (1981). Incision and postincision steps of pyrimidine dimer removal in excision-defective mutants of Saccharomyces cerevisiae. J Bacteriol *148*, 618-623.

Wilson, J.B., Yamamoto, K., Marriott, A.S., Hussain, S., Sung, P., Hoatlin, M.E., Mathew, C.G., Takata, M., Thompson, L.H., Kupfer, G.M*., et al.* (2008). FANCG promotes formation of a newly identified protein complex containing BRCA2, FANCD2 and XRCC3. Oncogene *27*, 3641-3652.

Winton, T., Livingston, R., Johnson, D., Rigas, J., Johnston, M., Butts, C., Cormier, Y., Goss, G., Inculet, R., Vallieres, E*., et al.* (2005). Vinorelbine plus cisplatin vs. observation in resected non-small-cell lung cancer. N Engl J Med *352*, 2589-2597.

Wood, R.D., and Burki, H.J. (1982). Repair capability and the cellular age response for killing and mutation induction after UV. Mutation research *95*, 505-514.

Wu, Y., Mitchell, T.R., and Zhu, X.D. (2008). Human XPF controls TRF2 and telomere length maintenance through distinctive mechanisms. Mechanisms of ageing and development *129*, 602-610.

Wu, Y., Zacal, N.J., Rainbow, A.J., and Zhu, X.D. (2007). XPF with mutations in its conserved nuclease domain is defective in DNA repair but functions in TRF2-mediated telomere shortening. DNA repair *6*, 157-166.

Yagi, T., Matsumura, Y., Sato, M., Nishigori, C., Mori, T., Sijbers, A.M., and Takebe, H. (1998). Complete restoration of normal DNA repair characteristics in group F xeroderma pigmentosum cells by over-expression of transfected XPF cDNA. Carcinogenesis *19*, 55-60.

Yagi, T., Tatsumi-Miyajima, J., Sato, M., Kraemer, K.H., and Takebe, H. (1991). Analysis of point mutations in an ultraviolet-irradiated shuttle vector plasmid propagated in cells from Japanese xeroderma pigmentosum patients in complementation groups A and F. Cancer research *51*, 3177-3182.

Yagi, T., Wood, R.D., and Takebe, H. (1997). A low content of ERCC1 and a 120 kDa protein is a frequent feature of group F xeroderma pigmentosum fibroblast cells. Mutagenesis *12*, 41-44.

Yamashita, T., Kupfer, G.M., Naf, D., Suliman, A., Joenje, H., Asano, S., and D'Andrea, A.D. (1998). The fanconi anemia pathway requires FAA phosphorylation and FAA/FAC nuclear accumulation. Proceedings of the National Academy of Sciences of the United States of America *95*, 13085-13090.

Yildiz, O., Kearney, H., Kramer, B.C., and Sekelsky, J.J. (2004). Mutational analysis of the Drosophila DNA repair and recombination gene mei-9. Genetics *167*, 263-273.

Yildiz, O., Majumder, S., Kramer, B., and Sekelsky, J.J. (2002). Drosophila MUS312 interacts with the nucleotide excision repair endonuclease MEI-9 to generate meiotic crossovers. Molecular cell *10*, 1503-1509.

Yin, J., Vogel, U., Gerdes, L.U., Dybdahl, M., Bolund, L., and Nexo, B.A. (2003). Twelve single nucleotide polymorphisms on chromosome 19q13.2-13.3: linkage disequilibria and associations with basal cell carcinoma in Danish psoriatic patients. Biochemical genetics *41*, 27-37.

Yu, J.J., Mu, C., Lee, K.B., Okamoto, A., Reed, E.L., Bostick-Bruton, F., Mitchell, K.C., and Reed, E. (1997). A nucleotide polymorphism in ERCC1 in human ovarian cancer cell lines and tumor tissues. Mutation research *382*, 13-20.

Yu, V.P., Koehler, M., Steinlein, C., Schmid, M., Hanakahi, L.A., van Gool, A.J., West, S.C., and Venkitaraman, A.R. (2000). Gross chromosomal rearrangements and genetic exchange between nonhomologous chromosomes following BRCA2 inactivation. Genes & development *14*, 1400-1406.

Zeng, L., Quilliet, X., Chevallier-Lagente, O., Eveno, E., Sarasin, A., and Mezzina, M. (1997). Retrovirus-mediated gene transfer corrects DNA repair defect of xeroderma pigmentosum cells of complementation groups A, B and C. Gene Ther *4*, 1077-1084.

Zhang, N., Kaur, R., Lu, X., Shen, X., Li, L., and Legerski, R.J. (2005). The Pso4 mRNA splicing and DNA repair complex interacts with WRN for processing of DNA interstrand cross-links. The Journal of biological chemistry *280*, 40559-40567.

Zhang, N., Lu, X., and Legerski, R.J. (2003). Partial reconstitution of human interstrand cross-link repair in vitro: characterization of the roles of RPA and PCNA. Biochemical and biophysical research communications *309*, 71-78.

Zhang, N., Lu, X., Zhang, X., Peterson, C.A., and Legerski, R.J. (2002). hMutSbeta is required for the recognition and uncoupling of psoralen interstrand cross-links in vitro. Molecular and cellular biology *22*, 2388-2397.

Zheng, Z., Chen, T., Li, X., Haura, E., Sharma, A., and Bepler, G. (2007). DNA synthesis and repair genes RRM1 and ERCC1 in lung cancer. The New England journal of medicine *356*, 800-808.

Zhu, X.D., Niedernhofer, L., Kuster, B., Mann, M., Hoeijmakers, J.H., and de Lange, T. (2003). ERCC1/XPF removes the 3' overhang from uncapped telomeres and represses formation of telomeric DNA-containing double minute chromosomes. Molecular cell *12*, 1489-1498.

Zienolddiny, S., Campa, D., Lind, H., Ryberg, D., Skaug, V., Stangeland, L., Phillips, D.H., Canzian, F., and Haugen, A. (2006). Polymorphisms of DNA repair genes and risk of non-small cell lung cancer. Carcinogenesis *27*, 560-567.